

UC Davis

UC Davis Previously Published Works

Title

Strontium isotope systematics for plagioclase of the Skaergaard intrusion (East Greenland): A window to crustal assimilation, differentiation, and magma dynamics

Permalink

<https://escholarship.org/uc/item/78p4d41h>

Journal

Geology, 47(4)

ISSN

0091-7613

Authors

Hagen-Peter, Graham

Tegner, Christian

Leshner, Charles E

Publication Date

2019-04-01

DOI

10.1130/g45639.1

Peer reviewed

Strontium isotope systematics for plagioclase of the Skaergaard intrusion (East Greenland): A window to crustal assimilation, differentiation, and magma dynamics

Graham Hagen-Peter^{1*}, Christian Tegner¹, and Charles E. Lesher^{1,2}

¹The Centre of Earth System Petrology and Aarhus Geochemistry and Isotope Research (AGiR) Platform, Department of Geoscience, Aarhus University, Høegh-Guldbergs Gade 2, 8000 Aarhus C, Denmark

²Department of Earth and Planetary Sciences, University of California, Davis, California 95616, USA

ABSTRACT

We present *in situ* laser ablation–multicollector–inductively coupled plasma–mass spectrometry Sr isotope data for plagioclase from a reference stratigraphic profile of the entire Layered Series and Upper Border Series of the Skaergaard intrusion (East Greenland). Plagioclase Sr isotope compositions and anorthite contents vary systematically from the margins of the intrusion inwards. The lowest $^{87}\text{Sr}/^{86}\text{Sr}_i$ (calculated at 56 Ma) values (~ 0.7041) occur near the base and top of the intrusion and systematically increase over several lithostratigraphic zones to a value of ~ 0.7044 , which is uniform throughout the middle ~ 2000 m of intrusion. Across this same profile, anorthite content of plagioclase varies smoothly from An_{65-70} at the base and top to $\sim \text{An}_{25}$ approaching the purported “Sandwich Horizon.” Plagioclase near the roof and proximal to rafts of partially assimilated basement gneiss are markedly more radiogenic ($^{87}\text{Sr}/^{86}\text{Sr}_i$ up to ~ 0.7046). We explain the stratigraphic relationships by progressive contamination of the magma during early stages of differentiation by basement gneiss rafts entrained during emplacement and accumulated near the top of the chamber. Contamination was transient, ceasing once the entrained gneiss was consumed or isolated from the main magma reservoir as the solidification front advanced. Modeling of fractionation–assimilation processes accounts for the observed isotopic trends with only a few percent assimilation (relative to the original magma mass). The record of contamination revealed by Sr in plagioclase supports the view that the bulk of the Skaergaard intrusion formed by closed-system differentiation with only minor *in situ* contamination and no magma recharge. Comparing plagioclase and bulk-rock Sr suggests that the latter may have witnessed late-stage metasomatic overprinting of phases other than plagioclase.

INTRODUCTION

The Skaergaard intrusion in central East Greenland is regarded as the archetypal natural example of closed-system magmatic differentiation. This is well supported by systematic changes in bulk-rock and mineral compositions indicating that solidification proceeded inward from the floor, roof, and walls, and terminated at what is known as the “Sandwich Horizon” (Wager and Deer, 1939; Wager, 1960; McBirney, 1975, 1998, 2002; Hunter and Sparks, 1987; Hoover, 1989; among others). Among the most compelling

observations is the regular variation in plagioclase composition from $\sim \text{An}_{65-70}$ at the exposed base, roof, and margins of the intrusion to $\sim \text{An}_{25}$ in the Sandwich Horizon (Fig. 1). Despite mineralogical evidence of closed-system magmatic differentiation, several studies (Leeman and Dasch, 1978; Stewart and DePaolo, 1990; McBirney and Creaser, 2003) drew attention to variations in the Sr and Nd isotope composition of bulk gabbroic rocks suggesting open-system behavior possibly involving magma recharge, crustal contamination, and/or post-cumulus melt infiltration.

Here, we present new Sr isotope data acquired by laser ablation–multicollector–inductively coupled plasma–mass spectrometry

(LA-MC-ICP-MS) for plagioclase from gabbroic and granophyric rocks of the Skaergaard intrusion. These new data include analyses of cores and rims of plagioclase primocrysts, as well as interstitial plagioclase, from each of the major subzones representing advancing solidification from the floor upward and the roof downward. Bulk-rock Sr data are also included for many of the samples, permitting direct comparison with plagioclase from the same samples and to previously published bulk-rock data. We evaluate these data in light of the possible open- and closed-system models for Skaergaard magmatic evolution.

GEOLOGICAL BACKGROUND

The Skaergaard intrusion is an $\sim 11 \times 8 \times 4$ km, box-shaped body bound by extensional faults emplaced at ca. 56 Ma on the eastern Greenland margin during the initial opening of the North Atlantic Ocean basin (Nielsen, 2004). The intrusion is in contact with Precambrian basement gneiss, Cretaceous–early Cenozoic sediments, and volcanic rocks of the east Greenland flood basalt province—the latter broadly contemporaneous with the intrusion. The upper ~ 2500 m of the intrusion is in contact with the basal unit of the flood basalt succession, whereas the lower part of the intrusion is in contact with ca. 2.86 Ga orthogneiss (Kays et al., 1989; Fig. 1; Fig. DR1 in the GSA Data Repository¹). Rafts and blocks of footwall gneiss are found included in gabbros near the roof of the intrusion (Fig. 2). These xenoliths are typically decimeter- to meter-size, although Wager and Deer (1939) mapped one gneiss block ~ 500 m wide. In contrast, blocks of basalt have been documented in the lower half of the stratigraphy of

*Current address: The Geological Survey of Norway, Leiv Eirikssons vei 39, 7040 Trondheim, Norway

¹GSA Data Repository item 2019106, description of the sample selections, methods, modeling details, map with sample locations, μXRF maps for all samples, a comparison of plagioclase and bulk-rock $^{87}\text{Sr}/^{86}\text{Sr}_i$, a comparison of plagioclase core and rim isotopic compositions, and data tables, is available online at <http://www.geosociety.org/datarepository/2019/>, or on request from editing@geosociety.org.

CITATION: Hagen-Peter, G., Tegner, C., and Lesher, C.E., 2019, Strontium isotope systematics for plagioclase of the Skaergaard intrusion (East Greenland): A window to crustal assimilation, differentiation, and magma dynamics: *Geology*, <https://doi.org/10.1130/G45639.1>

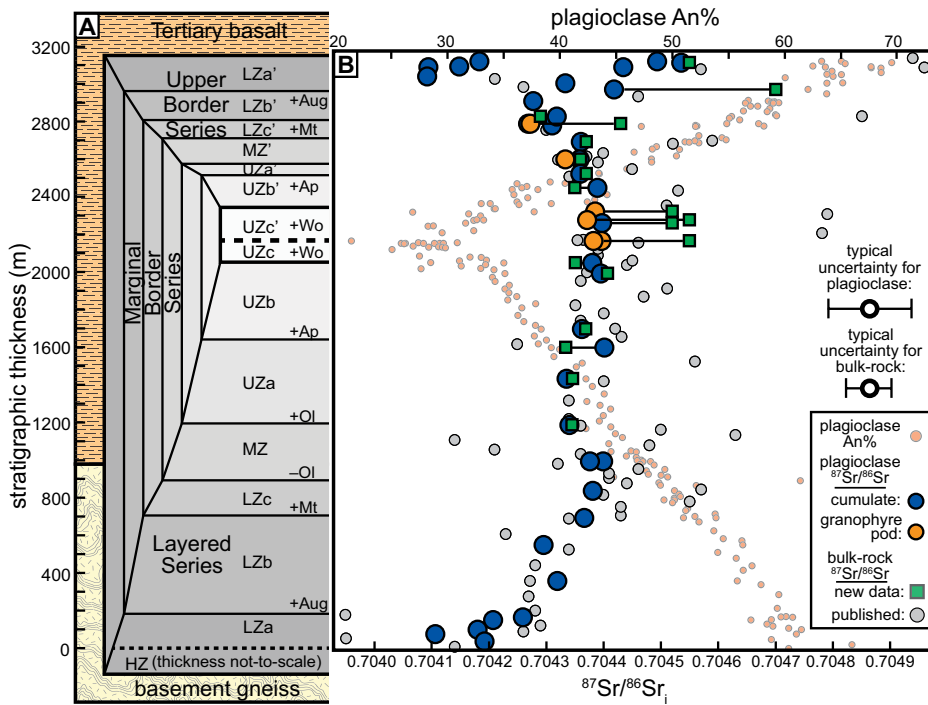


Figure 1. A: Schematic partial cross-section of the Skaergaard intrusion (East Greenland) showing the division of zones based on cumulus assemblages (modified from Salmonsén and Tegner, 2013). **B:** Plagioclase anorthite content and weighted-average $^{87}\text{Sr}/^{86}\text{Sr}_i$ across the stratigraphy of the intrusion along a reference profile of the Layered Series (LS) (Tegner et al., 2009) and several transects in the Upper Border Series (UBS) (Salmonsén and Tegner, 2013; sample locations are given in Fig. DR1 and Table DR3 [see footnote 1]). Anorthite contents are from Thy et al. (2009) and Salmonsén and Tegner (2013), as well as unpublished data. Each point is a weighted average of multiple analyses (6–26 for LS) per sample. Small squares show bulk-rock $^{87}\text{Sr}/^{86}\text{Sr}_i$ for a subset of samples. Tie lines connect bulk-rocks and constituent plagioclase. Uncertainties on $^{87}\text{Sr}/^{86}\text{Sr}_i$ for plagioclase are estimated as 2 standard error of the population and 2 standard deviation long-term reproducibility of a secondary standard added in quadrature. Published bulk-rock Sr data are from Stewart and DePaolo (1990) and McBirney and Creaser (2003) (see the Data Repository for explanation of the projection of these samples onto the reference profile).

the intrusion (Irvine et al., 1998). These features reflect stoping and sorting of xenoliths within the chamber due to density differences. Similar field relations are documented in the related Vandfaldsdalen and Mikis Fjord macrodikes (Rosing et al., 1989; Blichert-Toft et al., 1992).

The intrusion is divided into three distinct series: the Layered Series (LS), the Upper Border Series (UBS), and the Marginal Border Series (MBS). Each of these is subdivided into zones and subzones based on cumulate mineralogy that is correlated between series (UBS subzones denoted with apostrophes, e.g., LZa')—a result of the inward crystallization of the magma body (Fig. 1). Samples from the “Hidden Zone” and the MBS are not included in our study.

Published bulk-rock $^{87}\text{Sr}/^{86}\text{Sr}_i$ from Stewart and DePaolo (1990), and McBirney and Creaser (2003) mostly range from 0.70394 to 0.70495, with one sample as high as 0.70619. Stewart and DePaolo (1990) noted an increase in $^{87}\text{Sr}/^{86}\text{Sr}_i$ from the base of LS upwards and argued that a combination of progressive assimilation of Archean gneiss and periodic influx of new, less contaminated magma best explains the near-constant Sr isotope values. In contrast,

McBirney and Creaser (2003) determined that the most radiogenic gabbroic rocks occur in the middle zone (MZ) of the LS, roughly located in the center of intrusion. They also report several cases of isotopic disequilibrium between plagioclase and pyroxene in individual samples that, together with the bulk rock data, led them to posit that the Sr isotopic system was disturbed by infiltrating melt or late-stage metasomatic

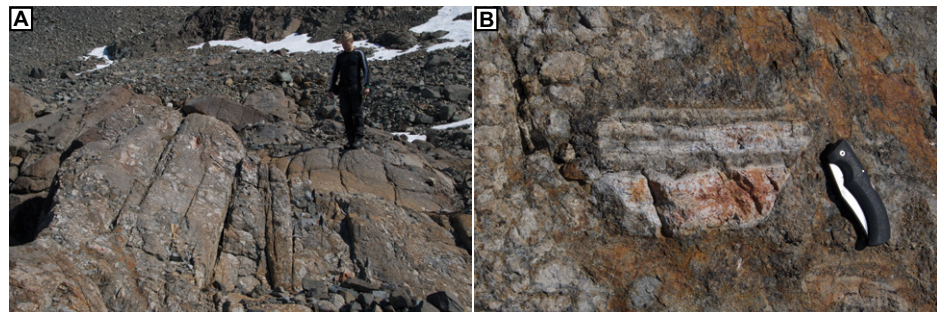


Figure 2. A: Abundant xenoliths of basement gneiss enveloped in gabbro of Upper Border Series (UBS) subzone LZa'. Xenoliths (light in color relative to enveloping gabbro) constitute > ~30% of the outcrop in the foreground, whereas the outcrop in the background (where the person is standing) has only sparse xenoliths. **B:** Close-up of a felsic gneiss xenolith in LZa' with the foliation still visible.

fluids. McBirney and Creaser (2003) found no evidence for recharge events as reported by Stewart and DePaolo (1990).

METHODS

Forty-one (41) surface and drill-core samples were selected for this study, representing all the major subzones of the intrusion, and are well characterized in terms of petrography, mineralogy, and geochemistry (Tegner et al., 2009; Salmonsén and Tegner, 2013). Of these, 33 are pristine gabbro from the LS and UBS, two are microgabbros collected near the roof of the intrusion, and six are granophyre-rich pods from the UBS and Sandwich Horizon.

In situ strontium isotope analyses were performed on polished rock billets using a Resonetics 193 nm excimer laser coupled to a Nu Plasma II MC-ICP-MS at the Aarhus Geochemistry and Isotope Research (AGiR) platform (Aarhus University, Denmark). Prior to Sr isotope measurements, billets were mapped by micro-X-ray fluorescence (μXRF) to provide compositional and petrographic context for laser spot placement (Fig. DR2). We targeted texturally variable plagioclase, including large euhedral primocrysts in cumulus textures, smaller intercumulus crystals, inclusions in other cumulus minerals, and crystals enveloped in interstitial granophyre. We were vigilant to analyze cores and rims of compositionally zoned primocrysts (Fig. DR2). Measurements of an in-house standard were accurate and repeatable to ± 0.000044 (2 standard deviations [SD] absolute; $n = 43$) over four analytical sessions, indicating excellent analytical precision. Bulk-rock Sr isotopes for a subset (18) of the samples were obtained by standard digestion, chemical purification, and MC-ICP-MS or thermal ionization mass spectrometry techniques. The bulk-rock data for samples from the UBS and Sandwich Horizon were previously presented by Salmonsén (2013). A detailed description of our analytical methods is provided in the Data Repository.

RESULTS

Figure 1 shows the variation in $^{87}\text{Sr}/^{86}\text{Sr}_i$ and anorthite content of plagioclase as a function of stratigraphic height in our reference profile.

Despite targeting texturally variable plagioclase, including cores and rims of individual crystals where possible (Fig. DR2), $^{87}\text{Sr}/^{86}\text{Sr}_i$ ratios for nearly every sample yield a single population with a mean square weighted deviation (MSWD) close to unity (Tables DR1 and DR2). Exceptions are samples SK08–65 from LZa' with $^{87}\text{Sr}/^{86}\text{Sr}_i$ ranging from 0.70432 to 0.70457, and SK08–129 from LZc' with $^{87}\text{Sr}/^{86}\text{Sr}_i$ of calcic cores up to 0.70551 and less calcic rims as low as 0.70424 (Fig. DR3). In Figure 1, we therefore plot the weighted average for each sample, including the roughly unimodal distribution of SK08–65 and the weighted average of the lower (and predominant) $^{87}\text{Sr}/^{86}\text{Sr}_i$ mode for sample SK08–129 (Fig. DR3). Also plotted in Figure 1 are bulk rock $^{87}\text{Sr}/^{86}\text{Sr}_i$ from this study and those reported by Stewart and DePaolo (1990), and McBirney and Creaser (2003).

Overall, plagioclase weighted-average $^{87}\text{Sr}/^{86}\text{Sr}_i$ range from ~0.7041–0.7046, with the least radiogenic values found in LZa of the LS and the equivalent zone (LZa') in UBS. LZa' also includes samples with the highest $^{87}\text{Sr}/^{86}\text{Sr}_i$. Through LZa and LZb, $^{87}\text{Sr}/^{86}\text{Sr}_i$ steadily increases, reaching a value of ~0.7044 in LZc that remains constant within uncertainty up to and including the Sandwich Horizon. This trend is mirrored in the equivalent zones of the UBS. These stratigraphic relations are in marked contrast to the steady decline in plagioclase anorthite content from An_{65-70} in LZa and LZa' to An_{25} in the Sandwich Horizon.

In contrast to the systematics of plagioclase, bulk rock $^{87}\text{Sr}/^{86}\text{Sr}_i$ are variable and commonly more radiogenic compared to plagioclase at a given stratigraphic level, with several exceptions in the LS (Fig. 1). We note here that where both bulk rock and constituent plagioclase have been analyzed, the bulk rock is either identical to (within uncertainty) or more radiogenic than its constituent plagioclase (Fig. 1; Fig. DR4).

DISCUSSION

Our new Sr isotope data for Skaergaard plagioclase reveal striking and systematic stratigraphic variations that bear directly on magmatic evolution. The perceptible increase in $^{87}\text{Sr}/^{86}\text{Sr}_i$ through LZa and LZb (and their UBS equivalents) is indicative of progressive contamination of the magma by a component with radiogenic Sr. An obvious source is the Precambrian basement gneiss hosting the lower portions of the intrusion, and, as noted above, found as partially assimilated rafts near the roof of the intrusion (Fig. 2). We interpret the samples with more radiogenic Sr from LZa' (and the absence of more radiogenic samples in LZa) as the result of reaction with entrained blocks of gneiss near the roof of the intrusion (Fig. 2) in a basaltic magma, even with an effective viscosity as high as 10^5 Pa s, Stokes' settling calculations permit 1-m-scale blocks of gneiss to ascend a distance equivalent to the thickness of the entire

intrusion in less than one year, explaining their concentration near the roof.

With the exception of several more radiogenic samples in LZa', the mirrored trend of increasing $^{87}\text{Sr}/^{86}\text{Sr}_i$ until LZc and LZc' in the LS and UBS suggests that the main reservoir of magma from which plagioclase crystallized remained well mixed. The uniform, elevated $^{87}\text{Sr}/^{86}\text{Sr}_i$ for the remaining stratigraphy requires that after an early period of contamination the source of radiogenic Sr was either exhausted or removed from interaction with the magma, for example, by trapping of the entrained gneiss blocks in the advancing solidification front by the time LZc' cumulates formed. This is consistent with the structural level of the large gneiss block mapped in the Lower Zone equivalents of the UBS (Wager and Deer, 1939; Naslund, 1984). The continuous evolution to more sodic plagioclase, terminating with the crystallization of An_{25} plagioclase in the Sandwich Horizon, further shows that fractional crystallization proceeded concurrently with assimilation during the early stages of evolution, and alone thereafter.

To further explore the scenario put forth above, we consider a simple forward model of fractionation and assimilation utilizing the formulation of Cribb and Barton (1996; a full description of the model is provided in the Data Repository). We tie fractionation to estimates of liquid remaining (F) as a function of stratigraphic height based on the mass balance model of Tegner et al. (2009), and permit the ratio of assimilation to crystallization (r) to vary with F . To constrain the latter functional relationship, we draw on our observation that $^{87}\text{Sr}/^{86}\text{Sr}_i$ ratios of plagioclase (excluding the radiogenic outliers in LZa') increase progressively from the bottom-up and top-down, reaching near uniform values by LZc and LZc', respectively. Thus, by the time LZc crystallized r is effectively zero. Additionally, the small overall range in $^{87}\text{Sr}/^{86}\text{Sr}_i$ in LZa and LZb requires that, even initially, r is relatively small. For simplicity, we assume that r varies linearly with F having a maximum value r_0 at $F = 1$ and a value of zero for $F = 0.34$, corresponding to the onset of crystallization in LZc and LZc'.

To implement our model, we constrain the Sr elemental and isotopic composition of the parental Skaergaard magma and consider plausible assimilants. For the parental magma, we use the composition of uncontaminated diabase from the adjacent Miki Fjord macrodike ($^{87}\text{Sr}/^{86}\text{Sr}_{56\text{Ma}} = 0.70392$; 264 ppm Sr; Blichert-Toft et al., 1992). For the assimilant, we consider a range based on the composition of the local basement gneiss, as well as partial melts of basement gneiss characterized by Blichert-Toft et al. (1992). Of these, we set the lower bounds as the least radiogenic felsic gneiss from Kays et al. (1989; $^{87}\text{Sr}/^{86}\text{Sr}_{56\text{Ma}} = 0.70967$; 224 ppm Sr) and the upper bounds as the most radiogenic granophyre formed by partial melting of felsic gneiss along the margin of the Miki Fjord macrodike (Blichert-Toft et al.,

1992; $^{87}\text{Sr}/^{86}\text{Sr}_{56\text{Ma}} = 0.78854$; 180 ppm Sr). While we do not consider that basement amphibolite contributed significantly to contamination of the Skaergaard magma—given its refractory nature, relatively high density, and marked low Sr—the bounds set for $^{87}\text{Sr}/^{86}\text{Sr}_i$ above span the isotope composition of analyzed amphibolites in the vicinity of Skaergaard.

With a visual best-fit to the data trends in the LS and UBS (Fig. 3), the models constrain r_0 to ~0.017–0.180 and the total mass assimilated to ~0.6%–6.3% (relative to the original mass of magma), with the lower and upper limits from the least and most radiogenic contaminant end-member, respectively. The precision of the estimates of assimilation is inherently limited by difficult-to-constrain assumptions about contaminant compositions. Regardless, the very modest effects of contamination are evident in the plagioclase record, which shows that this *in situ* contamination process apparently ceased once the assimilants were consumed or isolated from reaction with the main reservoir of magma.

Finally, as noted above, plagioclase from granophyre-rich pods in LZc'–UZc' are indistinguishable in $^{87}\text{Sr}/^{86}\text{Sr}_i$ from plagioclase in gabbroic rocks in the same interval. Several bulk samples, including granophyre-rich pods, have more radiogenic Sr than their constituent plagioclase (Fig. 1; Fig. DR4), suggesting that at least in some cases the plagioclase was not in equilibrium (compositionally and isotopically) with the host granophyre. The fact that the plagioclase generally defines the lower limit for $^{87}\text{Sr}/^{86}\text{Sr}_i$ at a given stratigraphic level supports the view of McBirney and Creaser (2003) that the scatter in the bulk rock is not a primary magmatic signature but a secondary overprint related to infiltration of late-stage melts or metasomatic fluids. Radiogenic granophyric melts contaminated by Archean crust (Hirschmann, 1992; Fig. DR4) are likely candidates. Whichever is the case, this overprinting did not alter the isotope composition of plagioclase.

In almost all samples, the $^{87}\text{Sr}/^{86}\text{Sr}_i$ of the plagioclase rims are indistinguishable from the cores (Fig. DR5), suggesting that infiltration of metasomatizing fluids and/or melts, even in samples with abundant interstitial granophyre, did not significantly perturb the isotope systematics of even the crystal margins. The one exception (sample SK08–129) contains several crystals with cores that are much more radiogenic ($^{87}\text{Sr}/^{86}\text{Sr}_i$ up to ~0.7055) than other plagioclase in the sample and, indeed, than any other samples measured in this study. We do not speculate to the origin of these few anomalously radiogenic crystal cores. However, the preservation of large isotopic heterogeneities in sample SK08–129 testifies to the absence of significant intracrystalline isotopic resetting.

In conclusion, the systematic and symmetric changes in chemical and isotopic compositions of plagioclase primocrysts across the LS and UBS are difficult to reconcile if the Skaergaard

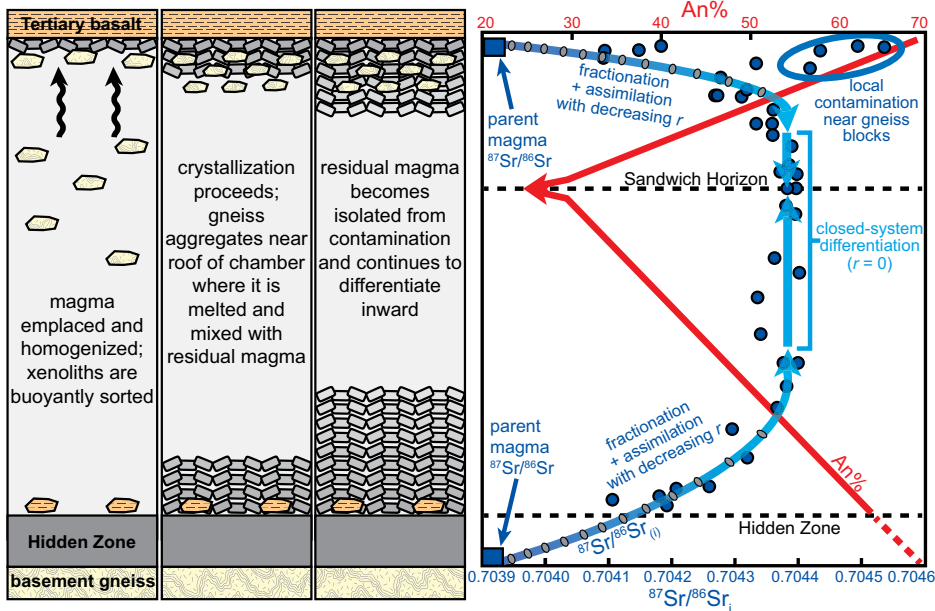


Figure 3. Conceptual model (left panels) summarizing the interpretations of the plagioclase Sr systematics and the corresponding quantitative fractionation-assimilation model (right panel). Gray ovals on fractionation-assimilation curves correspond to 0.5% increments of assimilation of the less radiogenic crustal end-member, but the model curves using either end-member coincide within the thickness of the curve shown.

magma chamber remained open to interaction with its wall rocks or experienced new inputs of primitive magma. We also find no evidence in the plagioclase record for a bull's-eye of radiogenic Sr centered on MZ as defined by McBirney and Creaser (2003), but do support McBirney and Creaser's (2003) contention bulk rock compositions were affected by late-stage melt infiltration and metasomatic processes. What this study does demonstrate are the opportunities to see beyond such secondary effects into the magmatic history by targeting plagioclases for *in situ* Sr isotopic analysis.

IMPLICATIONS

This study of Sr isotopes in plagioclase primocrysts *in situ* by LA-MC-ICP-MS has demonstrated that primary magmatic processes can be tracked precisely and accurately, avoiding later equilibration and alteration. As a result, we have elucidated the details of crystallization of the magma and subtle degrees of contamination in the Skaergaard chamber. The new data support the view that the Skaergaard intrusion differentiated from a common parental magma with entrained blocks of the host rocks. Minor contamination is detectable and can be ascribed to the interaction with gneiss xenoliths that eventually were consumed or buoyantly segregated from the main magma reservoir and became trapped by the advancing solidification front. There is no evidence for recharge or incremental emplacement of crystal slurries recorded in the plagioclase. In this regard, Skaergaard remains an example of *in situ* differentiation from a largely crystal-free

parental magma involving only a small amount of *in situ* contamination, reinforcing its value as a natural laboratory in which to study closed-system differentiation in a tank-like magma body.

ACKNOWLEDGMENTS

We thank Rasmus Andreasen for his analytical assistance at AGiR (Aarhus, Denmark). We thank three anonymous reviewers for insightful comments that improved the manuscript, and Chris Clark for efficient editorial handling. This work was funded by the Danish National Research Foundation Niels Bohr Professorship, awarded to C.E. Leshner, and the Carlsberg Foundation.

REFERENCES CITED

- Blichert-Toft, J., Leshner, C.E., and Rosing, M.T., 1992, Selectively contaminated magmas of the Tertiary East Greenland macrodike complex: Contributions to Mineralogy and Petrology, v. 110, p. 154–172, <https://doi.org/10.1007/BF00310736>.
- Cribb, J.W., and Barton, M., 1996, Geochemical effects of decoupled fractional crystallization and crustal assimilation: Lithos, v. 37, p. 293–307, [https://doi.org/10.1016/0024-4937\(95\)00027-5](https://doi.org/10.1016/0024-4937(95)00027-5).
- Hirschmann, M., 1992, Origin of the Transgressive granophyres from the Layered series of the Skaergaard intrusions, East Greenland: Journal of Volcanology and Geothermal Research, v. 52, p. 185–207.
- Hoover, J.D., 1989, Petrology of the Marginal Border Series of the Skaergaard intrusion: Journal of Petrology, v. 30, p. 399–439, <https://doi.org/10.1093/petrology/30.2.399>.
- Hunter, R.H., and Sparks, R.S.J., 1987, The differentiation of the Skaergaard intrusion: Contributions to Mineralogy and Petrology, v. 95, p. 451–461, <https://doi.org/10.1007/BF00402205>.
- Irvine, T.N., Andersen, J.C., and Brooks, C.K., 1998, Included blocks (and blocks within blocks) in the Skaergaard intrusion: Geologic relations and the origins of rhythmic modally graded layers:

- Geological Society of America Bulletin, v. 110, p. 1398–1447, [https://doi.org/10.1130/0016-7606\(1998\)110<1398:IBABWB>2.3.CO;2](https://doi.org/10.1130/0016-7606(1998)110<1398:IBABWB>2.3.CO;2).
- Kays, M.A., Goles, G.G., and Grover, T.W., 1989, Precambrian sequence bordering the Skaergaard Intrusion: Journal of Petrology, v. 30, p. 321–361, <https://doi.org/10.1093/petrology/30.2.321>.
- Leeman, W.P., and Dasch, E.J., 1978, Strontium, lead and oxygen isotopic investigation of the Skaergaard intrusion, East Greenland: Earth and Planetary Science Letters, v. 41, p. 47–59, [https://doi.org/10.1016/0012-821X\(78\)90040-7](https://doi.org/10.1016/0012-821X(78)90040-7).
- McBirney, A.R., 1975, Differentiation of the Skaergaard intrusion: Nature, v. 253, p. 691–694, <https://doi.org/10.1038/253691a0>.
- McBirney, A.R., 1998, The Skaergaard layered series. Part V. Included trace elements: Journal of Petrology, v. 39, p. 255–276, <https://doi.org/10.1093/ptro/39.2.255>.
- McBirney, A.R., 2002, The Skaergaard layered series. Part VI. Excluded trace elements: Journal of Petrology, v. 43, p. 535–556, <https://doi.org/10.1093/petrology/43.3.535>.
- McBirney, A.R., and Creaser, R.A., 2003, The Skaergaard layered series, part VII: Sr and Nd isotopes: Journal of Petrology, v. 44, p. 757–771, <https://doi.org/10.1093/petrology/44.4.757>.
- Naslund, H.R., 1984, Petrology of the Upper Border Series of the Skaergaard intrusion: Journal of Petrology, v. 25, p. 185–212, <https://doi.org/10.1093/petrology/25.1.185>.
- Nielsen, T.F., 2004, The shape and volume of the Skaergaard intrusion, Greenland: Implications for mass balance and bulk composition: Journal of Petrology, v. 45, p. 507–530, <https://doi.org/10.1093/petrology/egg092>.
- Rosing, M.T., Leshner, C.E., and Bird, D.K., 1989, Chemical modification of East Greenland Tertiary magmas by two-liquid interdiffusion: Geology, v. 17, p. 626–629, [https://doi.org/10.1130/0091-7613\(1989\)017<0626:CMOEGT>2.3.CO;2](https://doi.org/10.1130/0091-7613(1989)017<0626:CMOEGT>2.3.CO;2).
- Salmonsén, L.P., 2013, Petrology of the Upper Border Series of the Skaergaard Intrusion [Ph.D. thesis]: Aarhus, Denmark, Aarhus University, 97 p.
- Salmonsén, L.P., and Tegner, C., 2013, Crystallization sequence of the Upper Border Series of the Skaergaard Intrusion: Revised subdivision and implications for chamber-scale magma homogeneity: Contributions to Mineralogy and Petrology, v. 165, p. 1155–1171, <https://doi.org/10.1007/s00410-013-0852-y>.
- Stewart, B.W., and DePaolo, D.J., 1990, Isotopic studies of processes in mafic magma chambers: II. The Skaergaard Intrusion, East Greenland: Contributions to Mineralogy and Petrology, v. 104, p. 125–141, <https://doi.org/10.1007/BF00306438>.
- Tegner, C., Thy, P., Holness, M.B., Jakobsen, J.K., and Leshner, C.E., 2009, Differentiation and compaction in the Skaergaard intrusion: Journal of Petrology, v. 50, p. 813–840, <https://doi.org/10.1093/petrology/egg020>.
- Thy, P., Leshner, C.E., and Tegner, C., 2009, The Skaergaard liquid line of descent revisited: Contributions to Mineralogy and Petrology, v. 157, p. 735–747, <https://doi.org/10.1007/s00410-008-0361-6>.
- Wager, L.R., 1960, The major element variation of the layered series of the Skaergaard intrusion and a re-estimation of the average composition of the hidden layered series and of the successive residual magmas: Journal of Petrology, v. 1, p. 364–398, <https://doi.org/10.1093/petrology/1.3.364>.
- Wager, L.R., and Deer, W.A., eds., 1939, Geological investigations in East Greenland. Part III. The petrology of the Skaergaard Intrusion, Kangerdluqsuaq: East Greenland: Meddeleser om Grønland, v. 105, 352 p.

Printed in USA

Hagen-Peter, G., Tegner, C., and Leshner, C.E., 2019, Strontium isotope systematics for plagioclase of the Skaergaard intrusion (East Greenland): A window to crustal assimilation, differentiation, and magma dynamics: *Geology*, <https://doi.org/10.1130/G45639.1>

1 **SAMPLE SELECTION**

2 Samples from the Layered Series (LS) are from the reference profile of Tegner et al. (2009), which
3 extends from the base of LZa to a stratigraphic height of 2091 m at the top of the “90-22” drill core.
4 Additional samples assigned to the LS above the drill core extend to a stratigraphic height of 2169
5 m above the base of LZa, and the total thickness of the LS along the reference stratigraphic section
6 is 2177 m (Tenger et al., 2009). Samples from the Upper Border Series (UBS) come from three
7 different profiles in the southeastern part of the intrusion reported by Salmonsens and Tegner (2013),
8 with one additional sample from Skaergaardsbugt (“Skaergaard’s Bay”). The subzones have
9 different thicknesses in the different profiles. We have therefore scaled the stratigraphic position of
10 the samples from each profile (originally measured as distance from the roof contact for each
11 profile) to the idealized profile in Fig. 7 of Salmonsens and Tegner (2013). Naslund (1984) reported
12 a total thickness of 960 for the UBS, which is very similar to the idealized UBS section from
13 Salmonsens and Tegner (2013), and which we take as a representative thickness for the UBS.
14 Therefore, the total thickness of the stratigraphic profile reported in this study is 3137 m (2177 m
15 LS plus 960 m UBS). Two samples (SK08-110 and SK11-58) come from the “Sandwich Horizon”,
16 the boundary between the LS and UBS, interpreted to represent the horizon along which the most
17 evolved magma crystalized. The exact positions of the bulk-rock samples from Stewart and
18 DePaolo (1990) and McBirney and Creaser (2003) relative to our reference profile are unknown.
19 However, McBirney and Creaser (2003) did document the zone and subzone from which each
20 sample came (their Table 1 includes the samples from Stewart and DePaolo, 1990). The samples in
21 Table 1 of McBirney and Creaser (2003) are ordered by zone and subzone, and we assume that the
22 samples within a particular subzone are in relative stratigraphic order. We then linearly scaled the
23 positions of each sample within a particular subzone to the thickness of the given subzone in our

24 reference profile. That is, the samples from a particular subzone are equally spaced throughout that
25 subzone, with the lowermost at the basal contact and the uppermost at the upper contact.

26

27 **METHODS**

28 Approximately 1-cm-thick rock billets were cut, mounted in epoxy or Lexan, and polished.
29 Chemical composition maps with 20–30 μm pixel resolution were generated with a Bruker M4
30 Tornado micro-XRF equipped with two EDS detectors. Strontium isotopes in plagioclase were
31 measured by LA-MC-ICP-MS at the Aarhus Geochemistry and Isotope Research (AGiR) platform
32 during four separate sessions over a nine-month period. Ablations were done in a two-volume
33 Laurin Technic cell with a Resonetics 193 excimer using a 154- μm -diameter beam, 80 mJ energy at
34 the source, and 12 Hz repetition rate over a 45 s ablation period following a 35–40 s on-peak
35 baseline. Ablated material was transported by a He + Ar mixture to a Nu Plasma II MC-ICP-MS.
36 Ion beams with mass/charge ratios of 82–89, as well as the “half-masses” 83.5–87.5, were
37 measured in static mode on Faraday cups with 10^{11} Ω resistors over 0.5 s integration periods.

38 The data were reduced with Iolite v. 3.32 (Paton et al., 2011) using the following customized
39 routine: 1) Kr and other gas blank interferences were subtracted using on-peak baselines. 2) A
40 preliminary Sr mass bias factor (β_{pre}) was calculated using the baseline-subtracted mass/charge 88
41 and 86 signals and a reference $^{88}\text{Sr}/^{86}\text{Sr} = 8.37520938$. 3) CaAr interferences were subtracted from
42 ^{88}Sr and ^{86}Sr by monitoring $^{82}\text{CaAr}$ and using β_{pre} . 4) A revised Sr mass bias factor (β_{Sr}) was
43 calculated using the interference-corrected ^{88}Sr and ^{86}Sr signals and a reference $^{88}\text{Sr}/^{86}\text{Sr} =$
44 8.37520938 . 5) CaAr interferences were again subtracted from the raw ^{88}Sr and ^{86}Sr signals, as well
45 as the ^{84}Sr signal, by monitoring $^{82}\text{CaAr}$ and using β_{Sr} . 6) ^{87}Rb was subtracted from ^{87}Sr by
46 monitoring ^{85}Rb and with a Rb mass bias factor calculated using a bracketing rock standard (BCR-2
47 glass in this study) to solve the following equation for the Rb mass bias factor (β_{Rb}):

48

$$^{87}\text{Sr}/^{86}\text{Sr}_{\text{ref}} = [^{87}(\text{Sr},\text{Rb}) - ^{85}\text{Rb} * (^{87}\text{Rb}/^{85}\text{Rb}_{\text{ref}}) * (\text{mass}^{87}\text{Rb}/\text{mass}^{85}\text{Rb})^{\beta\text{Rb}}] * (\text{mass}^{87}\text{Sr}/\text{mass}^{86}\text{Sr})^{\beta\text{Sr}} * (1/^{86}\text{Sr}_{\text{cor}})$$

51

52

where:

53

$^{87}\text{Sr}/^{86}\text{Sr}_{\text{ref}}$ is the Sr isotope ratio of the bracketing standard

54

$^{87}(\text{Sr},\text{Rb})$ is the signal on mass 87 with all other interferences subtracted

55

^{85}Rb is the raw signal on mass 85

56

$^{87}\text{Rb}/^{85}\text{Rb}$ is a canonical natural Rb isotope ratio

57

$^{86}\text{Sr}_{\text{cor}}$ is the interference-corrected ^{86}Sr signal

58

59

60 7) Final Sr isotope ratios (and $^{87}\text{Rb}/^{86}\text{Sr}$) were calculated using the interference-corrected Sr signals
61 and β_{Sr} .

62

63

64

65

66

67

68

69

70

71

Two in-house plagioclase standards were used for normalization and to assess data accuracy and precision. A gem-quality single-crystal bytownite was used to normalize the interference-corrected $^{87}\text{Sr}/^{86}\text{Sr}$ ratios. The magnitude of the normalization (i.e., the relative offset between the normalized and non-normalized values) was typically less than 100 ppm. A fused plagioclase standard, "T21", was used as a secondary standard to evaluate data accuracy and reproducibility across analytical sessions. It yielded an average $^{87}\text{Sr}/^{86}\text{Sr}$ value of 0.704691 ± 44 (2 SD; $n = 43$; 3 outliers rejected), in good agreement with the reference value of $^{87}\text{Sr}/^{86}\text{Sr}$ 0.704701 ± 16 (see section on in-house plagioclase standard calibration below). Initial (56 Ma) $^{87}\text{Sr}/^{86}\text{Sr}$ values were calculated using the normalized present-day $^{87}\text{Sr}/^{86}\text{Sr}$, normalized $^{87}\text{Rb}/^{86}\text{Sr}$ (using BCR-2 glass as an external standard to correct for Rb-Sr instrumental element fractionation), and $\lambda^{87}\text{Rb} =$

72 $1.3972 \times 10^{-11} \text{ yr}^{-1}$ (Villa et al., 2015). The magnitude of the age correction was small (typically <
73 0.00001 in $^{87}\text{Sr}/^{86}\text{Sr}$) due to the relatively young age and low Rb/Sr of the plagioclase. Six to
74 twenty-six individual analyses in individual samples typically yielded single populations in
75 $^{87}\text{Sr}/^{86}\text{Sr}$. Therefore, the data are presented as weighted means for each sample, with uncertainties
76 calculated as quadratic additions of the standard error of each population and the external
77 reproducibility of the T21 secondary standard.

78 Bulk-rock Sr data from the UBS, reported by Salmonsén (2013), were obtained by powdering,
79 digestion, Sr isolation, and isotopic measurements by MC-ICP-MS at the University of California,
80 Davis. Previously unpublished bulk-rock Sr data from the 90-22 drill core (Fig. DR1, Table DR1)
81 were measured on a VG 54-30 TIMS at the Geological Institute, University of Copenhagen.

82

83 **Calibration of In-House Plagioclase Standards for LA-MC-ICPMS Measurements**

84 The Sr isotope standards used in this study are: 1) a gem-quality single-crystal bytownite acquired
85 from the American Museum of Natural History (“AMNH-107160”), and 2) a plagioclase grain from
86 Samoa (“T21”) fused in a furnace at $1500 \text{ }^\circ\text{C}$ for 48 hours at Arizona State University (Mathew
87 Jackson and Mark Edwards, personal communication, 2018; Edwards et al., in review). To
88 determine Sr isotope composition and evaluate isotopic homogeneity, we performed digestion, Sr
89 purification by standard ion chromatography protocols, and Sr isotope analysis by solution MC-
90 ICPMS (Nu Plasma II at Aarhus University) on nine fragments of AMNH-107160 and four
91 fragments of T21. The AMNH-107160 plagioclase yielded $^{87}\text{Sr}/^{86}\text{Sr} = 0.704371 \pm 24$ (2 SD). The
92 T21 plagioclase yielded $^{87}\text{Sr}/^{86}\text{Sr} = 0.704701 \pm 16$ (2 SD), including quadruplicate analysis of one
93 of the fractions. The latter is in agreement with a TIMS value of 0.704720 ± 9 (Mathew Jackson
94 and Mark Edwards, personal communication, 2018; Edwards et al., in review; renormalized to
95 $^{87}\text{Sr}/^{86}\text{Sr} = 0.710248$ for NIST SRM 987). The $^{87}\text{Sr}/^{86}\text{Sr}$ are relative to $^{87}\text{Sr}/^{86}\text{Sr} = 0.710248$ for

96 NIST SRM 987. At least three different fragments of AMNH-107160 were used for normalization
97 in the LA-MC-ICP-MS measurements, yielding a single $^{87}\text{Sr}/^{86}\text{Sr}$ population with ~62 ppm 2 RSD
98 for the secondary T21 standard, adding further confidence in AMNH-107160 as a robust primary
99 standard.

100

101 **MIXING AND FRACTIONATION-ASSIMILATION MODELS**

102 Fractional crystallization-assimilation (“FCA”; Cribb and Barton, 1996) models were used to
103 evaluate the magnitude of country rock assimilation by the Skaergaard magma. The FCA models
104 were used instead of the widely used AFC equations (DePaolo, 1981) because the latter were
105 derived for a constant ratio of the rate of assimilation to fractional crystallization (r), which
106 demonstrably varied in the Skaergaard intrusion. The FCA equations allow r to be changed in
107 incremental steps of F (fraction of remaining magma) in the models. However, when using a
108 constant r , the results of both FCA and AFC models converge for small steps of F and the very
109 small r values required by our data. The $^{87}\text{Sr}/^{86}\text{Sr}$ and Sr concentration of the initial magma were set
110 to 0.70392 and 264.1 ppm, respectively, the composition of an uncontaminated diabase sample
111 from Vandfaldsdalen macrodyke, related in space and time to the Skaergaard intrusion (Bichert-
112 Toft et al., 1992). This assumes that the least radiogenic plagioclase from this study ($^{87}\text{Sr}/^{86}\text{Sr}_i \approx$
113 0.7041) crystallized from a magma that had already experienced some degree of contamination. For
114 the LS, this is consistent with fact that the stratigraphic position and anorthite contents of
115 plagioclase from the lowermost exposed rocks correspond to $F = 0.76$ (i.e., after 24% of the magma
116 had crystallized; Tegner et al., 2009). If the parental magma had $^{87}\text{Sr}/^{86}\text{Sr} = 0.70392$, it might be
117 expected that plagioclase in the Hidden Zone and in LZa’ in the UBS would record lower $^{87}\text{Sr}/^{86}\text{Sr}_i$
118 than 0.7041. However, several samples from LZa’ contain plagioclase with the most radiogenic Sr
119 observed in this study, which we attribute to local contamination during the assimilation of gneiss

120 xenoliths. The most anorthite-rich sample from this study ($\sim\text{An}_{70}$), in-fact, also has the most
121 radiogenic Sr. Two samples with $^{87}\text{Sr}/^{86}\text{Sr}_i \approx 0.7041$ in LZa' have plagioclase with $\sim\text{An}_{65}$,
122 suggesting that they crystallized from magma that had already undergone some degree of
123 differentiation and contamination. It is also noteworthy that the least radiogenic samples reported
124 by McBirney and Creaser (2003) have $^{87}\text{Sr}/^{86}\text{Sr}_i \approx 0.70394$, very similar to the parental end-member
125 in the models, although these samples come from a stratigraphic position in LZa where the
126 plagioclase records $^{87}\text{Sr}/^{86}\text{Sr}_i \geq 0.7041$. There is an extreme range of published $^{87}\text{Sr}/^{86}\text{Sr}$ from
127 ~ 0.70967 to 0.84810 (calculated at 56 Ma) for basement rocks in the vicinity of the Skaergaard
128 intrusion (Stewart and DePaolo, 1990; Blichert-Toft et al., 1992; Kays et al., 1989). Clearly, the
129 choice of the assimilant end-member in the models will have a large effect on the calculated degree
130 of contamination. The least radiogenic felsic gneiss from Kays et al. (1989) ($^{87}\text{Sr}/^{86}\text{Sr}_{55\text{Ma}} \approx$
131 0.70967 ; ~ 224 ppm Sr) and the most most radiogenic granophyre derived from partial melting of
132 basement gneiss from Blichert-Toft et al. (1992) ($^{87}\text{Sr}/^{86}\text{Sr}_{56\text{Ma}} \approx 0.78854$; ~ 180 ppm Sr) were used
133 in the models to represent a reasonable range of assimilant end-member compositions. Bulk Sr
134 partition coefficients (D_{Sr}) for each step in the model were calculated for mineral assemblages that
135 vary with F according to the Skaergaard liquid line of descent model from Thy et al. (2006) and
136 mineral partition coefficients from the Geochemical Earth Reference Model ("GERM";
137 earthref.org). The curvature of the array of Sr data in Figures 1 and 3 of the main text is consistent a
138 decreasing value of r with progressive crystallization, with r approaching 0 at $F \approx 0.34$ (at the base
139 of LZc and LZc') where the $^{87}\text{Sr}/^{86}\text{Sr}_i$ become uniform. The r values in the models were decreased
140 linearly as a function of F from an initial value (r_0 , at the first step in the models) to 0 at $F = 0.34$.
141 The r_0 was adjusted for each end-member to generate a visual "best-fit" model curve.

142

143

144 **Appendix references**

145

146 Blichert-Toft, J., Leshner, C. E., and Rosing, M. T., 1992, Selectively contaminated magmas of the
147 Tertiary East Greenland macrodike complex: *Contributions to Mineralogy and Petrology*, v. 110,
148 p. 154–172.

149

150 Cribb, J. W., and Barton, M., 1996, Geochemical effects of decoupled fractional crystallization and
151 crustal assimilation: *Lithos*, v. 37, p. 293–307.

152

153 DePaulo, D. J., 1981, Trace element and isotopic effects of combined wallrock assimilation and
154 fractional crystallization: *Earth and planetary science letters*, v. 53, p. 189–202.

155

156 Edwards, M.A., Jackson, M.G., Kylander-Clark, A.R.C., Harvey, J., Hagen-Peter, G.A., Seward,
157 G.G.E., Till, C.B., Adams, J.V., Cottle, J.M., Hacker, B.R., and Spera, F.J., in revision, Extreme
158 enriched and heterogeneous $^{87}\text{Sr}/^{86}\text{Sr}$ ratios recorded in magmatic plagioclase from the Samoan
159 hotspot: *Earth and Planetary Science Letters*.

160

161 Kays, M. A., Goles, G. G., and Grover, T. W., 1989, Precambrian sequence bordering the
162 Skaergaard Intrusion: *Journal of Petrology*, v. 30, p. 321–361.

163

164 McBirney, A. R., and Creaser, R. A., 2003, The Skaergaard layered series, part VII: Sr and Nd
165 isotopes: *Journal of Petrology*, v. 44, p. 757–771.

166

167 Naslund, H. R., 1984, Petrology of the Upper Border Series of the Skaergaard intrusion: Journal of
168 Petrology, v. 25, p. 185–212.
169

170 Paton, C., Hellstrom, J., Paul, B., Woodhead, J., and Hergt, J., 2011, Iolite: Freeware for the
171 visualisation and processing of mass spectrometric data: Journal of Analytical Atomic
172 Spectrometry, v. 26, p. 2508–2518.
173

174 Salmonsens, L. P., 2013, Petrology of the Upper Border Series of the Skaergaard Intrusion [Ph.D.
175 thesis]: Aarhus University, Denmark, 97 p.
176

177 Salmonsens, L. P., and Tegner, C., 2013, Crystallization sequence of the Upper Border Series of the
178 Skaergaard Intrusion: revised subdivision and implications for chamber-scale magma
179 homogeneity: Contributions to Mineralogy and Petrology, v. 165, p. 1155–1171.
180

181 Stewart, B. W., and DePaolo, D. J., 1990, Isotopic studies of processes in mafic magma chambers:
182 II. The Skaergaard Intrusion, East Greenland: Contributions to Mineralogy and Petrology, v.
183 104, p. 125–141.
184

185 Tegner, C., Thy, P., Holness, M. B., Jakobsen, J. K., and Leshner, C. E., 2009, Differentiation and
186 compaction in the Skaergaard intrusion: Journal of Petrology, v. 50, p. 813–840.
187

188 Thy, P., Leshner, C. E., Nielsen, T. F. D., and Brooks, C. K., 2006, Experimental constraints on the
189 Skaergaard liquid line of descent: Lithos, v. 92, p. 154–180.
190

191 Villa, I. M., De Bièvre, P., Holden, N. E., and Renne, P. R., 2015, IUPAC-IUGS recommendation
192 on the half life of ^{87}Rb : *Geochimica et Cosmochimica Acta*, v. 164, p. 382–385.

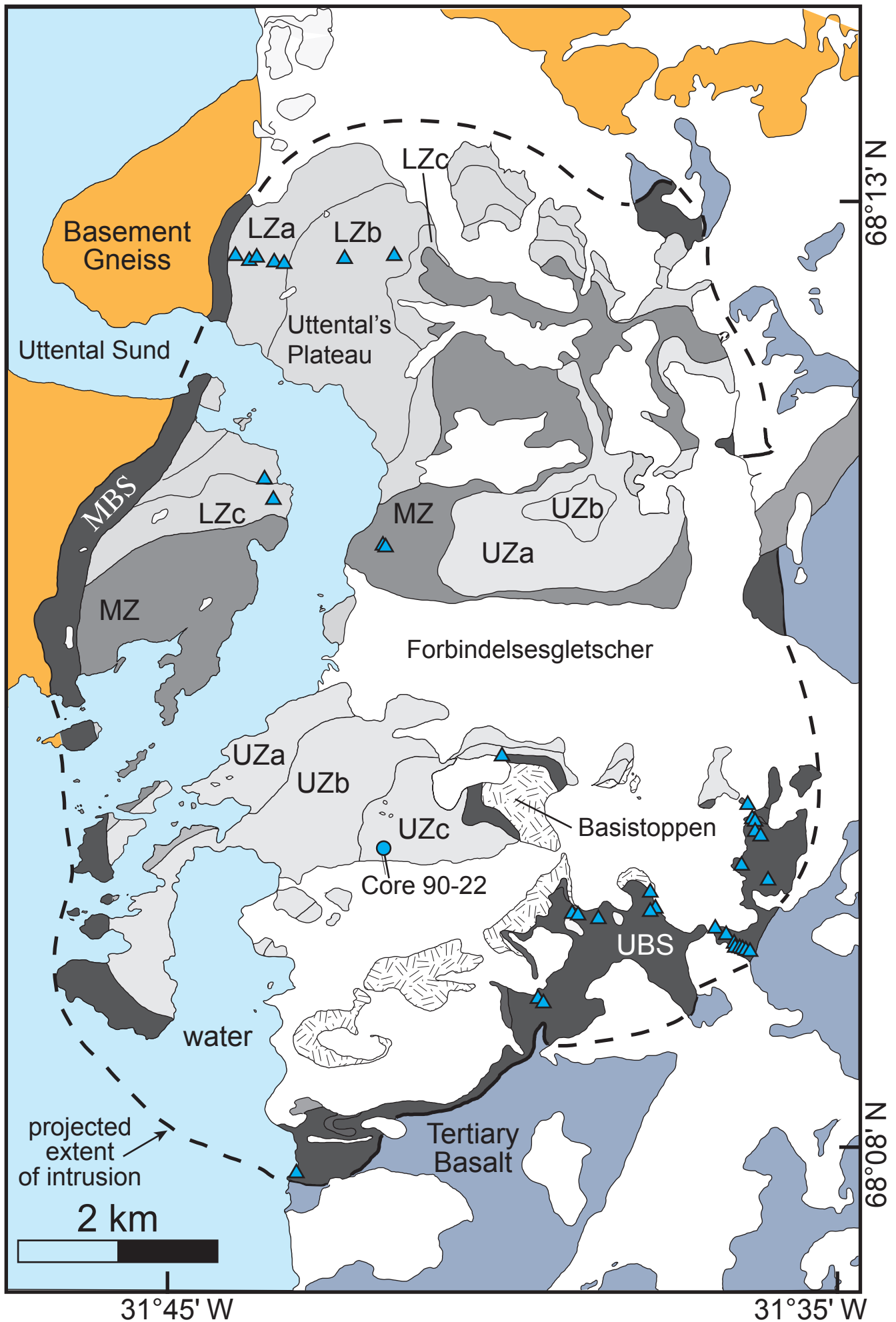
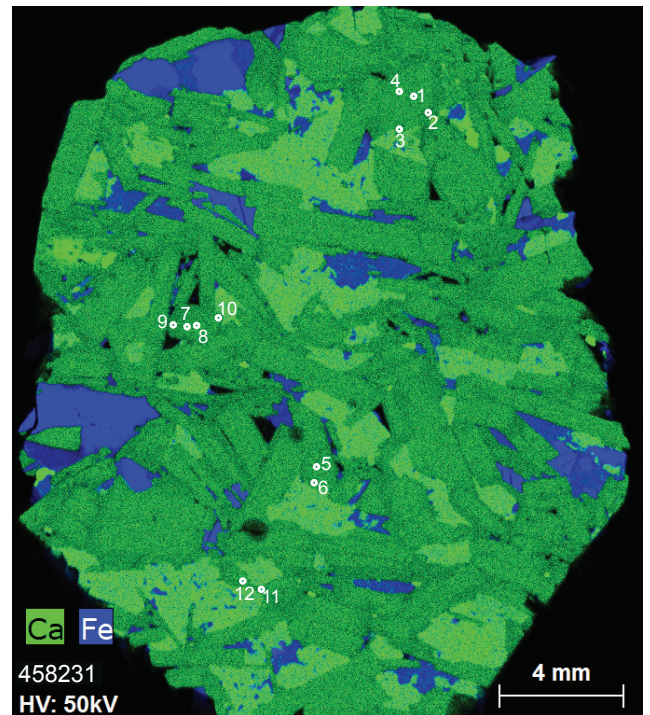
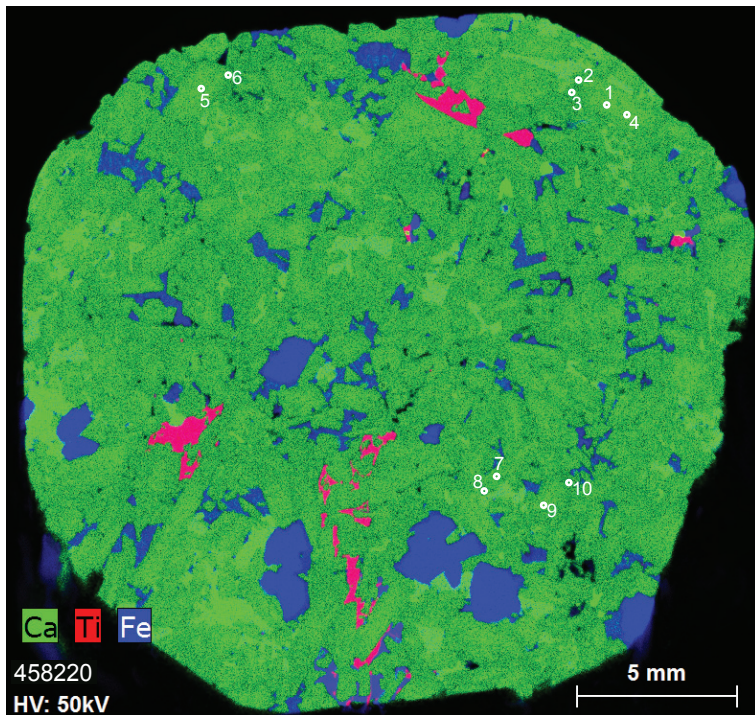
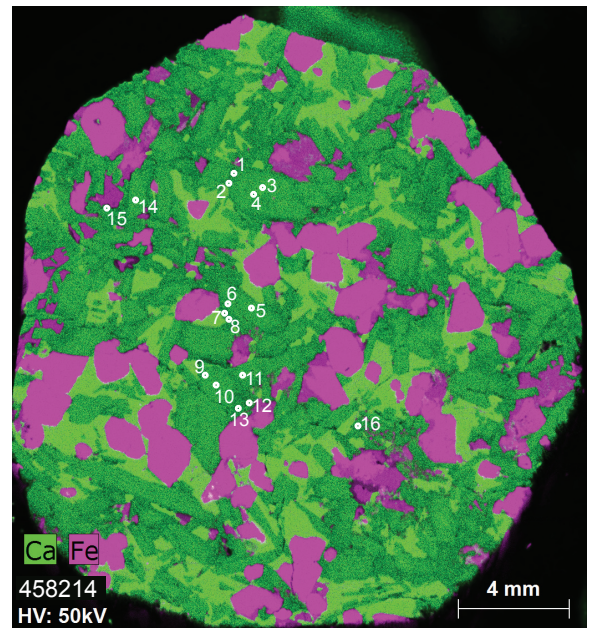
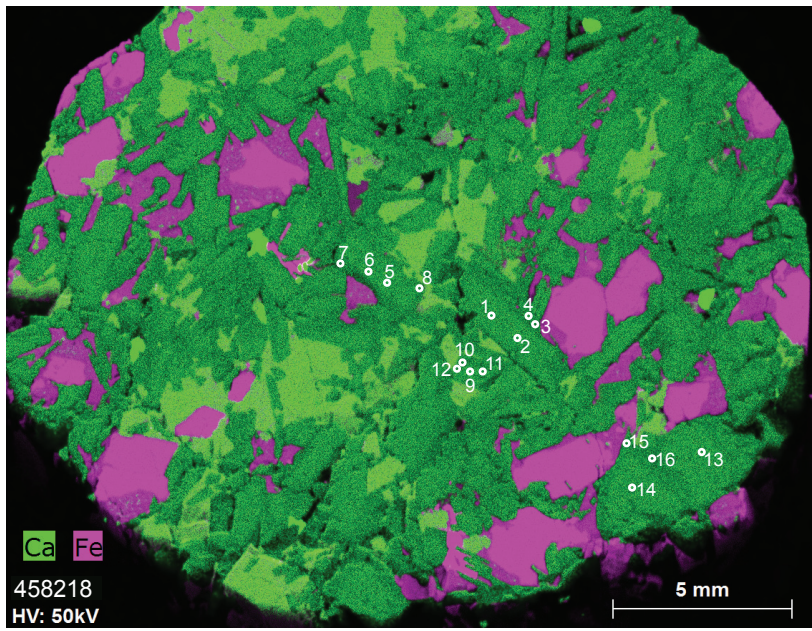
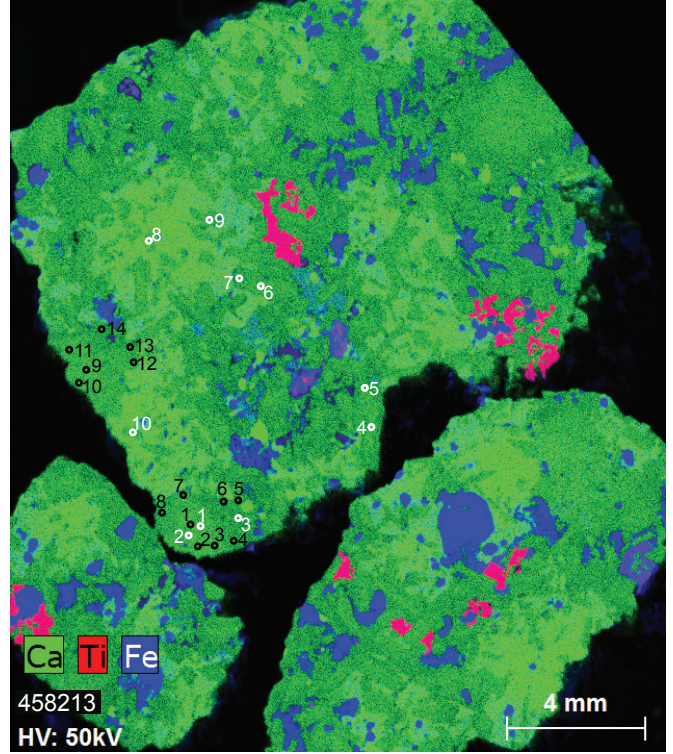
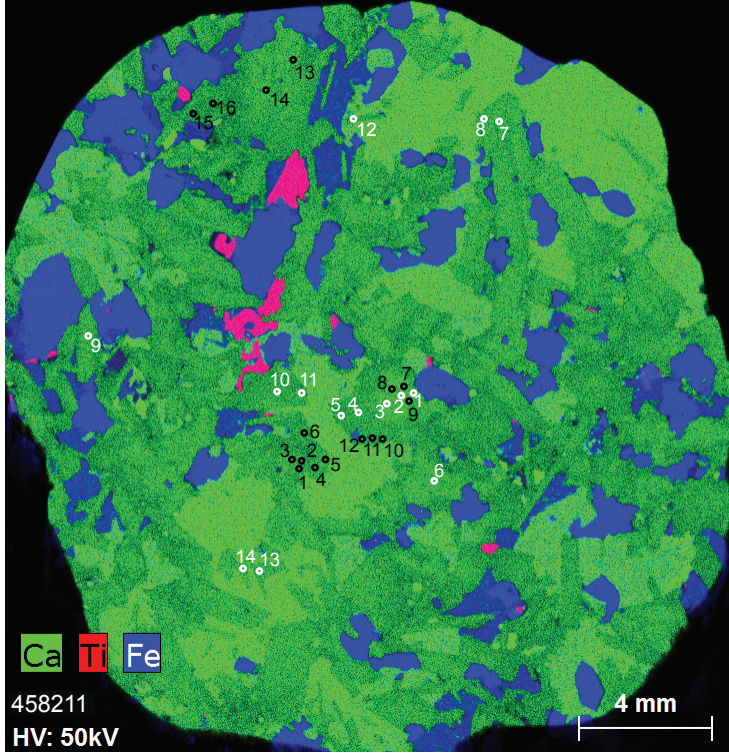
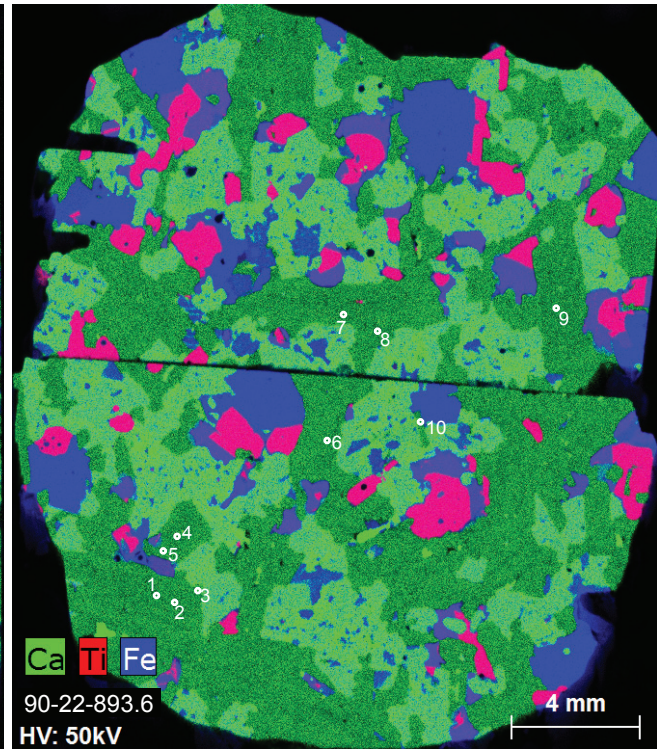
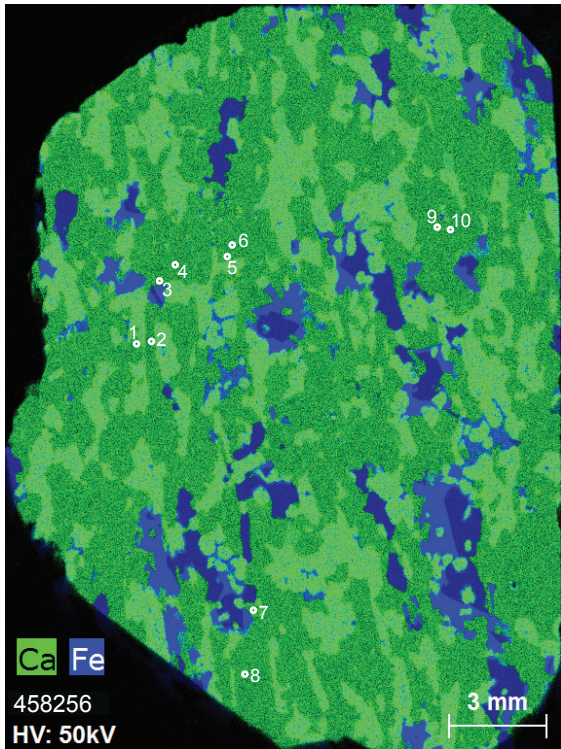
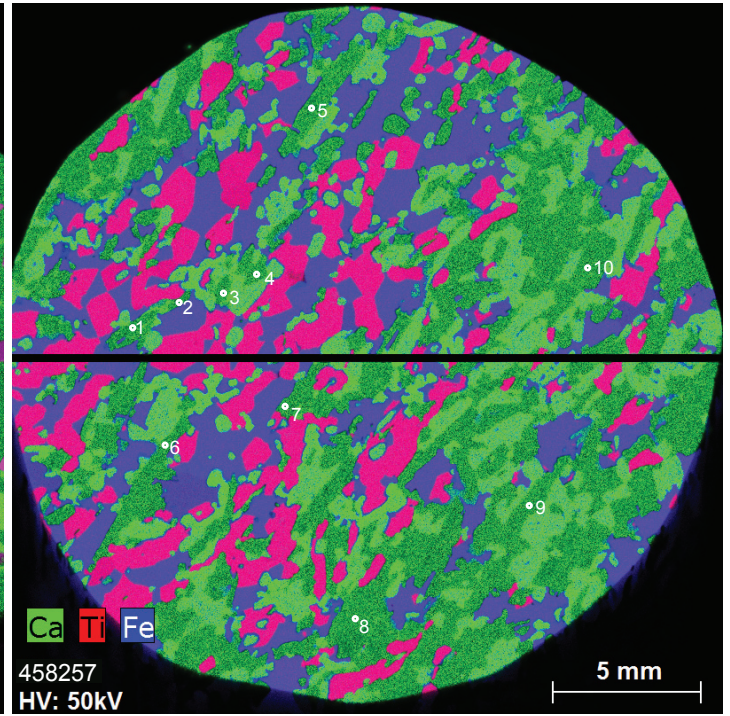
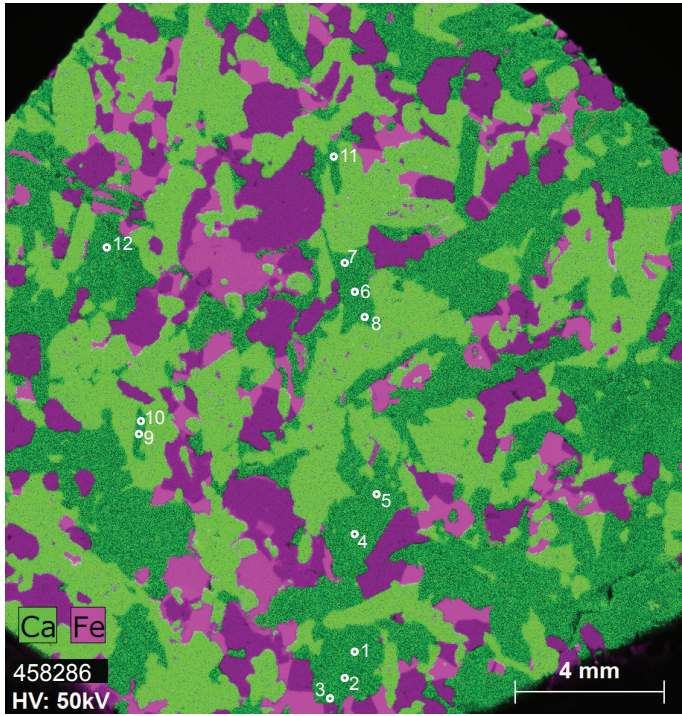
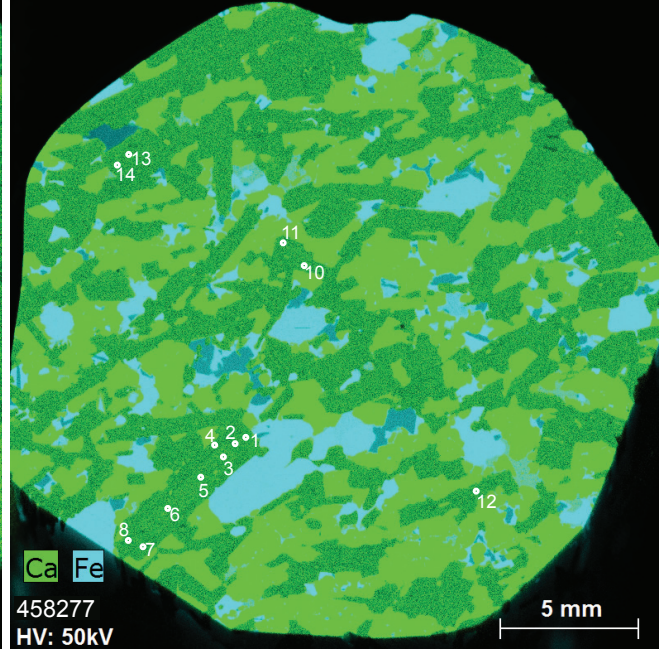
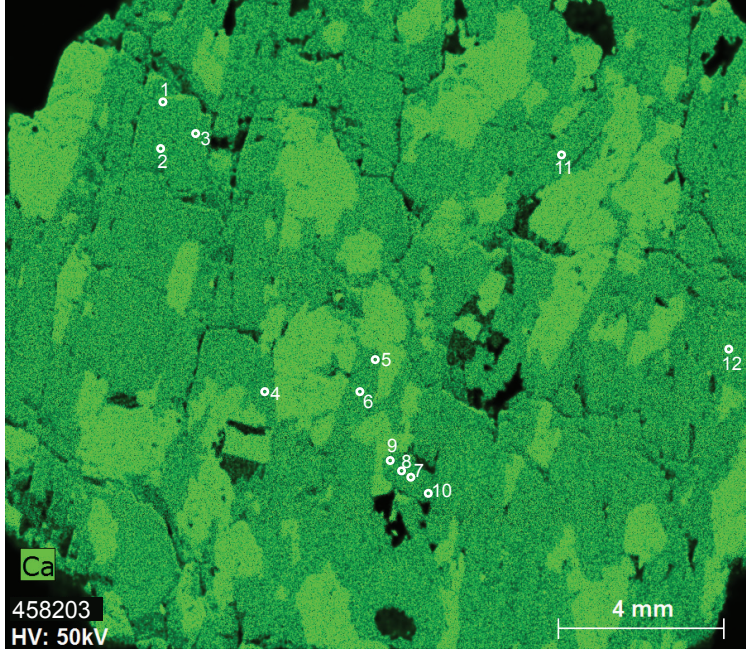
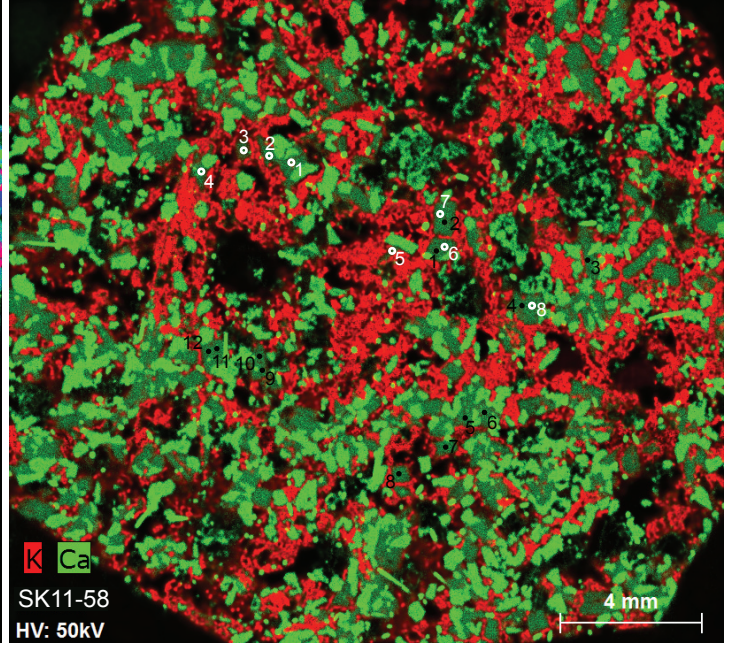
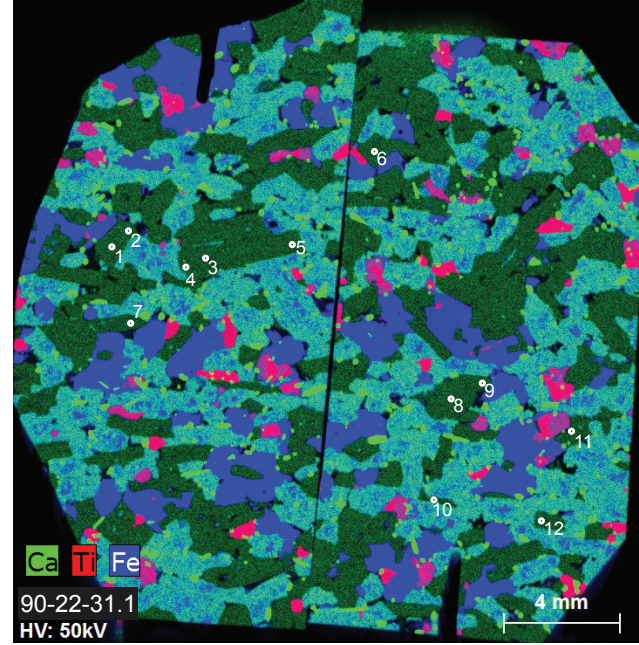
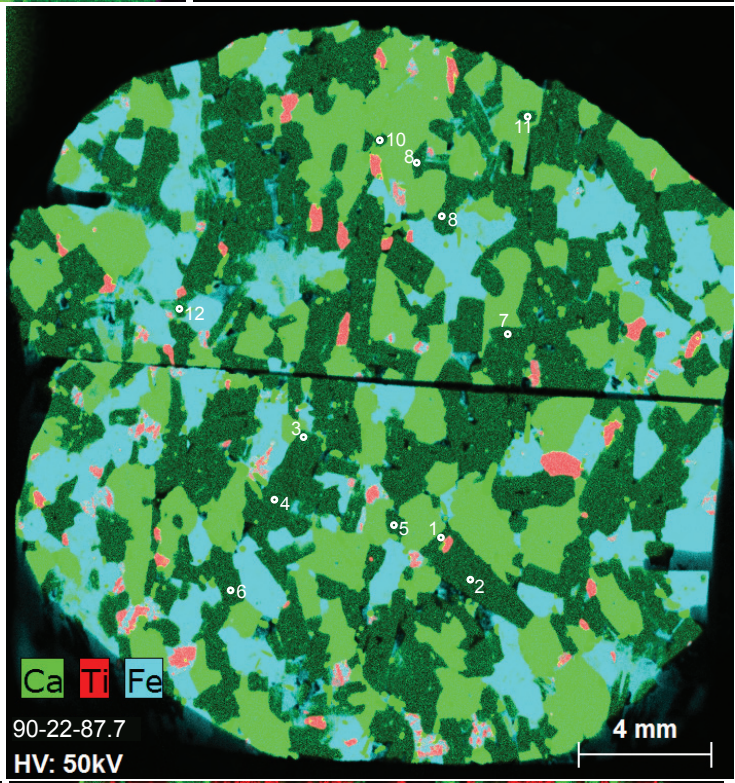
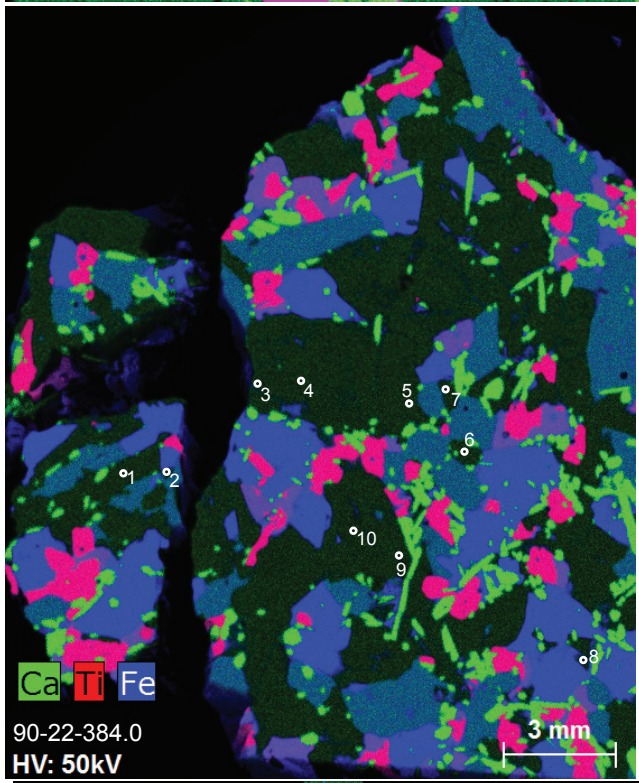
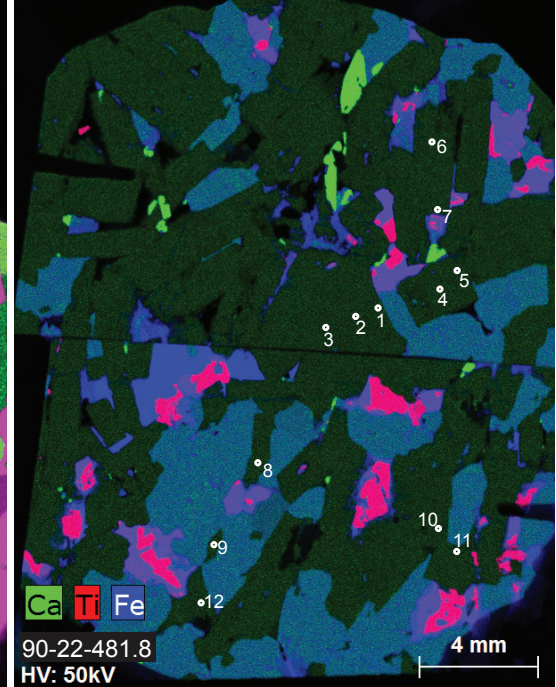
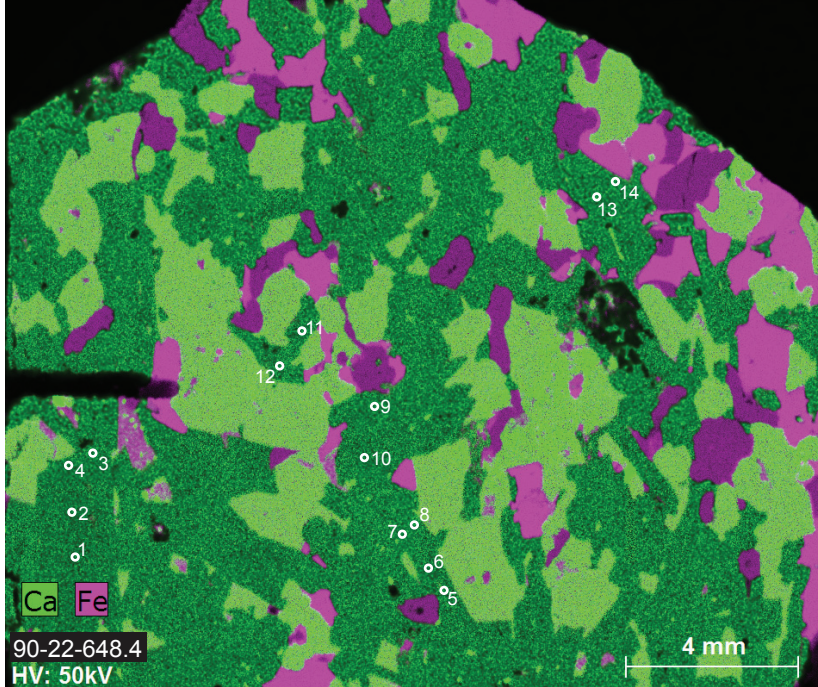
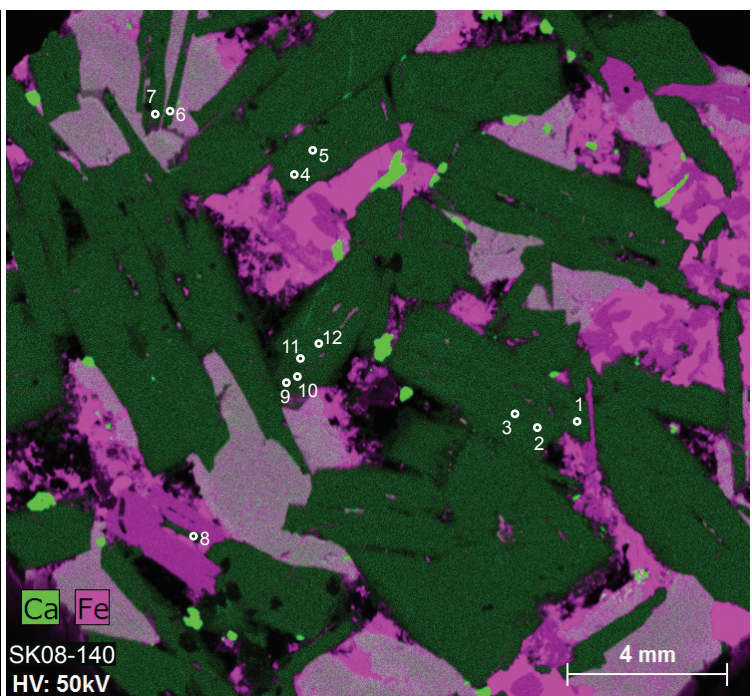
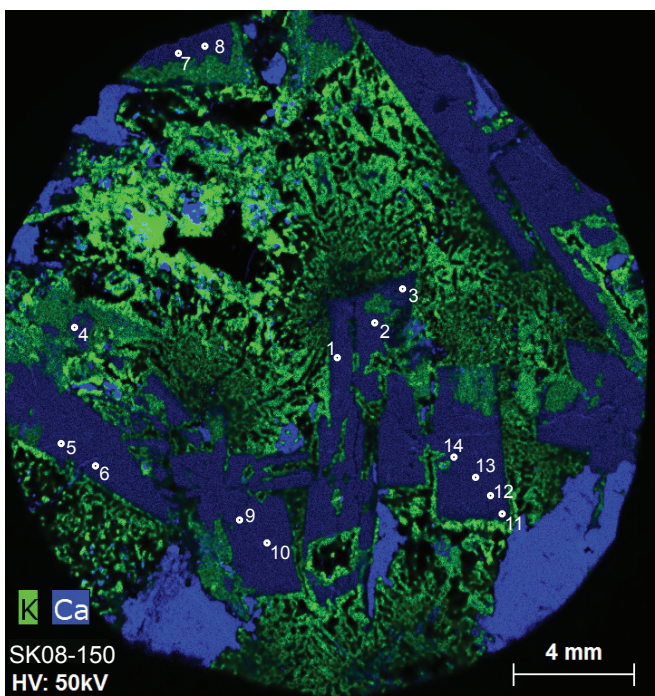
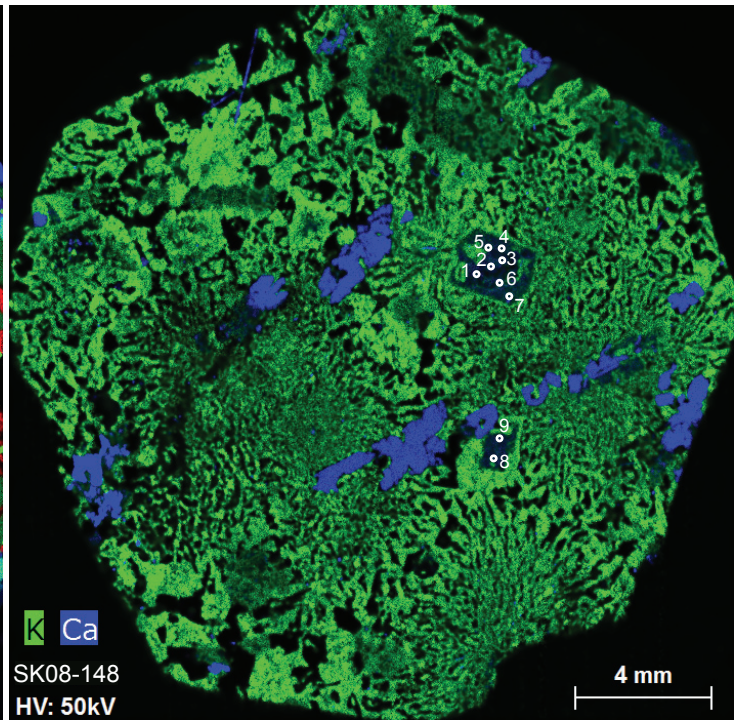
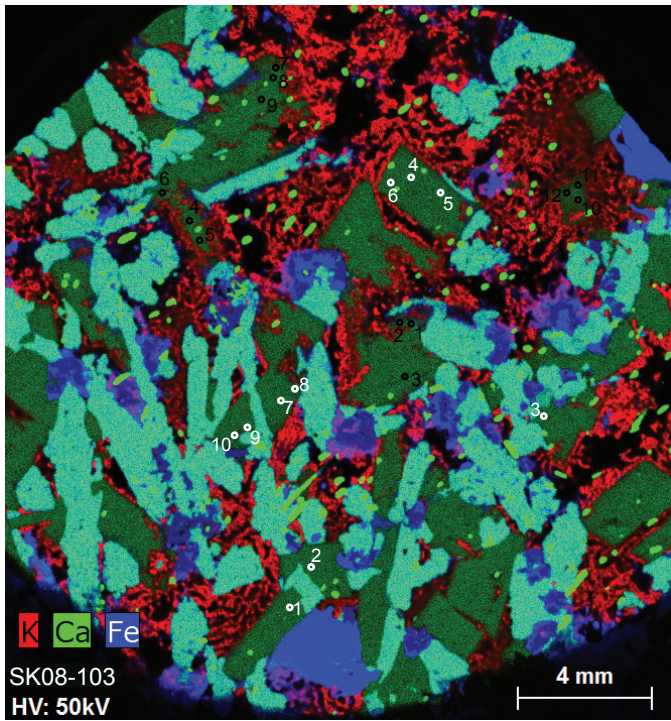
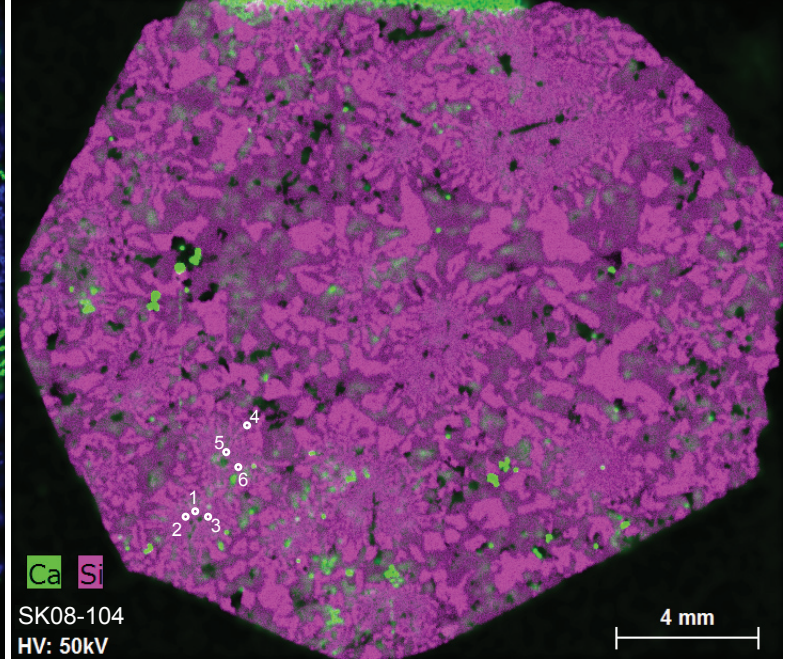
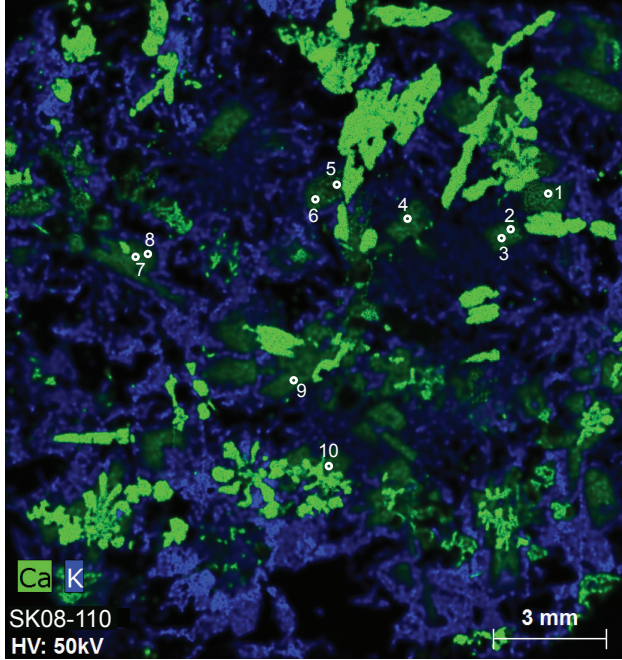


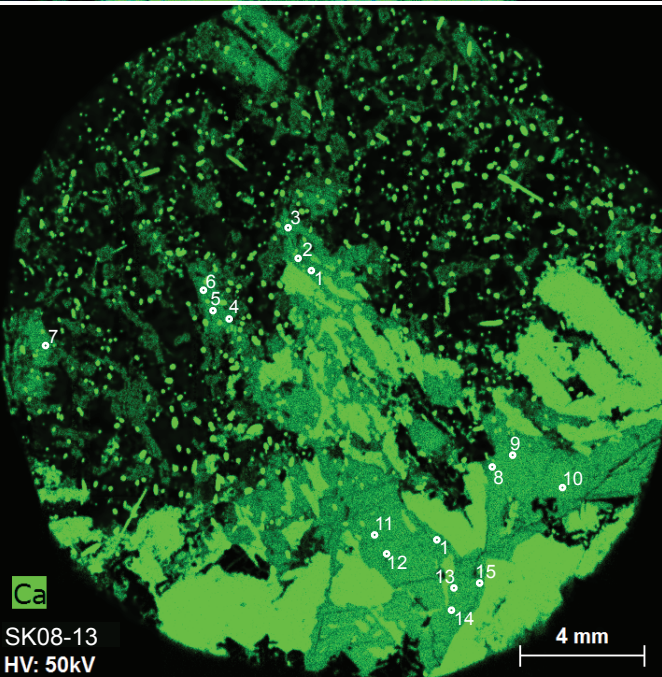
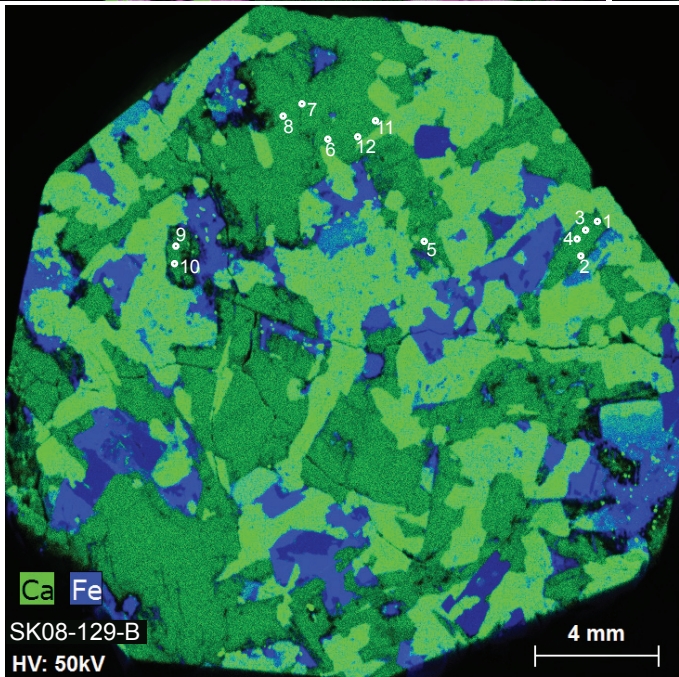
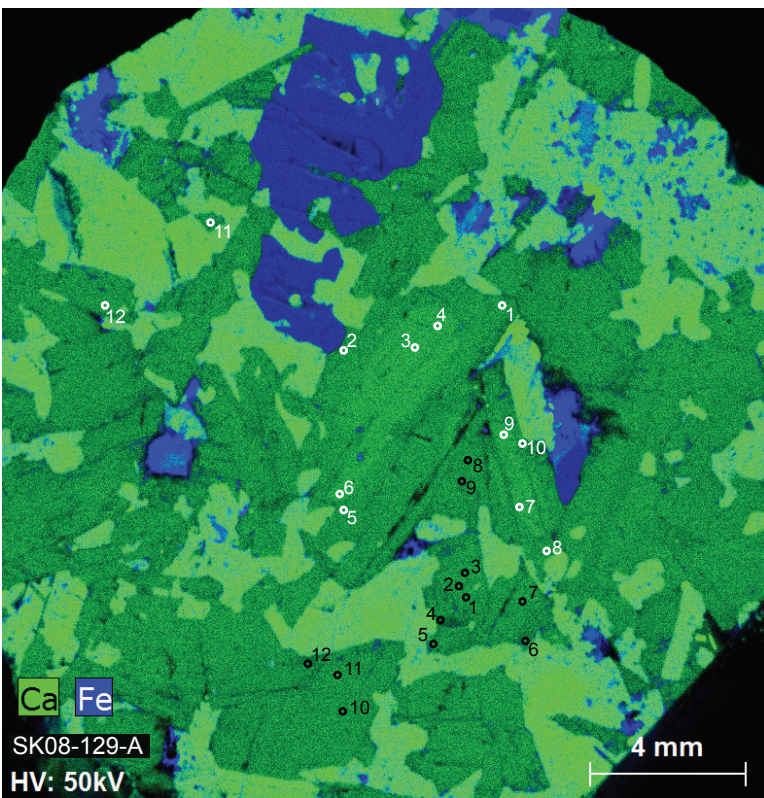
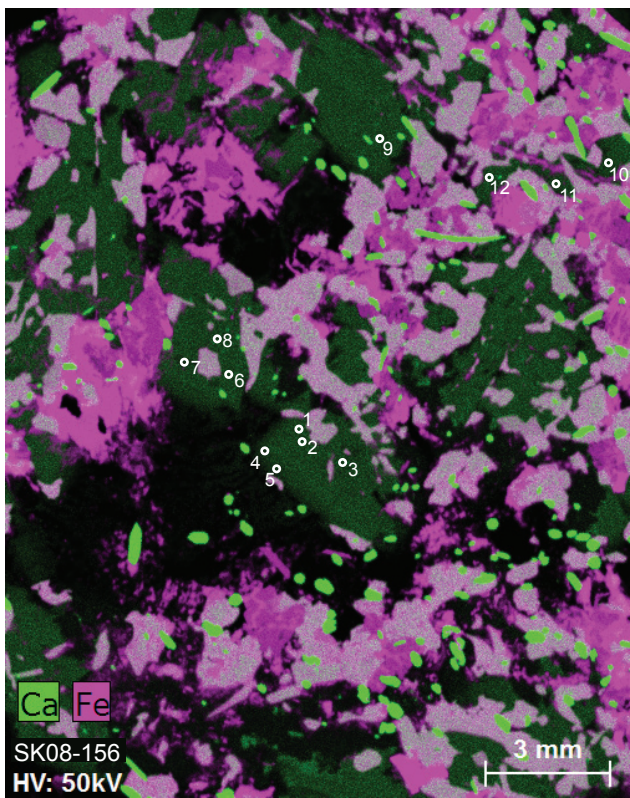
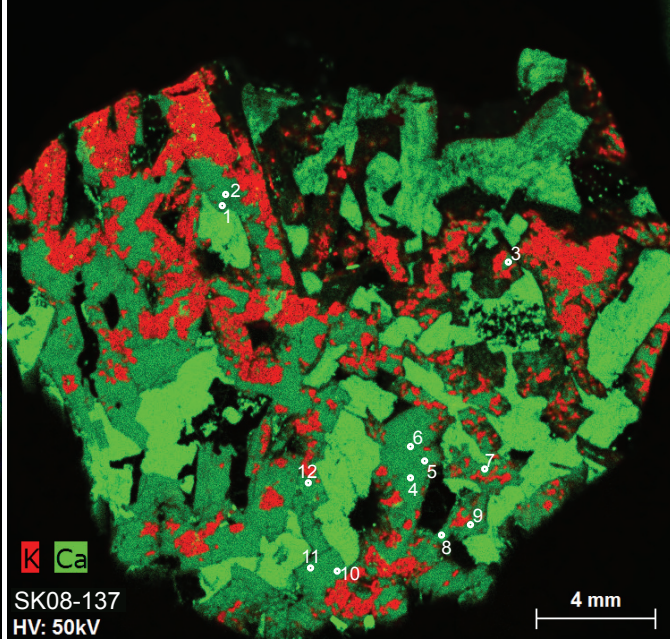
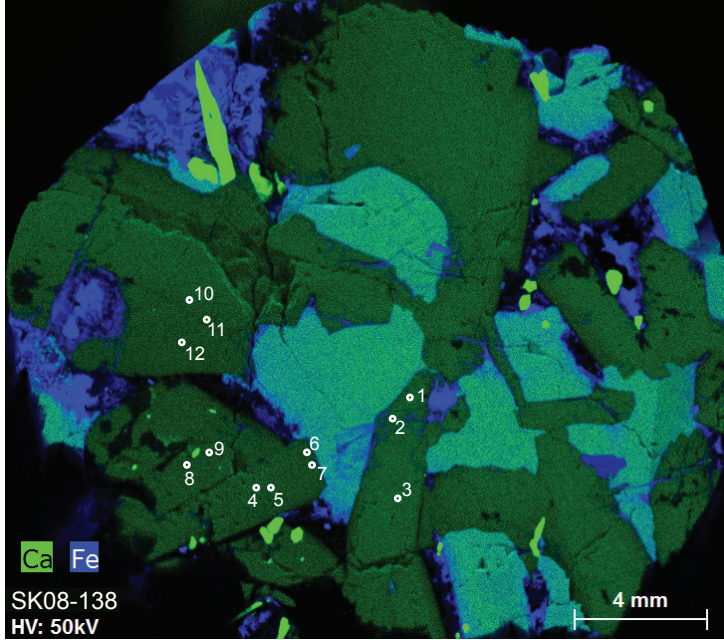
Figure DR1: Geologic map of the Skaergaard intrusion (modified from Tegner et al., 2009) showing locations of samples from this study. Six samples were taken from core 90-22.

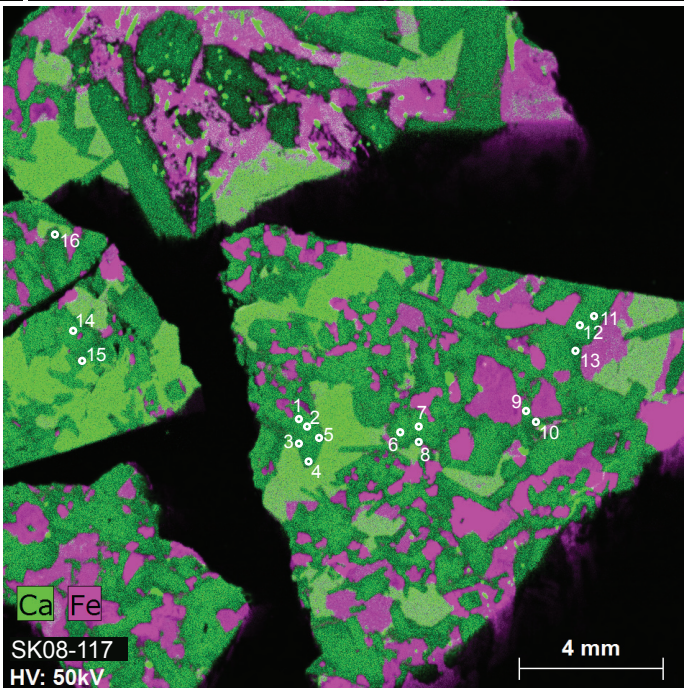
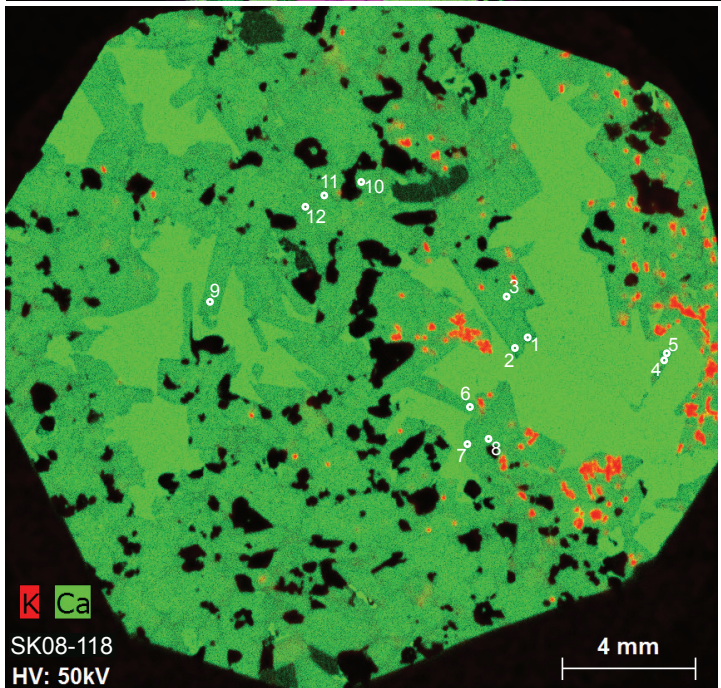
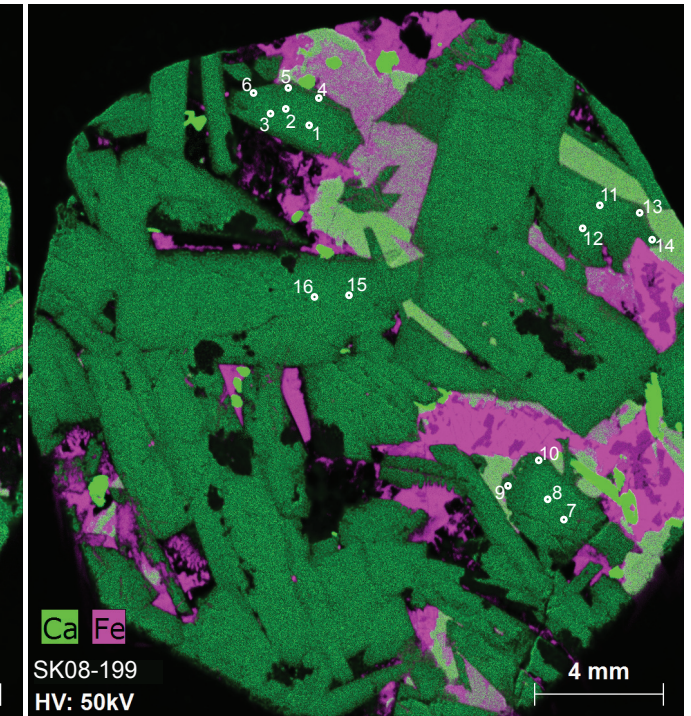
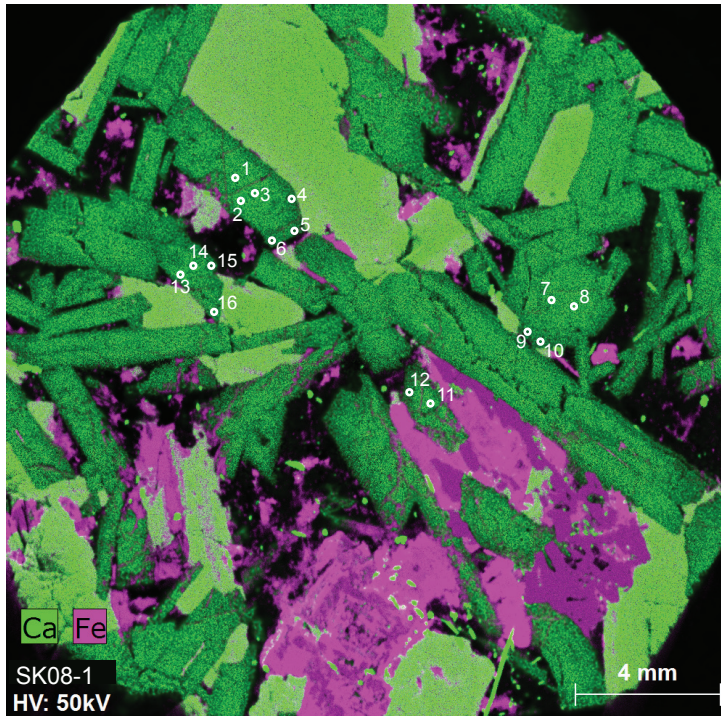
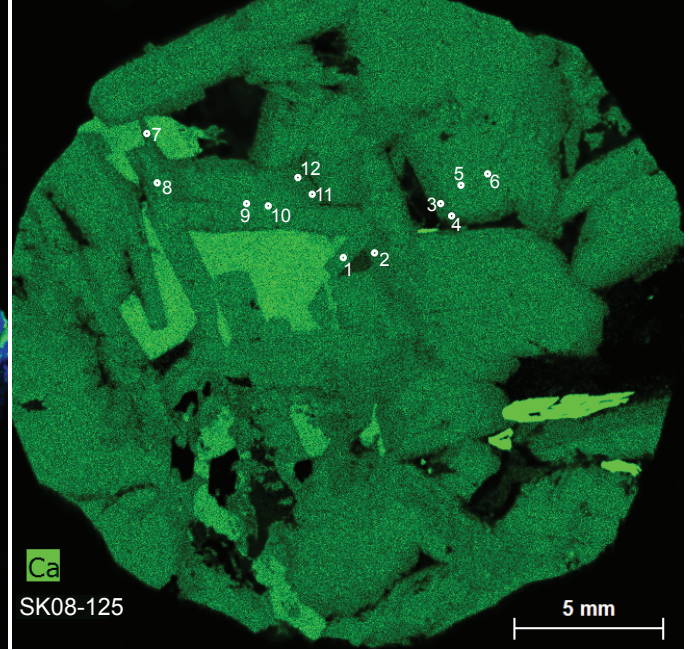
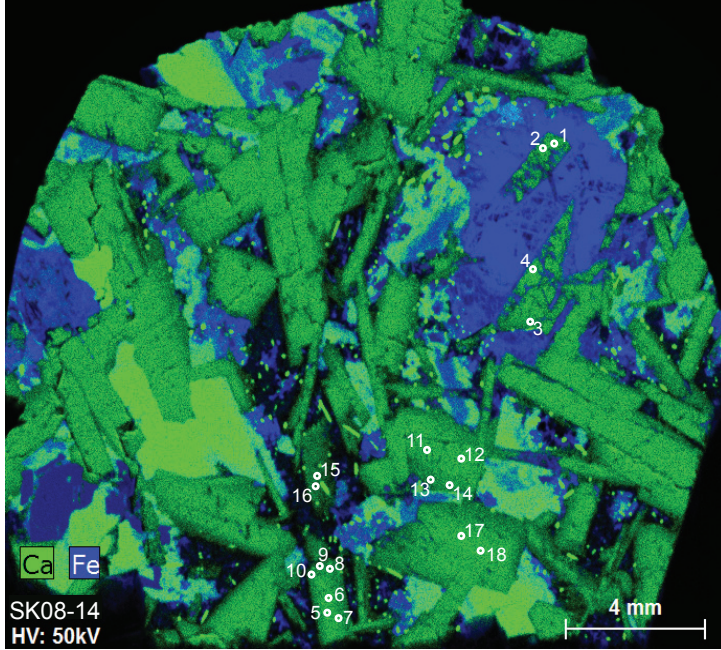


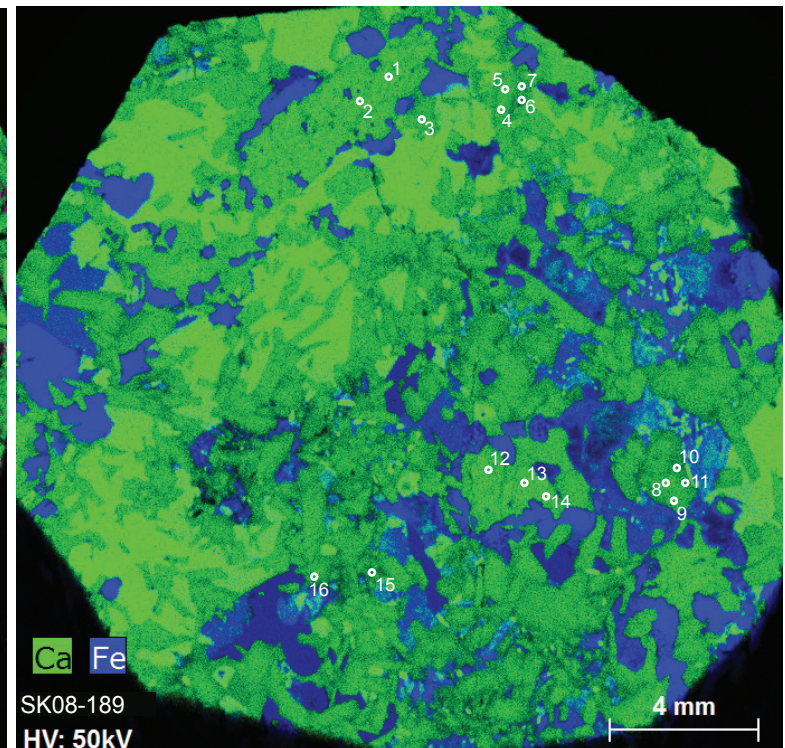
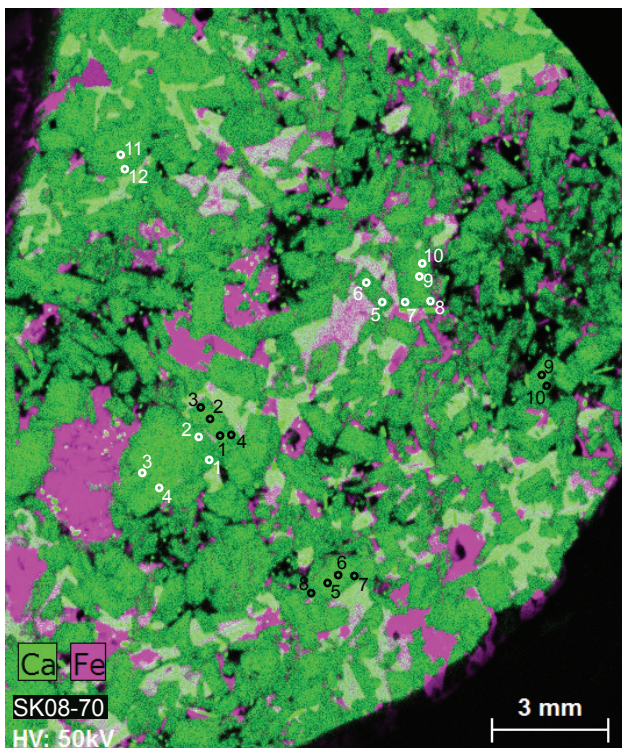
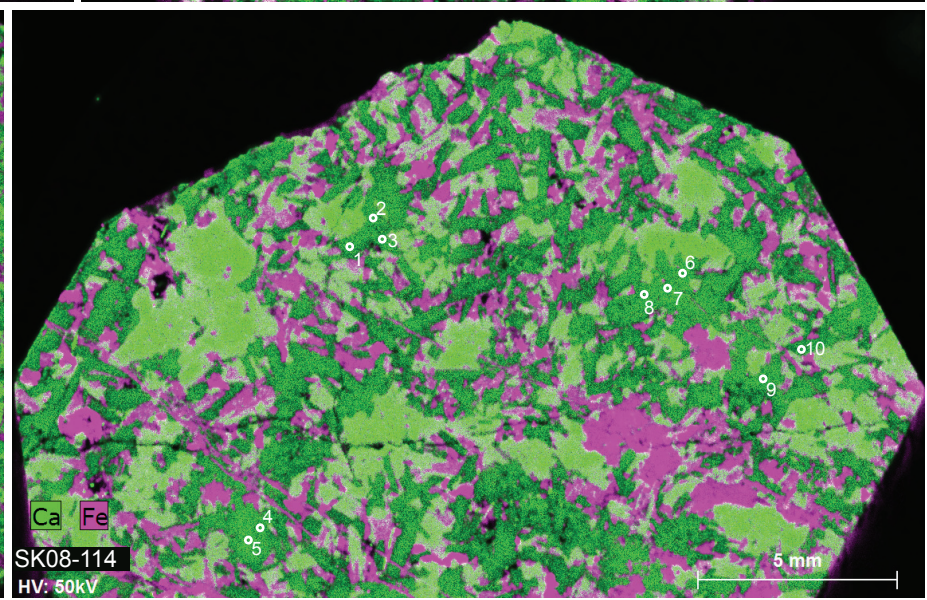
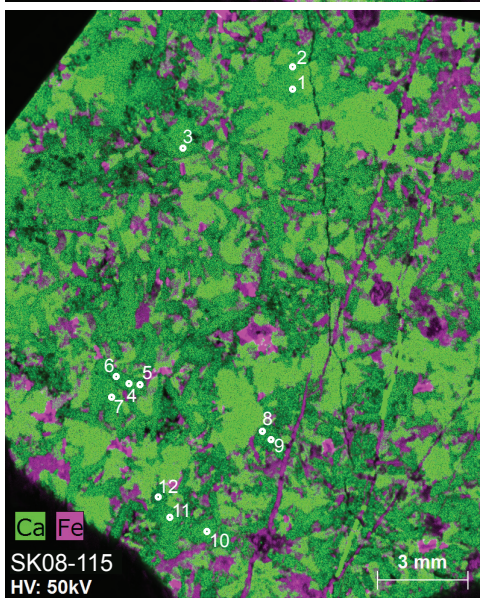
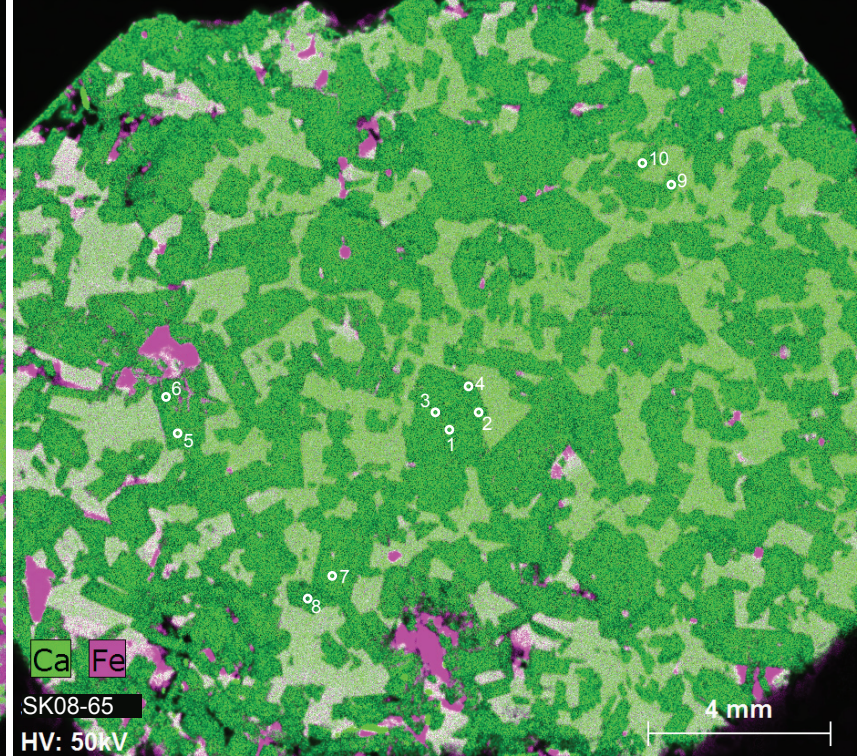
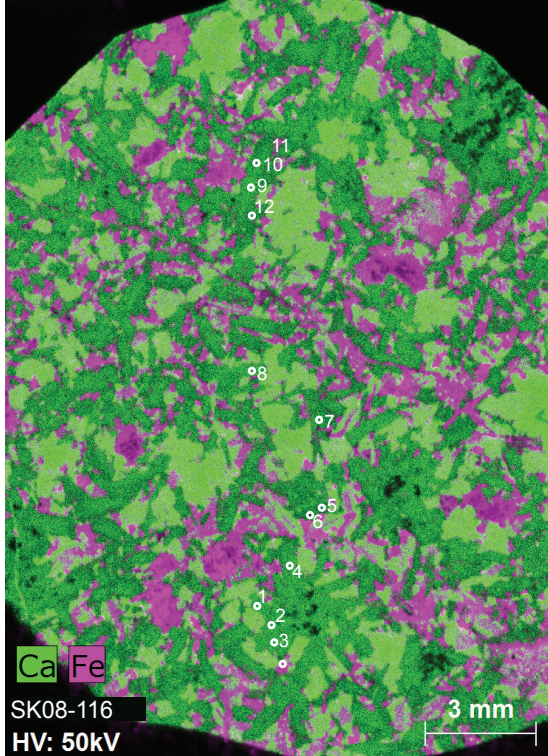












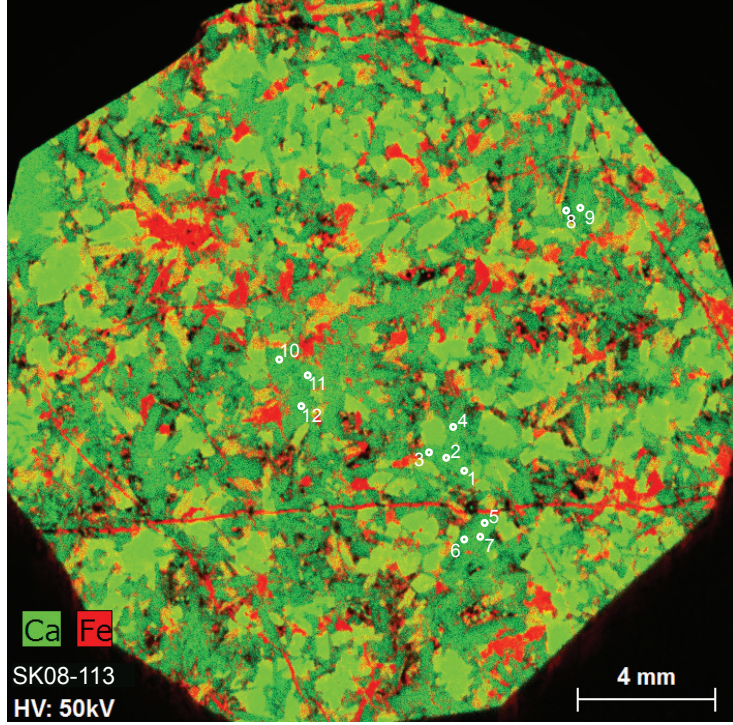


Figure DR2: Micro-XRF maps showing the locations of laser spot analyses of all samples from this study. Numbers next to the spot locations correspond to the analysis numbers in Table DR2. For samples measured in multiple sessions, white spots and numbers indicate analyses from the earlier session and black spots and numbers indicate analyses from the later session.

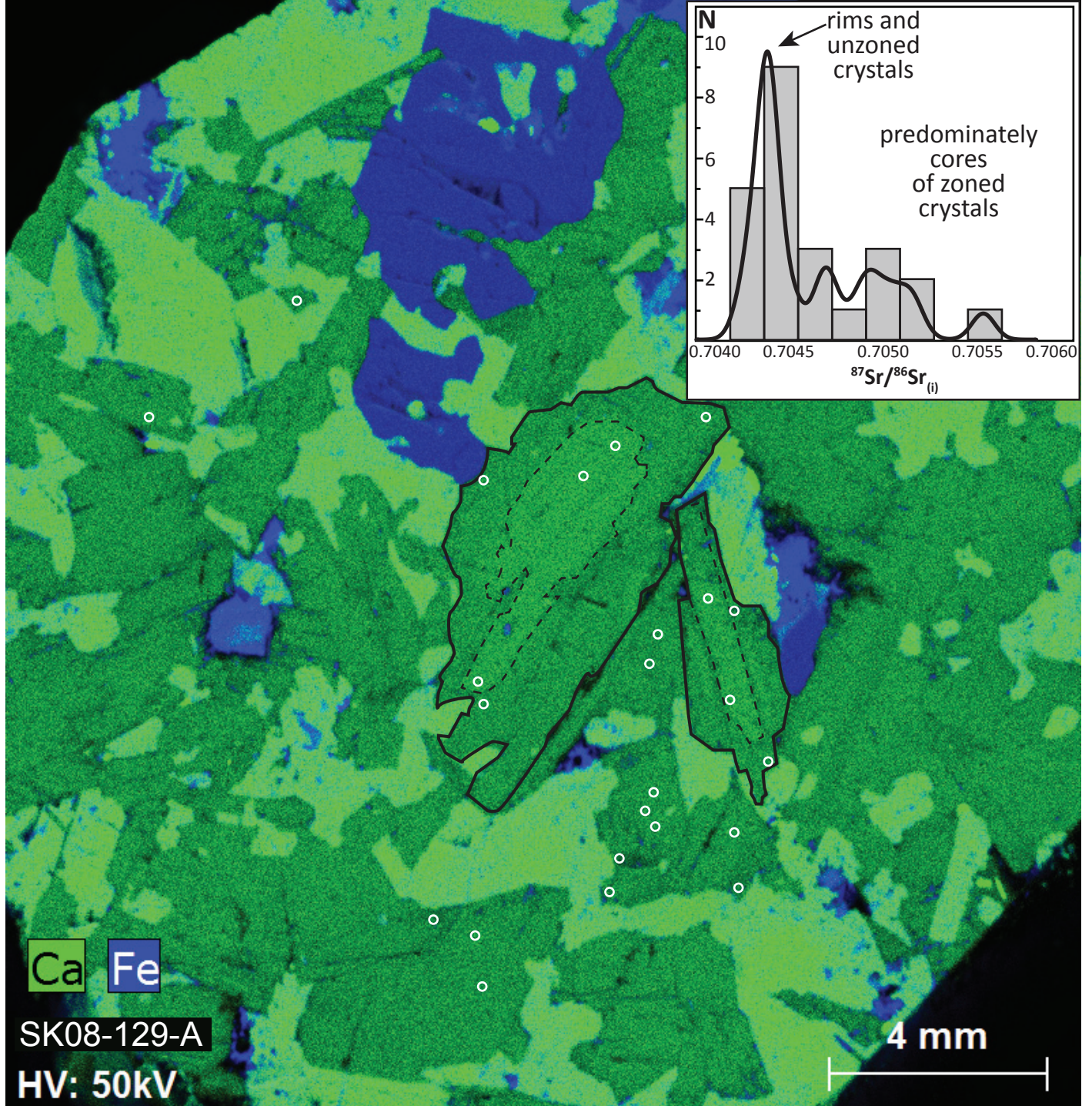


Figure DR3: Micro-XRF map of sample SK08-129 (billet A) showing the locations of laser spot analyses. The inset histogram and probability distribution function of the $^{87}\text{Sr}/^{86}\text{Sr}_i$ show a strong mode at ~ 0.7044 along with significantly more radiogenic compositions, particularly in the cores of two large crystals (dashed outlines) with slightly higher Ca contents.

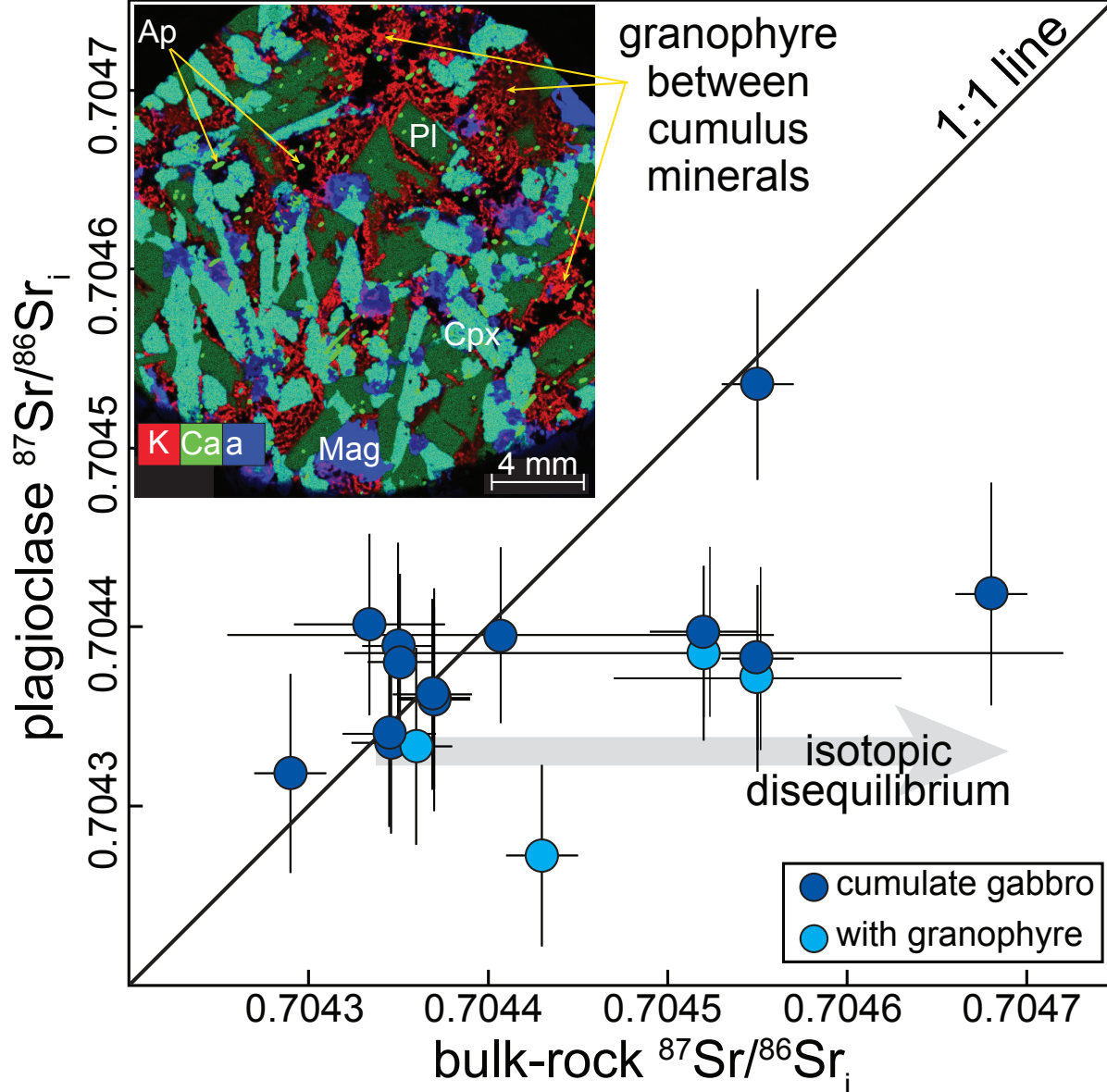


Figure DR4. Weighted-average $^{87}\text{Sr}/^{86}\text{Sr}_i$ in plagioclase versus corresponding bulk-rock $^{87}\text{Sr}/^{86}\text{Sr}_i$ for gabbro, some with abundant interstitial granophyre. Most of the samples plot along the 1:1, as would be expected if plagioclase and all other phases in the rock had the same $^{87}\text{Sr}/^{86}\text{Sr}_i$. Systematic discrepancies between the *in situ* and bulk-rock methods would result in all the samples systematically offset from the 1:1 line. Several samples plot off the 1:1 line to more radiogenic bulk-rock values, revealing some component of the samples with higher $^{87}\text{Sr}/^{86}\text{Sr}_i$ than the constituent plagioclase. The inset micro-XRF map shows one of the samples that plots off the 1:1 line with abundant granophyre (intergrown quartz and K-feldspar with Apatite - "Ap") in between euhedral to subhedral primocrysts of plagioclase (Pl), clinopyroxene (Cpx), and oxide minerals (Mag = magnetite). The late-stage granophyre may carry Sr with higher $^{87}\text{Sr}/^{86}\text{Sr}_i$ that is in isotopic disequilibrium with the primocrysts minerals. It is also possible that clinopyroxene or apatite (brightest green) carry the more radiogenic Sr. Regardless of the explanation for these particular samples, a bulk analysis of a rock composed of phases with variable Sr isotope compositions would yield a mixed $^{87}\text{Sr}/^{86}\text{Sr}_i$ of a heterogeneous system.

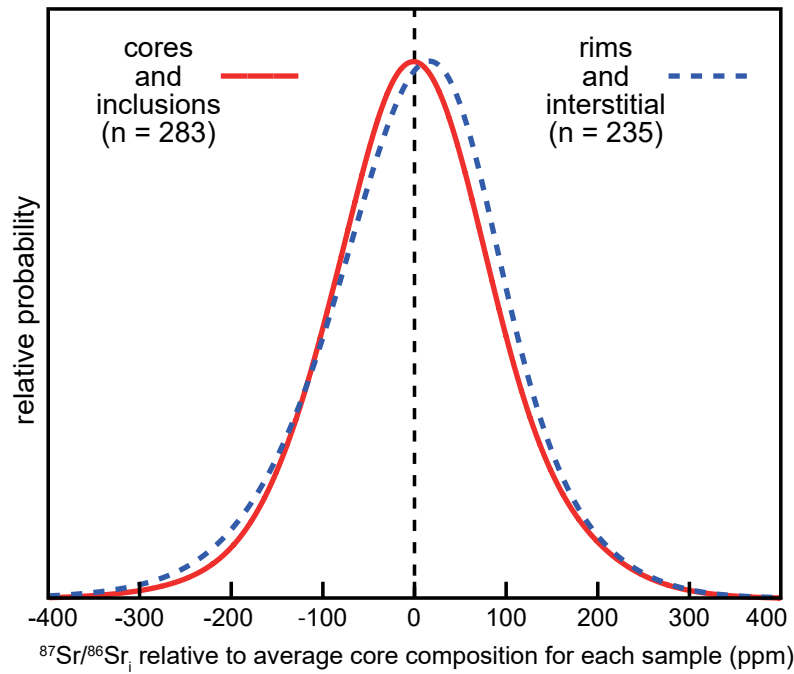


Figure DR5. Relative probability distribution functions of $^{87}\text{Sr}/^{86}\text{Sr}_i$ of core, rim, inclusion, and interstitial plagioclase analyses relative to the average core composition for each sample, enabling comparison of the core and rim compositions among all samples. As expected, the self-relative core analyses form a normal distribution centered around 0. The mode of rim and interstitial plagioclase distribution is offset to slightly higher $^{87}\text{Sr}/^{86}\text{Sr}_i$ (<25 ppm). However, the rims and interstitial plagioclase are not significantly more radiogenic than the cores (i.e., the vast majority of the areas under the probability distributions overlap). The distributions are calculated only for the analyses included in the weighted-average for each samples, and which could be confidently classified as a core, rim, etc. (Table DR2). Plagioclase inclusions in other primocryst minerals were included with core analyses.

TABLE DR1. SUMMARY OF PLAGIOCLASE AND BULK-ROCK RESULTS

Sample	Zone	Profile	Stratigraphic height (m)	Rock type	Plagioclase An%	Plagioclase $^{87}\text{Sr}/^{86}\text{Sr}_i$	Uncertainty*	n	MSWD	Bulk rock $^{87}\text{Sr}/^{86}\text{Sr}_i$ †	Uncertainty
<u>Upper Border Series</u>											
SK08-113	LZa'	Hammerpas	3135	chilled margin	65.05	0.704183	0.000058	12	0.6	N.D.	N.D.
SK08-189	LZa'	Skaergaardsbugt	3134	chilled margin	63.28	0.704493	0.000053	15	1.0	N.D.	N.D.
SK08-70	LZa'	Sydtoppen	3128	cumulate	69.52	0.704535	0.000053	21	1.1	0.704550	0.000020
SK08-114	LZa'	Hammerpas	3108	cumulate	62.51	0.704148	0.000051	7	0.6	N.D.	N.D.
SK08-115	LZa'	Hammerpas	3104	cumulate	63.63	0.704094	0.000054	11	2.3	N.D.	N.D.
SK08-65	LZa'	Sydtoppen	3104	cumulate	67.68	0.704434 §	0.000070	10	4.7	N.D.	N.D.
SK08-116	LZa'	Hammerpas	3054	cumulate	64.31	0.704092	0.000050	10	1.8	N.D.	N.D.
SK08-117	LZa'	Hammerpas	3017	cumulate	63.77	0.704333	0.000048	15	1.1	N.D.	N.D.
SK08-118	LZa'	Hammerpas	2984	cumulate	57.98	0.704418	0.000062	12	1.4	0.704680	0.000020
SK08-1	LZb'	Brødretoppen	2922	cumulate	58.55	0.704277	0.000046	16	0.7	N.D.	N.D.
SK08-125	LZb'	Hammerpas	2841	cumulate	50.26	0.704318	0.000056	12	0.3	0.704290	0.000020
SK08-14	LZb'	Brødretoppen	2803	cumulate	53.87	0.704268	0.000057	17	1.6	N.D.	N.D.
SK08-13	LZb'	Brødretoppen	2803	granophyre pod	N.D.	0.704272	0.000051	16	0.7	0.704430	0.000020
SK08-199	LZb'	Kilen	2793	cumulate	52.07	0.704310	0.000047	16	0.8	N.D.	N.D.
SK08-129	LZc'	Hammerpas	2706	cumulate	53.76	0.70436 #	0.000051	26	1.2	0.704370	0.000020
SK08-137	MZ'	Hammerpas	2613	cumulate	46.45	0.704358	0.000057	12	1.2	N.D.	N.D.
SK08-138	MZ'	Hammerpas	2613	granophyre pod	N.D.	0.704333	0.000055	13	1.3	0.704360	0.000020
SK08-140	UZa'	Hammerpas	2535	cumulate	43.61	0.704359	0.000062	12	1.2	0.704370	0.000020
SK08-156	UZb'	Kilen	2460	cumulate	31.47	0.704389	0.000057	11	1.3	0.704350	0.000020
SK08-150	UZb'/UZc'	Kilen	2334	granophyre pod	N.D.	0.704385	0.000049	13	1.1	0.704520	0.000200
SK08-148	UZb'/UZc'	Kilen	2290	granophyre pod	N.D.	0.704371	0.000052	8	0.8	0.704550	0.000080
SK08-103	UZc'	Kilen	2273	cumulate	31.62	0.704397	0.000048	21	1.1	0.704520	0.000030
<u>Sandwich Horizon</u>											
SK08-110	SH	Kilen	2177	granophyre pod	21.47	0.704396	0.000046	8	1.1	N.D.	N.D.
SK11-58	SH	N.D.	2177	granophyre pod	N.D.	0.704388	0.000051	19	0.8	0.704550	0.000020
<u>Layered Series</u>											

90-22-31.1	UZc	LS Reference Profile	2061	cumulate	N.D.	0.704380	0.000049	12	0.9	0.704351	0.000018
90-22-87.7	UZb	LS Reference Profile	2004	cumulate	35.10	0.704395	0.000049	12	0.9	0.704407	0.000152
90-22-384.0	UZb	LS Reference Profile	1708	cumulate	38.30	0.704362	0.000053	10	0.8	0.704369	0.000022
90-22-481.8	UZa	LS Reference Profile	1610	cumulate	39.20	0.704401	0.000051	12	1.0	0.704334	0.000042
90-22-648.4	UZa	LS Reference Profile	1443	cumulate	42.3	0.704335	0.000051	13	1.6	0.704346	0.000022
90-22-893.6	UZa	LS Reference Profile	1198	cumulate	N.D.	0.704340	0.000052	10	0.6	0.704345	0.000026
458256	MZ	LS Reference Profile	1003	cumulate	48.10	0.704399	0.000069	9	2.8	N.D.	N.D.
458257	MZ	LS Reference Profile	1003	cumulate	47.40	0.704376	0.000054	10	1.2	N.D.	N.D.
458286	LZc	LS Reference Profile	847	cumulate	50.2	0.704381	0.000052	11	1.4	N.D.	N.D.
458277	LZb	LS Reference Profile	703	cumulate	51.00	0.704366	0.000050	13	0.5	N.D.	N.D.
458203	LZb	LS Reference Profile	558	cumulate	56.3	0.704295	0.000052	12	1.4	N.D.	N.D.
458231	LZb	LS Reference Profile	367	cumulate	55.80	0.704319	0.000050	12	0.3	N.D.	N.D.
458220	LZa	LS Reference Profile	173	cumulate	60.70	0.704259	0.000052	10	0.5	N.D.	N.D.
458218	LZa	LS Reference Profile	159	cumulate	57	0.704207	0.000048	16	0.8	N.D.	N.D.
458214	LZa	LS Reference Profile	107	cumulate	61.5	0.704180	0.000047	15	1.1	N.D.	N.D.
458213	LZa	LS Reference Profile	84	cumulate	61.10	0.704106	0.000051	22	1.2	N.D.	N.D.
458211	LZa	LS Reference Profile	7	cumulate	60.40	0.704192	0.000048	30	1.4	N.D.	N.D.

* Plagioclase $^{87}\text{Sr}/^{86}\text{Sr}_i$ are weighted means of multiple analyses with uncertainties estimated from the 2 SE of the sample population and the 2 SD reproducibility of the T21 secondary standard added in quadrature.

† Bulk-rock Sr data from the Upper Border Series are from Salmonsén (2013, unpublished PhD thesis from Aarhus University). Bulk-rock Sr from the Layered Series are previously unpublished data.

§ Sample SK08-65 shows excess scatter (high MSWD) in $^{87}\text{Sr}/^{86}\text{Sr}_i$ with a roughly unimodal distribution ranging 0.70432 to 0.70457. However, the weighted average is plotted in the Figures in the text.

Sample SK08-129 shows a polymodal distribution in $^{87}\text{Sr}/^{86}\text{Sr}_i$, with radiogenic values up to ~0.70551 in the cores of grains (Fig. DR3). The average of a less radiogenic mode is used here.

TABLE DR2. DATA FOR INDIVIDUAL LA-MC-ICP-MS Sr ANALYSES

Sample	analysis #	position*	session date	Sr signal (V)	approximate Sr (ppm) [†]	βSr	⁸⁴ Sr/ ⁸⁸ Sr	internal 2SE	⁸⁴ Sr/ ⁸⁶ Sr	internal 2SE	⁸⁷ Sr/ ⁸⁶ Sr ₀	internal 2SE	⁸⁷ Rb/ ⁸⁶ Sr	internal 2SE	⁸⁷ Sr/ ⁸⁶ Sr _i	internal 2SE
<u>Upper Border Series</u>																
SK08-113	1	rim?	7/28/2017	2.1	287	-1.922	0.006703	0.000050	0.05614	0.00042	0.704235	0.000160	0.00428	0.00010	0.704232	0.000163
SK08-113	2	core	7/28/2017	2.1	296	-1.916	0.006692	0.000050	0.05605	0.00042	0.704175	0.000120	0.03210	0.00260	0.704150	0.000147
SK08-113	3	core	7/28/2017	2.3	316	-1.900	0.006695	0.000041	0.05607	0.00034	0.704135	0.000120	0.02800	0.00120	0.704113	0.000143
SK08-113	4	core	7/28/2017	2.1	291	-1.889	0.006697	0.000047	0.05609	0.00040	0.704155	0.000140	0.00608	0.00029	0.704150	0.000145
SK08-113	5	rim	7/28/2017	2.0	277	-1.900	0.006703	0.000053	0.05613	0.00044	0.704195	0.000130	0.00259	0.00011	0.704193	0.000132
SK08-113	6	rim	7/28/2017	2.6	353	-1.901	0.006732	0.000035	0.05638	0.00030	0.704125	0.000094	0.00517	0.00010	0.704121	0.000098
SK08-113	7	core	7/28/2017	2.1	285	-1.890	0.006716	0.000055	0.05625	0.00046	0.704185	0.000120	0.00810	0.00074	0.704179	0.000127
SK08-113	8	rim	7/28/2017	2.7	369	-1.918	0.006651	0.000034	0.05571	0.00028	0.704199	0.000095	0.01185	0.00015	0.704190	0.000104
SK08-113	9	core	7/28/2017	2.1	294	-1.902	0.006723	0.000050	0.05631	0.00042	0.704275	0.000130	0.00552	0.00040	0.704271	0.000135
SK08-113	10	core	7/28/2017	2.1	282	-1.905	0.006698	0.000052	0.05610	0.00044	0.704275	0.000120	0.02660	0.00120	0.704254	0.000142
SK08-113	11	core	7/28/2017	2.1	292	-1.904	0.006722	0.000054	0.05630	0.00045	0.704265	0.000110	0.03800	0.00270	0.704235	0.000142
SK08-113	12	core	7/28/2017	2.1	285	-1.894	0.006690	0.000050	0.05603	0.00042	0.704195	0.000140	0.03410	0.00400	0.704168	0.000170
SK08-189[§]	1	core	7/28/2017	1.8	251	-1.883	0.006691	0.000069	0.05604	0.00058	0.704225	0.000130	0.00567	0.00011	0.704221	0.000135
SK08-189	2	core	7/28/2017	1.7	238	-1.885	0.006651	0.000048	0.05570	0.00040	0.704555	0.000130	0.05650	0.00370	0.704511	0.000177
SK08-189	3	core	7/28/2017	2.1	287	-1.883	0.006754	0.000045	0.05656	0.00037	0.704535	0.000130	0.01470	0.00035	0.704523	0.000142
SK08-189	4	core	7/28/2017	2.1	285	-1.875	0.006726	0.000046	0.05633	0.00039	0.704585	0.000110	0.00697	0.00009	0.704580	0.000116
SK08-189	5	core	7/28/2017	2.1	290	-1.875	0.006722	0.000059	0.05630	0.00049	0.704555	0.000110	0.00769	0.00014	0.704549	0.000116
SK08-189	6	interstitial	7/28/2017	2.3	319	-1.871	0.006729	0.000047	0.05636	0.00039	0.704483	0.000086	0.01229	0.00011	0.704473	0.000096
SK08-189	7	interstitial	7/28/2017	2.4	325	-1.866	0.006714	0.000047	0.05623	0.00040	0.704558	0.000092	0.01323	0.00025	0.704548	0.000103
SK08-189	8	core	7/28/2017	2.1	283	-1.866	0.006743	0.000053	0.05647	0.00044	0.704365	0.000140	0.00495	0.00009	0.704361	0.000144
SK08-189	9	core	7/28/2017	2.1	295	-1.857	0.006743	0.000049	0.05648	0.00041	0.704425	0.000120	0.00519	0.00020	0.704421	0.000124
SK08-189	10	rim	7/28/2017	2.4	333	-1.873	0.006721	0.000037	0.05629	0.00031	0.704495	0.000100	0.00830	0.00026	0.704489	0.000107
SK08-189	11	rim	7/28/2017	2.4	337	-1.871	0.006729	0.000037	0.05636	0.00031	0.704515	0.000110	0.00822	0.00020	0.704509	0.000117
SK08-189	12	core	7/28/2017	2.0	272	-1.863	0.006725	0.000053	0.05633	0.00044	0.704475	0.000120	0.00946	0.00018	0.704468	0.000128
SK08-189	13	core	7/28/2017	2.0	282	-1.859	0.006757	0.000040	0.05659	0.00034	0.704445	0.000140	0.01440	0.00034	0.704434	0.000152
SK08-189	14	core	7/28/2017	1.9	268	-1.858	0.006713	0.000055	0.05622	0.00046	0.704405	0.000140	0.02026	0.00096	0.704389	0.000157
SK08-189	15	interstitial	7/28/2017	2.3	316	-1.849	0.006705	0.000039	0.05616	0.00032	0.704565	0.000100	0.00947	0.00071	0.704558	0.000108
SK08-189	16	core?	7/28/2017	2.2	302	-1.865	0.006720	0.000049	0.05628	0.00041	0.704465	0.000100	0.00301	0.00010	0.704463	0.000102

SK08-70	1	rim	5/18/2017	1.8	302	-1.863	0.006665	0.000072	0.05582	0.00061	0.704465	0.000140	0.00601	0.00021	0.704460	0.000145
SK08-70	2	rim	5/18/2017	1.7	291	-1.864	0.006660	0.000110	0.05580	0.00089	0.704465	0.000140	0.00266	0.00004	0.704463	0.000142
SK08-70	3	core	5/18/2017	1.5	258	-1.860	0.006652	0.000097	0.05571	0.00082	0.704455	0.000120	0.00285	0.00019	0.704453	0.000122
SK08-70	4	core	5/18/2017	1.7	282	-1.848	0.006719	0.000073	0.05627	0.00061	0.704515	0.000140	0.00123	0.00003	0.704514	0.000141
SK08-70	5	core	5/18/2017	1.7	293	-1.855	0.006706	0.000092	0.05617	0.00077	0.704435	0.000160	0.00273	0.00004	0.704433	0.000162
SK08-70	6	core	5/18/2017	1.7	292	-1.857	0.006704	0.000083	0.05615	0.00069	0.704545	0.000120	0.00274	0.00004	0.704543	0.000122
SK08-70	7	rim	5/18/2017	1.8	312	-1.862	0.006712	0.000083	0.05622	0.00069	0.704495	0.000130	0.00340	0.00013	0.704492	0.000133
SK08-70	8	rim	5/18/2017	1.8	308	-1.869	0.006744	0.000094	0.05649	0.00079	0.704465	0.000120	0.00420	0.00012	0.704462	0.000123
SK08-70	9	core	5/18/2017	1.6	268	-1.862	0.006680	0.000120	0.05600	0.00100	0.704575	0.000160	0.00865	0.00018	0.704568	0.000167
SK08-70	10	core	5/18/2017	1.6	273	-1.866	0.006716	0.000090	0.05624	0.00076	0.704595	0.000140	0.00389	0.00005	0.704592	0.000143
SK08-70	11	core	5/18/2017	1.5	261	-1.862	0.006730	0.000110	0.05634	0.00089	0.704595	0.000160	0.00361	0.00037	0.704592	0.000163
SK08-70	12	rim	5/18/2017	1.7	297	-1.866	0.006775	0.000094	0.05674	0.00078	0.704465	0.000150	0.00389	0.00008	0.704462	0.000153
SK08-70	1	core	7/28/2017	2.0	281	-1.932	0.006718	0.000050	0.05627	0.00042	0.704705	0.000140	0.01728	0.00066	0.704691	0.000154
SK08-70	2	core	7/28/2017	2.0	290	-1.933	0.006747	0.000037	0.05651	0.00031	0.704595	0.000120	0.00213	0.00007	0.704593	0.000122
SK08-70	3	rim	7/28/2017	2.3	329	-1.929	0.006735	0.000044	0.05641	0.00037	0.704485	0.000120	0.00400	0.00020	0.704482	0.000123
SK08-70	4	rim	7/28/2017	2.4	340	-1.930	0.006710	0.000048	0.05620	0.00040	0.704515	0.000100	0.00347	0.00006	0.704512	0.000103
SK08-70	5	core	7/28/2017	1.8	263	-1.954	0.006744	0.000057	0.05648	0.00048	0.704635	0.000130	0.00482	0.00013	0.704631	0.000134
SK08-70	6	core	7/28/2017	1.9	275	-1.959	0.006737	0.000050	0.05643	0.00042	0.704545	0.000130	0.00226	0.00008	0.704543	0.000132
SK08-70	7	rim	7/28/2017	2.3	326	-1.956	0.006711	0.000037	0.05620	0.00031	0.704575	0.000120	0.00691	0.00026	0.704570	0.000126
SK08-70	8	rim	7/28/2017	2.1	297	-1.955	0.006311	0.000072	0.05286	0.00061	0.704595	0.000150	0.02264	0.00096	0.704577	0.000168
SK08-70	9	core	7/28/2017	2.3	329	-1.948	0.006728	0.000041	0.05635	0.00034	0.704691	0.000092	0.04500	0.00310	0.704656	0.000130
SK08-70	10	rim	7/28/2017	1.6	232	-1.936	0.006684	0.000064	0.05598	0.00054	0.704725	0.000200	1.22300	0.04000	0.703768	0.001189
SK08-104	1	vesitiges in granophyre	7/28/2017	1.8	245	-1.961	0.006564	0.000076	0.05497	0.00064	0.704955	0.000150	0.47300	0.02000	0.704585	0.000536
SK08-104	2	vesitiges in granophyre	7/28/2017	1.3	180	-1.953	0.006578	0.000078	0.05509	0.00065	0.704805	0.000210	0.92200	0.01400	0.704083	0.000943
SK08-104	3	vesitiges in granophyre	7/28/2017	1.2	171	-1.952	0.006540	0.000120	0.05480	0.00100	0.705285	0.000250	0.83800	0.02800	0.704629	0.000928
SK08-104	4	vesitiges in granophyre	7/28/2017	1.3	186	-1.895	0.006564	0.000077	0.05497	0.00065	0.705045	0.000190	0.61300	0.02900	0.704565	0.000693
SK08-104	5	vesitiges in granophyre	7/28/2017	1.5	213	-1.924	0.005420	0.000170	0.04540	0.00140	0.705185	0.000220	0.73900	0.01500	0.704607	0.000810
SK08-104	6	vesitiges in granophyre	7/28/2017	1.3	185	-1.937	0.006628	0.000077	0.05551	0.00064	0.705305	0.000180	0.93300	0.01700	0.704575	0.000924
SK08-114	1	core?	11/29/2017	5.9	332	-1.631	0.006745	0.000044	0.05649	0.00037	0.704151	0.000058	0.00433	0.00015	0.704148	0.000062
SK08-114	2	interstitial?	11/29/2017	5.2	292	-1.627	0.006762	0.000047	0.05663	0.00040	0.704268	0.000061	0.00324	0.00018	0.704265	0.000064
SK08-114	3	core?	11/29/2017	5.3	296	-1.621	0.006746	0.000036	0.05650	0.00030	0.704164	0.000063	0.00416	0.00014	0.704161	0.000066
SK08-114	4	rim	11/29/2017	5.0	280	-1.631	0.006729	0.000051	0.05636	0.00043	0.703837	0.000064	0.00233	0.00007	0.703835	0.000066
SK08-114	5	core	11/29/2017	5.6	318	-1.623	0.006746	0.000038	0.05650	0.00032	0.704022	0.000066	0.01040	0.00041	0.704014	0.000074
SK08-114	6	interstitial?	11/29/2017	5.3	296	-1.615	0.006754	0.000032	0.05656	0.00027	0.704170	0.000062	0.00857	0.00032	0.704163	0.000069

SK08-114	7	core	11/29/2017	5.7	320	-1.624	0.006730	0.000044	0.05637	0.00037	0.704231	0.000062	0.04815	0.00066	0.704193	0.000100
SK08-114	8	core	11/29/2017	5.6	315	-1.622	0.006711	0.000032	0.05621	0.00027	0.704127	0.000065	0.00912	0.00023	0.704120	0.000072
SK08-114	9	cor	11/29/2017	5.7	319	-1.624	0.006725	0.000036	0.05632	0.00030	0.704180	0.000060	0.01030	0.00035	0.704172	0.000068
SK08-114	10	interstitial?	11/29/2017	5.9	334	-1.630	0.006753	0.000035	0.05656	0.00030	0.704113	0.000057	0.00297	0.00004	0.704111	0.000059
SK08-115	1	core	11/29/2017	5.0	283	-1.641	0.006742	0.000049	0.05647	0.00041	0.704253	0.000088	0.03880	0.00370	0.704223	0.000121
SK08-115	2	interstitial?	11/29/2017	5.4	306	-1.644	0.006736	0.000041	0.05641	0.00034	0.704176	0.000052	0.00930	0.00100	0.704169	0.000060
SK08-115	3	core	11/29/2017	5.8	323	-1.640	0.006745	0.000039	0.05649	0.00033	0.704046	0.000054	0.01097	0.00039	0.704037	0.000063
SK08-115	4	core	11/29/2017	5.2	294	-1.620	0.006736	0.000046	0.05641	0.00038	0.704116	0.000071	0.00339	0.00023	0.704113	0.000074
SK08-115	5	rim	11/29/2017	6.2	350	-1.645	0.006750	0.000036	0.05653	0.00030	0.704039	0.000051	0.00583	0.00010	0.704034	0.000056
SK08-115	6	rim	11/29/2017	5.8	324	-1.652	0.006726	0.000030	0.05634	0.00025	0.704083	0.000057	0.00866	0.00056	0.704076	0.000064
SK08-115	7	core	11/29/2017	5.1	287	-1.628	0.006725	0.000047	0.05632	0.00039	0.704153	0.000063	0.00574	0.00031	0.704149	0.000068
SK08-115	8	interstitial?	11/29/2017	5.8	327	-1.631	0.006747	0.000039	0.05651	0.00033	0.704071	0.000050	0.00339	0.00009	0.704068	0.000053
SK08-115	9	interstitial?	11/29/2017	5.9	333	-1.633	0.006726	0.000035	0.05634	0.00030	0.704085	0.000057	0.00446	0.00011	0.704082	0.000061
SK08-115	10	core	11/29/2017	5.4	304	-1.628	0.006763	0.000032	0.05664	0.00027	0.704139	0.000061	0.00451	0.00019	0.704135	0.000065
SK08-115	11	core	11/29/2017	5.7	317	-1.629	0.006749	0.000042	0.05652	0.00035	0.704128	0.000047	0.00445	0.00006	0.704125	0.000051
SK08-115	12	core?	11/29/2017	6.0	334	-1.657	0.006732	0.000041	0.05639	0.00035	0.704055	0.000064	0.02217	0.00062	0.704038	0.000082
SK08-65	1	core	11/29/2017	4.1	258	-1.672	0.006757	0.000058	0.05659	0.00049	0.704540	0.000076	0.00198	0.00002	0.704538	0.000078
SK08-65	2	core	11/29/2017	4.3	268	-1.675	0.006752	0.000041	0.05655	0.00034	0.704466	0.000077	0.00273	0.00005	0.704464	0.000079
SK08-65	3	rim	11/29/2017	4.2	263	-1.677	0.006754	0.000046	0.05657	0.00039	0.704576	0.000081	0.00203	0.00002	0.704574	0.000083
SK08-65	4	rim	11/29/2017	4.2	265	-1.677	0.006734	0.000048	0.05639	0.00040	0.704470	0.000065	0.00362	0.00004	0.704467	0.000068
SK08-65	5	core	11/29/2017	4.2	263	-1.673	0.006746	0.000054	0.05650	0.00045	0.704319	0.000061	0.00241	0.00024	0.704317	0.000063
SK08-65	6	rim	11/29/2017	4.5	285	-1.673	0.006763	0.000041	0.05664	0.00034	0.704439	0.000065	0.00374	0.00044	0.704436	0.000068
SK08-65	7	core	11/29/2017	4.2	268	-1.676	0.006752	0.000039	0.05655	0.00033	0.704394	0.000081	0.00101	0.00001	0.704393	0.000082
SK08-65	8	core	11/29/2017	4.4	279	-1.677	0.006762	0.000054	0.05664	0.00045	0.704448	0.000058	0.00281	0.00003	0.704446	0.000060
SK08-65	9	core	11/29/2017	4.0	258	-1.675	0.006726	0.000059	0.05633	0.00049	0.704440	0.000074	0.00246	0.00005	0.704438	0.000076
SK08-65	10	core	11/29/2017	4.3	271	-1.673	0.006749	0.000049	0.05652	0.00041	0.704344	0.000067	0.00182	0.00001	0.704343	0.000068
SK08-116	1	rim	11/29/2017	4.8	295	-1.647	0.006744	0.000037	0.05648	0.00031	0.704121	0.000065	0.00202	0.00005	0.704119	0.000067
SK08-116	2	core	11/29/2017	4.9	296	-1.661	0.006739	0.000043	0.05644	0.00036	0.704177	0.000063	0.00437	0.00021	0.704174	0.000067
SK08-116	3	core	11/29/2017	4.7	286	-1.656	0.006743	0.000050	0.05648	0.00042	0.704228	0.000064	0.00384	0.00041	0.704225	0.000067
SK08-116	4	core	11/29/2017	4.7	286	-1.644	0.006742	0.000048	0.05646	0.00040	0.704116	0.000067	0.01736	0.00084	0.704102	0.000081
SK08-116	5	rim	11/29/2017	5.8	353	-1.670	0.006575	0.000056	0.05507	0.00047	0.704126	0.000064	0.01719	0.00066	0.704113	0.000078
SK08-116	6	rim	11/29/2017	5.4	333	-1.677	0.006732	0.000035	0.05638	0.00030	0.704045	0.000050	0.04980	0.00260	0.704006	0.000091
SK08-116	7	core	11/29/2017	5.5	339	-1.680	0.006746	0.000044	0.05650	0.00036	0.703997	0.000067	0.01770	0.00038	0.703983	0.000081

SK08-116	8	core	11/29/2017	4.9	300	-1.654	0.006739	0.000043	0.05644	0.00036	0.704070	0.000061	0.00247	0.00004	0.704068	0.000063
SK08-116	9	core	11/29/2017	5.1	312	-1.656	0.006738	0.000032	0.05643	0.00027	0.704092	0.000063	0.00488	0.00044	0.704088	0.000067
SK08-116	10	core	11/29/2017	5.5	337	-1.661	0.006746	0.000045	0.05650	0.00038	0.704111	0.000057	0.00549	0.00045	0.704107	0.000062
SK08-116	11	rim	11/29/2017	5.3	327	-1.684	0.006736	0.000038	0.05641	0.00032	0.704024	0.000059	0.03090	0.00250	0.704000	0.000085
SK08-116	12	rim	11/29/2017	5.2	323	-1.676	0.006759	0.000044	0.05661	0.00037	0.704083	0.000069	0.02558	0.00090	0.704063	0.000090
SK08-117	1	core	11/29/2017	5.0	281	-1.627	0.006719	0.000039	0.05627	0.00032	0.704361	0.000061	0.00113	0.00003	0.704360	0.000062
SK08-117	2	core	11/29/2017	4.9	278	-1.627	0.006727	0.000060	0.05634	0.00050	0.704317	0.000064	0.01830	0.00039	0.704303	0.000079
SK08-117	3	rim	11/29/2017	5.0	282	-1.633	0.006754	0.000051	0.05656	0.00043	0.704334	0.000062	0.02083	0.00082	0.704318	0.000079
SK08-117	4	rim	11/29/2017	5.0	279	-1.632	0.006749	0.000043	0.05652	0.00036	0.704293	0.000061	0.03477	0.00043	0.704266	0.000089
SK08-117	5	rim	11/29/2017	5.1	286	-1.635	0.006736	0.000035	0.05642	0.00029	0.704289	0.000069	0.01350	0.00110	0.704278	0.000080
SK08-117	6	core	11/29/2017	5.1	285	-1.639	0.006732	0.000038	0.05638	0.00032	0.704302	0.000054	0.00357	0.00006	0.704299	0.000057
SK08-117	7	core	11/29/2017	5.3	295	-1.644	0.006749	0.000042	0.05652	0.00035	0.704367	0.000070	0.01140	0.00120	0.704358	0.000080
SK08-117	8	rim	11/29/2017	5.6	314	-1.645	0.006755	0.000037	0.05657	0.00031	0.704434	0.000057	0.00442	0.00005	0.704431	0.000061
SK08-117	9	interstitial	11/29/2017	5.0	282	-1.640	0.006734	0.000046	0.05640	0.00039	0.704306	0.000061	0.00667	0.00005	0.704301	0.000066
SK08-117	10	interstitial	11/29/2017	5.5	309	-1.647	0.006725	0.000041	0.05633	0.00034	0.704402	0.000051	0.02820	0.00150	0.704380	0.000074
SK08-117	11	core	11/29/2017	5.1	284	-1.635	0.006749	0.000050	0.05652	0.00042	0.704378	0.000071	0.00206	0.00003	0.704376	0.000073
SK08-117	12	core	11/29/2017	5.2	293	-1.628	0.006764	0.000044	0.05665	0.00037	0.704320	0.000067	0.00254	0.00006	0.704318	0.000069
SK08-117	13	interstitial	11/29/2017	5.2	290	-1.647	0.006748	0.000041	0.05652	0.00035	0.704383	0.000061	0.01055	0.00040	0.704375	0.000070
SK08-117	14	core	11/29/2017	4.9	276	-1.636	0.006752	0.000042	0.05655	0.00035	0.704383	0.000074	0.00147	0.00002	0.704382	0.000075
SK08-117	15	rim	11/29/2017	4.9	277	-1.646	0.006748	0.000044	0.05652	0.00037	0.704320	0.000055	0.00485	0.00005	0.704316	0.000059
SK08-117	16	rim	11/29/2017	5.3	297	-1.652	0.006737	0.000037	0.05642	0.00031	0.704359	0.000061	0.00807	0.00015	0.704353	0.000067
SK08-118	1	rim	5/18/2017	1.5	253	-1.854	0.006701	0.000093	0.05612	0.00078	0.704455	0.000180	0.00967	0.00050	0.704447	0.000188
SK08-118	2	rim	5/18/2017	1.5	259	-1.845	0.006753	0.000091	0.05656	0.00076	0.704315	0.000150	0.00482	0.00018	0.704311	0.000154
SK08-118	3	core	5/18/2017	1.5	255	-1.849	0.006700	0.000110	0.05613	0.00094	0.704265	0.000140	0.00329	0.00007	0.704262	0.000143
SK08-118	4	inclusion	5/18/2017	1.6	270	-1.849	0.006726	0.000084	0.05633	0.00071	0.704485	0.000140	0.01416	0.00051	0.704474	0.000151
SK08-118	5	inclusion	5/18/2017	1.6	276	-1.860	0.006741	0.000091	0.05646	0.00076	0.704455	0.000140	0.00479	0.00009	0.704451	0.000144
SK08-118	6	interstitial	5/18/2017	1.5	254	-1.867	0.006727	0.000088	0.05634	0.00074	0.704475	0.000160	0.00496	0.00005	0.704471	0.000164
SK08-118	7	rim	5/18/2017	1.5	257	-1.854	0.006740	0.000130	0.05650	0.00110	0.704265	0.000150	0.00579	0.00004	0.704260	0.000155
SK08-118	8	core	5/18/2017	1.5	257	-1.861	0.006732	0.000073	0.05638	0.00061	0.704435	0.000150	0.00421	0.00008	0.704432	0.000153
SK08-118	9	rim	5/18/2017	1.5	255	-1.861	0.006693	0.000096	0.05605	0.00080	0.704485	0.000130	0.00629	0.00019	0.704480	0.000135
SK08-118	10	rim	5/18/2017	1.5	255	-1.860	0.006687	0.000096	0.05600	0.00080	0.704515	0.000130	0.00820	0.00008	0.704509	0.000136
SK08-118	11	rim	5/18/2017	1.5	258	-1.862	0.006706	0.000082	0.05617	0.00069	0.704485	0.000170	0.00828	0.00006	0.704479	0.000177
SK08-118	12	core	5/18/2017	1.5	261	-1.860	0.006751	0.000098	0.05654	0.00082	0.704455	0.000160	0.00823	0.00005	0.704449	0.000166

SK08-1	1	core	11/29/2017	5.2	303	-1.624	0.006762	0.000054	0.05663	0.00045	0.704278	0.000066	0.00163	0.00004	0.704277	0.000067
SK08-1	2	core	11/29/2017	4.9	283	-1.621	0.006770	0.000038	0.05670	0.00032	0.704246	0.000073	0.00163	0.00001	0.704245	0.000074
SK08-1	3	core	11/29/2017	5.3	305	-1.629	0.006756	0.000053	0.05658	0.00045	0.704232	0.000066	0.00176	0.00003	0.704231	0.000067
SK08-1	4	rim	11/29/2017	6.3	365	-1.634	0.006756	0.000035	0.05658	0.00029	0.704283	0.000059	0.00341	0.00008	0.704280	0.000062
SK08-1	5	rim	11/29/2017	6.8	392	-1.656	0.006752	0.000035	0.05655	0.00030	0.704275	0.000047	0.00555	0.00021	0.704271	0.000052
SK08-1	6	rim	11/29/2017	7.0	407	-1.636	0.006763	0.000033	0.05664	0.00028	0.704306	0.000042	0.00165	0.00002	0.704305	0.000043
SK08-1	7	core	11/29/2017	4.9	283	-1.630	0.006776	0.000044	0.05675	0.00037	0.704240	0.000068	0.00453	0.00011	0.704236	0.000072
SK08-1	8	core	11/29/2017	5.1	294	-1.629	0.006756	0.000038	0.05658	0.00032	0.704257	0.000067	0.00444	0.00006	0.704254	0.000071
SK08-1	9	rim	11/29/2017	6.7	387	-1.633	0.006751	0.000038	0.05654	0.00032	0.704303	0.000045	0.00575	0.00044	0.704298	0.000050
SK08-1	10	rim	11/29/2017	7.3	418	-1.630	0.006753	0.000031	0.05656	0.00026	0.704290	0.000046	0.00221	0.00003	0.704288	0.000048
SK08-1	11	core	11/29/2017	5.1	289	-1.621	0.006764	0.000042	0.05665	0.00035	0.704283	0.000060	0.00171	0.00002	0.704282	0.000061
SK08-1	12	rim	11/29/2017	7.1	408	-1.645	0.006753	0.000033	0.05656	0.00028	0.704296	0.000042	0.00399	0.00011	0.704293	0.000045
SK08-1	13	core	11/29/2017	5.1	294	-1.618	0.006744	0.000039	0.05649	0.00033	0.704285	0.000063	0.00193	0.00005	0.704283	0.000065
SK08-1	14	core	11/29/2017	5.2	295	-1.626	0.006745	0.000043	0.05649	0.00036	0.704256	0.000064	0.00180	0.00002	0.704255	0.000065
SK08-1	15	rim	11/29/2017	7.2	412	-1.647	0.006731	0.000031	0.05637	0.00026	0.704251	0.000045	0.00682	0.00022	0.704246	0.000051
SK08-1	16	rim	11/29/2017	5.9	334	-1.631	0.006706	0.000037	0.05616	0.00031	0.704308	0.000060	0.00484	0.00030	0.704304	0.000064
SK08-125	1	core	5/17/2017	2.2	326	-1.811	0.006699	0.000067	0.05610	0.00056	0.704325	0.000120	0.00210	0.00004	0.704323	0.000122
SK08-125	2	interstitial	5/17/2017	2.2	333	-1.814	0.006727	0.000061	0.05634	0.00051	0.704335	0.000110	0.00297	0.00007	0.704333	0.000112
SK08-125	3	rim	5/17/2017	2.1	309	-1.810	0.006711	0.000076	0.05621	0.00063	0.704325	0.000130	0.00940	0.00100	0.704318	0.000138
SK08-125	4	rim	5/17/2017	2.2	325	-1.819	0.006707	0.000058	0.05617	0.00048	0.704358	0.000098	0.00919	0.00034	0.704351	0.000105
SK08-125	5	core	5/17/2017	2.2	326	-1.793	0.006709	0.000046	0.05619	0.00038	0.704285	0.000110	0.00427	0.00006	0.704282	0.000113
SK08-125	6	core	5/17/2017	2.1	308	-1.789	0.006702	0.000069	0.05613	0.00058	0.704325	0.000110	0.00192	0.00003	0.704323	0.000112
SK08-125	7	interstitial	5/17/2017	2.3	337	-1.814	0.006706	0.000084	0.05617	0.00070	0.704305	0.000120	0.00901	0.00054	0.704298	0.000127
SK08-125	8	core	5/17/2017	2.1	311	-1.798	0.006728	0.000074	0.05634	0.00062	0.704375	0.000110	0.00352	0.00005	0.704372	0.000113
SK08-125	9	core	5/17/2017	2.1	311	-1.796	0.006714	0.000075	0.05623	0.00063	0.704275	0.000120	0.00176	0.00003	0.704274	0.000121
SK08-125	10	core	5/17/2017	2.2	325	-1.802	0.006715	0.000072	0.05624	0.00060	0.704355	0.000120	0.00213	0.00004	0.704353	0.000122
SK08-125	11	rim	5/17/2017	2.1	312	-1.815	0.006660	0.000087	0.05578	0.00073	0.704315	0.000110	0.01241	0.00089	0.704305	0.000120
SK08-125	12	rim	5/17/2017	2.2	326	-1.816	0.006707	0.000044	0.05617	0.00037	0.704255	0.000140	0.00422	0.00036	0.704252	0.000144
SK08-14	1	inclusion	7/28/2017	2.1	290	-1.875	0.006719	0.000045	0.05627	0.00037	0.704285	0.000120	0.00769	0.00035	0.704279	0.000126
SK08-14	2	inclusion	7/28/2017	2.0	273	-1.870	0.006733	0.000050	0.05639	0.00042	0.704365	0.000150	0.00577	0.00004	0.704360	0.000155
SK08-14	3	rim	7/28/2017	2.4	336	-1.879	0.006705	0.000038	0.05615	0.00032	0.704185	0.000110	0.00513	0.00020	0.704181	0.000114
SK08-14	4	rim	7/28/2017	2.1	286	-1.849	0.006709	0.000046	0.05619	0.00038	0.704275	0.000120	0.00250	0.00007	0.704273	0.000122
SK08-14	5	core	7/28/2017	2.3	312	-1.847	0.006736	0.000046	0.05642	0.00038	0.704305	0.000100	0.00215	0.00003	0.704303	0.000102
SK08-14	6	core	7/28/2017	2.4	325	-1.842	0.006707	0.000047	0.05617	0.00040	0.704355	0.000100	0.00264	0.00024	0.704353	0.000102

SK08-14	7	core	7/28/2017	2.7	364	-1.874	0.006736	0.000039	0.05641	0.00033	0.704245	0.000110	0.00452	0.00010	0.704241	0.000114
SK08-14	8	rim	7/28/2017	2.9	391	-1.867	0.006709	0.000039	0.05619	0.00033	0.704217	0.000082	0.00400	0.00015	0.704214	0.000085
SK08-14	9	rim	7/28/2017	2.9	401	-1.897	0.006727	0.000033	0.05634	0.00028	0.704240	0.000099	0.00456	0.00015	0.704236	0.000103
SK08-14	10	rim	7/28/2017	2.0	278	-1.865	0.006693	0.000060	0.05606	0.00051	0.704115	0.000130	0.00648	0.00023	0.704110	0.000135
SK08-14	11	core	7/28/2017	2.1	285	-1.863	0.006716	0.000050	0.05625	0.00042	0.704195	0.000130	0.00295	0.00006	0.704193	0.000132
SK08-14	12	core	7/28/2017	2.7	380	-1.882	0.006723	0.000032	0.05631	0.00027	0.704211	0.000098	0.00632	0.00020	0.704206	0.000103
SK08-14	13	rim	7/28/2017	2.8	388	-1.884	0.006715	0.000036	0.05624	0.00030	0.704357	0.000095	0.00469	0.00020	0.704353	0.000099
SK08-14	14	rim	7/28/2017	2.1	293	-1.910	0.006704	0.000062	0.05614	0.00052	0.704255	0.000140	0.00922	0.00021	0.704248	0.000147
SK08-14	15	interstitial	7/28/2017	2.4	333	-1.905	0.006727	0.000039	0.05634	0.00033	0.704265	0.000100	0.00778	0.00014	0.704259	0.000106
SK08-14	16	interstitial	7/28/2017	2.0	286	-1.862	0.006693	0.000057	0.05606	0.00047	0.704365	0.000110	0.00282	0.00013	0.704363	0.000112
SK08-14	17	core	7/28/2017	2.1	294	-1.858	0.006746	0.000053	0.05650	0.00044	0.704365	0.000120	0.00214	0.00008	0.704363	0.000122
SK08-13	1	rim	7/28/2017	3.1	472	-2.000	0.006705	0.000030	0.05616	0.00025	0.704284	0.000096	0.00684	0.00026	0.704279	0.000102
SK08-13	2	interstitial	7/28/2017	3.2	479	-1.993	0.006703	0.000029	0.05614	0.00024	0.704241	0.000084	0.00441	0.00045	0.704238	0.000088
SK08-13	3	interstitial	7/28/2017	2.9	442	-2.004	0.006727	0.000036	0.05634	0.00030	0.704292	0.000093	0.00690	0.00028	0.704287	0.000099
SK08-13	4	interstitial	7/28/2017	2.9	439	-1.991	0.006708	0.000036	0.05618	0.00030	0.704317	0.000090	0.00958	0.00034	0.704310	0.000098
SK08-13	5	interstitial	7/28/2017	3.1	467	-1.982	0.006700	0.000029	0.05611	0.00024	0.704236	0.000096	0.00507	0.00018	0.704232	0.000100
SK08-13	6	interstitial	7/28/2017	3.0	450	-1.979	0.006704	0.000034	0.05615	0.00028	0.704355	0.000100	0.00509	0.00011	0.704351	0.000104
SK08-13	7	core	7/28/2017	3.4	504	-1.981	0.006714	0.000028	0.05623	0.00023	0.704283	0.000076	0.00839	0.00037	0.704276	0.000083
SK08-13	8	rim	7/28/2017	2.9	434	-1.966	0.006731	0.000033	0.05637	0.00028	0.704228	0.000089	0.00272	0.00003	0.704226	0.000091
SK08-13	9	rim	7/28/2017	2.7	402	-1.957	0.006714	0.000035	0.05623	0.00029	0.704255	0.000100	0.00287	0.00002	0.704253	0.000102
SK08-13	10	core	7/28/2017	2.7	394	-1.961	0.006709	0.000041	0.05619	0.00034	0.704325	0.000100	0.00336	0.00010	0.704322	0.000103
SK08-13	11	core	7/28/2017	2.7	400	-1.958	0.006725	0.000040	0.05632	0.00034	0.704345	0.000100	0.00372	0.00003	0.704342	0.000103
SK08-13	12	core	7/28/2017	2.7	397	-1.956	0.006718	0.000036	0.05627	0.00030	0.704285	0.000120	0.00449	0.00003	0.704281	0.000124
SK08-13	13	rim	7/28/2017	2.6	383	-1.951	0.006713	0.000038	0.05622	0.00032	0.704195	0.000100	0.00660	0.00004	0.704190	0.000105
SK08-13	14	rim	7/28/2017	2.6	386	-1.953	0.006736	0.000040	0.05642	0.00034	0.704255	0.000110	0.00499	0.00004	0.704251	0.000114
SK08-13	15	rim	7/28/2017	2.8	407	-1.952	0.006741	0.000033	0.05645	0.00027	0.704266	0.000095	0.00638	0.00003	0.704261	0.000100
SK08-13	16	rim	7/28/2017	2.7	391	-1.946	0.006731	0.000037	0.05638	0.00031	0.704285	0.000110	0.00919	0.00007	0.704278	0.000117
SK08-199	1	core	11/29/2017	5.2	299	-1.647	0.006733	0.000036	0.05639	0.00030	0.704315	0.000052	0.00393	0.00014	0.704312	0.000055
SK08-199	2	core	11/29/2017	5.4	309	-1.645	0.006753	0.000040	0.05656	0.00034	0.704330	0.000060	0.00392	0.00017	0.704327	0.000063
SK08-199	3	core	11/29/2017	5.3	304	-1.641	0.006734	0.000047	0.05640	0.00039	0.704302	0.000063	0.00251	0.00004	0.704300	0.000065
SK08-199	4	rim	11/29/2017	5.6	321	-1.654	0.006747	0.000038	0.05650	0.00031	0.704329	0.000064	0.00359	0.00003	0.704326	0.000067
SK08-199	5	rim	11/29/2017	5.5	315	-1.658	0.006739	0.000042	0.05644	0.00035	0.704362	0.000057	0.01450	0.00030	0.704351	0.000069
SK08-199	6	rim	11/29/2017	4.9	285	-1.677	0.006741	0.000044	0.05645	0.00037	0.704333	0.000069	0.00603	0.00008	0.704328	0.000074
SK08-199	7	core	11/29/2017	5.3	310	-1.639	0.006763	0.000052	0.05664	0.00044	0.704299	0.000058	0.00200	0.00001	0.704297	0.000060

SK08-199	8	core	11/29/2017	5.6	326	-1.640	0.006753	0.000041	0.05656	0.00034	0.704291	0.000069	0.00201	0.00001	0.704289	0.000071
SK08-199	9	rim	11/29/2017	5.6	330	-1.674	0.006745	0.000029	0.05649	0.00024	0.704341	0.000062	0.00793	0.00032	0.704335	0.000068
SK08-199	10	rim	11/29/2017	5.4	319	-1.666	0.006762	0.000035	0.05663	0.00029	0.704328	0.000059	0.01633	0.00021	0.704315	0.000072
SK08-199	11	core	11/29/2017	5.3	312	-1.650	0.006776	0.000044	0.05675	0.00037	0.704261	0.000059	0.00760	0.00100	0.704255	0.000066
SK08-199	12	core	11/29/2017	5.3	313	-1.645	0.006751	0.000042	0.05654	0.00035	0.704270	0.000047	0.00354	0.00035	0.704267	0.000050
SK08-199	13	rim	11/29/2017	5.3	310	-1.664	0.006721	0.000045	0.05629	0.00038	0.704342	0.000069	0.00630	0.00041	0.704337	0.000074
SK08-199	14	rim	11/29/2017	5.5	323	-1.667	0.006717	0.000034	0.05625	0.00028	0.704315	0.000070	0.00413	0.00012	0.704312	0.000073
SK08-199	15	core	11/29/2017	5.3	313	-1.653	0.006743	0.000044	0.05648	0.00037	0.704352	0.000059	0.00240	0.00002	0.704350	0.000061
SK08-199	16	core	11/29/2017	5.4	321	-1.651	0.006749	0.000043	0.05653	0.00036	0.704297	0.000066	0.00229	0.00002	0.704295	0.000068
SK08-129-A	1	rim	5/17/2017	2.2	327	-1.800	0.006730	0.000069	0.05637	0.00057	0.704245	0.000120	0.00190	0.00004	0.704244	0.000122
SK08-129-A	2	rim	5/17/2017	2.2	320	-1.806	0.006709	0.000071	0.05619	0.00059	0.704375	0.000120	0.00344	0.00006	0.704372	0.000123
SK08-129-A	3	core	5/17/2017	1.9	281	-1.792	0.006690	0.000079	0.05603	0.00066	0.705115	0.000150	0.00244	0.00009	0.705113	0.000152
SK08-129-A	4	core	5/17/2017	2.0	296	-1.795	0.006675	0.000059	0.05591	0.00049	0.704915	0.000130	0.00201	0.00006	0.704913	0.000132
SK08-129-A	5	rim	5/17/2017	2.1	312	-1.796	0.006730	0.000062	0.05636	0.00052	0.704685	0.000120	0.00380	0.00011	0.704682	0.000123
SK08-129-A	6	core	5/17/2017	2.1	313	-1.790	0.006736	0.000075	0.05642	0.00063	0.705135	0.000120	0.00485	0.00012	0.705131	0.000124
SK08-129-A	7	core	5/17/2017	2.1	319	-1.789	0.006687	0.000067	0.05601	0.00056	0.704855	0.000120	0.00261	0.00012	0.704853	0.000122
SK08-129-A	8	rim	5/17/2017	2.4	354	-1.795	0.006700	0.000046	0.05611	0.00038	0.704675	0.000120	0.01422	0.00023	0.704664	0.000131
SK08-129-A	9	core	5/17/2017	2.0	299	-1.784	0.006736	0.000074	0.05641	0.00062	0.705515	0.000120	0.00187	0.00004	0.705514	0.000121
SK08-129-A	10	rim	5/17/2017	2.2	324	-1.799	0.006701	0.000062	0.05612	0.00052	0.704935	0.000120	0.00249	0.00006	0.704933	0.000122
SK08-129-A	11	inclusion	5/17/2017	2.2	320	-1.803	0.006722	0.000048	0.05630	0.00040	0.704315	0.000110	0.00555	0.00023	0.704311	0.000115
SK08-129-A	12	rim	5/17/2017	2.2	329	-1.796	0.006702	0.000071	0.05613	0.00059	0.704275	0.000110	0.00252	0.00013	0.704273	0.000112
SK08-129-A	1	core	7/28/2017	2.4	345	-1.962	0.006751	0.000036	0.05654	0.00030	0.704385	0.000100	0.00319	0.00005	0.704383	0.000103
SK08-129-A	2	core	7/28/2017	2.5	352	-1.951	0.006753	0.000037	0.05656	0.00031	0.704365	0.000100	0.00282	0.00005	0.704363	0.000102
SK08-129-A	3	core	7/28/2017	2.4	337	-1.960	0.006745	0.000039	0.05649	0.00033	0.704345	0.000100	0.00209	0.00007	0.704343	0.000102
SK08-129-A	4	rim	7/28/2017	2.5	358	-1.967	0.006726	0.000032	0.05633	0.00027	0.704515	0.000100	0.00285	0.00012	0.704513	0.000102
SK08-129-A	5	rim	7/28/2017	2.5	356	-1.967	0.006716	0.000031	0.05625	0.00026	0.704395	0.000110	0.00364	0.00006	0.704392	0.000113
SK08-129-A	6	rim	7/28/2017	2.3	332	-1.966	0.006728	0.000045	0.05635	0.00038	0.704375	0.000100	0.00882	0.00068	0.704368	0.000107
SK08-129-A	7	core	7/28/2017	2.4	342	-1.954	0.006715	0.000043	0.05624	0.00036	0.704355	0.000100	0.01100	0.00430	0.704346	0.000112
SK08-129-A	8	core	7/28/2017	2.5	355	-1.962	0.006718	0.000034	0.05627	0.00028	0.704705	0.000130	0.00911	0.00064	0.704698	0.000138
SK08-129-A	9	core	7/28/2017	2.5	352	-1.962	0.006741	0.000041	0.05646	0.00034	0.705025	0.000110	0.00297	0.00011	0.705023	0.000112
SK08-129-A	10	core	7/28/2017	2.3	328	-1.965	0.006736	0.000045	0.05642	0.00037	0.704425	0.000120	0.00216	0.00004	0.704423	0.000122
SK08-129-A	11	core	7/28/2017	2.5	359	-1.969	0.006733	0.000037	0.05639	0.00031	0.704405	0.000110	0.00852	0.00032	0.704398	0.000117
SK08-129-A	12	rim	7/28/2017	2.5	358	-1.947	0.006725	0.000031	0.05632	0.00026	0.704407	0.000096	0.00251	0.00008	0.704405	0.000098
SK08-129-B	1	rim	7/28/2017	2.5	362	-1.844	0.006714	0.000048	0.05623	0.00040	0.704475	0.000110	0.01179	0.00060	0.704466	0.000120
SK08-129-B	2	rim	7/28/2017	2.4	344	-1.839	0.006717	0.000049	0.05625	0.00041	0.704305	0.000110	0.00588	0.00006	0.704300	0.000115

SK08-129-B	3	core	7/28/2017	2.5	357	-1.833	0.006738	0.000032	0.05644	0.00027	0.704265	0.000130	0.00287	0.00005	0.704263	0.000132
SK08-129-B	4	core	7/28/2017	2.5	362	-1.835	0.006740	0.000043	0.05645	0.00036	0.704318	0.000098	0.00307	0.00003	0.704316	0.000100
SK08-129-B	5	interstitial	7/28/2017	2.3	333	-1.835	0.006744	0.000054	0.05649	0.00045	0.704325	0.000110	0.00342	0.00005	0.704322	0.000113
SK08-129-B	6	rim	7/28/2017	2.2	322	-1.833	0.006732	0.000035	0.05638	0.00029	0.704365	0.000120	0.00405	0.00007	0.704362	0.000123
SK08-129-B	7	core	7/28/2017	2.2	322	-1.829	0.006746	0.000042	0.05650	0.00036	0.704425	0.000110	0.00263	0.00010	0.704423	0.000112
SK08-129-B	8	core	7/28/2017	2.2	315	-1.824	0.006705	0.000055	0.05616	0.00046	0.704305	0.000130	0.00227	0.00005	0.704303	0.000132
SK08-129-B	9	core	7/28/2017	2.5	359	-1.825	0.006718	0.000041	0.05627	0.00034	0.704365	0.000110	0.02500	0.00110	0.704345	0.000130
SK08-129-B	10	core	7/28/2017	2.5	359	-1.820	0.006723	0.000045	0.05631	0.00038	0.704405	0.000110	0.00430	0.00015	0.704402	0.000113
SK08-129-B	11	rim	7/28/2017	2.3	332	-1.824	0.006727	0.000046	0.05634	0.00038	0.704305	0.000100	0.00292	0.00006	0.704303	0.000102
SK08-129-B	12	rim	7/28/2017	2.4	345	-1.822	0.006716	0.000037	0.05625	0.00031	0.704365	0.000100	0.00361	0.00009	0.704362	0.000103
SK08-137	1	rim	7/28/2017	2.7	376	-1.868	0.006722	0.000038	0.05629	0.00031	0.704303	0.000096	0.00695	0.00010	0.704298	0.000102
SK08-137	2	core	7/28/2017	2.8	388	-1.868	0.006718	0.000038	0.05626	0.00032	0.704355	0.000088	0.00668	0.00023	0.704350	0.000093
SK08-137	3	interstitial	7/28/2017	2.8	393	-1.845	0.006714	0.000032	0.05623	0.00027	0.704355	0.000100	0.01054	0.00037	0.704347	0.000109
SK08-137	4	core	7/28/2017	2.6	366	-1.850	0.006701	0.000042	0.05612	0.00035	0.704385	0.000110	0.00189	0.00003	0.704384	0.000112
SK08-137	5	rim	7/28/2017	2.6	370	-1.869	0.006728	0.000034	0.05635	0.00028	0.704434	0.000091	0.00228	0.00004	0.704432	0.000093
SK08-137	6	core	7/28/2017	2.6	371	-1.858	0.006729	0.000032	0.05636	0.00027	0.704293	0.000096	0.01005	0.00076	0.704285	0.000104
SK08-137	7	interstitial	7/28/2017	2.5	357	-1.861	0.006719	0.000042	0.05627	0.00035	0.704363	0.000093	0.01394	0.00045	0.704352	0.000104
SK08-137	8	interstitial	7/28/2017	2.5	358	-1.859	0.006708	0.000039	0.05618	0.00033	0.704285	0.000110	0.03260	0.00320	0.704259	0.000138
SK08-137	9	interstitial	7/28/2017	2.7	384	-1.848	0.006732	0.000036	0.05639	0.00030	0.704348	0.000091	0.01660	0.00270	0.704335	0.000106
SK08-137	10	rim	7/28/2017	2.5	356	-1.843	0.006735	0.000037	0.05641	0.00031	0.704445	0.000110	0.00197	0.00004	0.704443	0.000112
SK08-137	11	rim	7/28/2017	2.6	376	-1.852	0.006741	0.000033	0.05646	0.00028	0.704342	0.000093	0.00221	0.00005	0.704340	0.000095
SK08-137	12	core	7/28/2017	2.7	382	-1.857	0.006740	0.000040	0.05645	0.00034	0.704435	0.000100	0.00469	0.00017	0.704431	0.000104
SK08-138	1	rim	7/28/2017	2.4	340	-1.878	0.006743	0.000040	0.05647	0.00034	0.704355	0.000120	0.00623	0.00051	0.704350	0.000125
SK08-138	2	rim	7/28/2017	2.4	337	-1.883	0.006709	0.000041	0.05619	0.00034	0.704364	0.000082	0.00278	0.00006	0.704362	0.000084
SK08-138	3	core	7/28/2017	2.5	349	-1.875	0.006716	0.000042	0.05625	0.00035	0.704285	0.000100	0.00377	0.00019	0.704282	0.000103
SK08-138	4	core	7/28/2017	2.9	407	-1.889	0.006702	0.000033	0.05613	0.00028	0.704298	0.000096	0.00272	0.00002	0.704296	0.000098
SK08-138	5	core	7/28/2017	2.9	411	-1.889	0.006709	0.000028	0.05619	0.00024	0.704395	0.000095	0.00325	0.00003	0.704392	0.000098
SK08-138	6	rim	7/28/2017	2.9	417	-1.899	0.006714	0.000038	0.05623	0.00032	0.704359	0.000076	0.01186	0.00018	0.704350	0.000085
SK08-138	7	rim	7/28/2017	3.1	437	-1.894	0.006727	0.000035	0.05634	0.00029	0.704335	0.000110	0.01290	0.00038	0.704325	0.000120
SK08-138	8	core	7/28/2017	3.0	433	-1.913	0.006713	0.000038	0.05623	0.00032	0.704445	0.000083	0.00379	0.00004	0.704442	0.000086
SK08-138	9	rim?	7/28/2017	3.0	431	-1.877	0.006758	0.000037	0.05660	0.00031	0.704265	0.000110	0.00344	0.00012	0.704262	0.000113
SK08-138	10	core	7/28/2017	3.0	433	-1.891	0.006706	0.000033	0.05616	0.00028	0.704337	0.000088	0.00237	0.00002	0.704335	0.000090
SK08-138	11	core	7/28/2017	2.1	295	-1.870	0.006719	0.000041	0.05627	0.00035	0.704315	0.000130	0.00613	0.00023	0.704310	0.000135
SK08-138	12	core	7/28/2017	3.1	448	-1.894	0.006752	0.000032	0.05655	0.00027	0.704247	0.000086	0.00273	0.00002	0.704245	0.000088

SK08-138	13		7/28/2017	3.3	479	-1.897	0.006725	0.000030	0.05632	0.00025	0.704327	0.000069	0.00296	0.00002	0.704325	0.000071
SK08-140	1	rim	5/17/2017	2.3	358	-1.819	0.006734	0.000052	0.05640	0.00044	0.704435	0.000100	0.00807	0.00004	0.704429	0.000106
SK08-140	2	rim	5/17/2017	2.2	337	-1.815	0.006759	0.000060	0.05661	0.00051	0.704215	0.000120	0.00641	0.00021	0.704210	0.000125
SK08-140	3	core	5/17/2017	2.2	341	-1.817	0.006714	0.000078	0.05623	0.00065	0.704325	0.000120	0.00589	0.00013	0.704320	0.000125
SK08-140	4	rim	5/17/2017	2.2	351	-1.829	0.006729	0.000060	0.05636	0.00050	0.704455	0.000110	0.00761	0.00021	0.704449	0.000116
SK08-140	5	core	5/17/2017	2.2	343	-1.815	0.006733	0.000053	0.05639	0.00045	0.704415	0.000130	0.00448	0.00003	0.704411	0.000134
SK08-140	6	inclusion	5/17/2017	2.6	403	-1.829	0.006758	0.000056	0.05660	0.00047	0.704325	0.000110	0.00836	0.00003	0.704318	0.000117
SK08-140	7	inclusion	5/17/2017	2.3	367	-1.809	0.006719	0.000072	0.05628	0.00060	0.704405	0.000100	0.02940	0.00120	0.704382	0.000124
SK08-140	8	inclusion	5/17/2017	2.0	317	-1.845	0.006717	0.000071	0.05626	0.00060	0.704405	0.000140	0.01754	0.00010	0.704391	0.000154
SK08-140	9	rim	5/18/2017	1.9	305	-1.805	0.006728	0.000054	0.05635	0.00045	0.704445	0.000120	0.03820	0.00160	0.704415	0.000151
SK08-140	10	rim	5/18/2017	2.0	315	-1.828	0.006722	0.000058	0.05630	0.00049	0.704345	0.000140	0.02097	0.00018	0.704329	0.000157
SK08-140	11	core	5/18/2017	1.9	301	-1.829	0.006740	0.000061	0.05645	0.00052	0.704335	0.000110	0.02944	0.00068	0.704312	0.000134
SK08-140	12	core	5/18/2017	2.3	363	-1.822	0.006708	0.000055	0.05618	0.00046	0.704335	0.000110	0.00883	0.00003	0.704328	0.000117
SK08-156	1	rim	5/18/2017	2.8	449	-1.840	0.006728	0.000062	0.05635	0.00052	0.704366	0.000084	0.00306	0.00003	0.704364	0.000086
SK08-156	2	rim	5/18/2017	2.8	445	-1.825	0.006746	0.000050	0.05650	0.00042	0.704432	0.000077	0.00257	0.00002	0.704430	0.000079
SK08-156	3	rim?	5/18/2017	2.5	394	-1.823	0.006702	0.000068	0.05613	0.00057	0.704308	0.000083	0.00670	0.00003	0.704303	0.000088
SK08-156	4	rim	5/18/2017	1.3	212	-1.826	0.006730	0.000130	0.05630	0.00100	0.704385	0.000160	0.12150	0.00730	0.704290	0.000261
SK08-156	5	rim	5/18/2017	2.2	353	-1.840	0.006737	0.000047	0.05642	0.00040	0.704457	0.000091	0.01525	0.00015	0.704445	0.000103
SK08-156	6	core?	5/18/2017	2.5	405	-1.823	0.006718	0.000061	0.05627	0.00051	0.704405	0.000110	0.00393	0.00010	0.704402	0.000113
SK08-156	7	core?	5/18/2017	2.5	405	-1.825	0.006740	0.000053	0.05645	0.00044	0.704335	0.000099	0.00944	0.00017	0.704328	0.000107
SK08-156	8	core?	5/18/2017	2.4	386	-1.831	0.006731	0.000057	0.05637	0.00048	0.704455	0.000110	0.00376	0.00003	0.704452	0.000113
SK08-156	9	core	5/18/2017	2.5	403	-1.827	0.006748	0.000046	0.05652	0.00039	0.704455	0.000110	0.01210	0.00140	0.704446	0.000121
SK08-156	10	core?	5/18/2017	2.8	459	-1.846	0.006750	0.000051	0.05653	0.00043	0.704393	0.000093	0.00341	0.00007	0.704390	0.000096
SK08-156	11	core	5/18/2017	2.6	419	-1.830	0.005160	0.000180	0.04330	0.00150	0.704448	0.000096	0.00526	0.00054	0.704444	0.000101
SK08-156	12	core	5/18/2017	2.8	447	-1.818	0.006722	0.000056	0.05630	0.00047	0.704328	0.000087	0.00247	0.00005	0.704326	0.000089
SK08-150	1	core	7/28/2017	4.2	608	-1.922	0.006732	0.000026	0.05638	0.00022	0.704392	0.000071	0.00203	0.00001	0.704390	0.000073
SK08-150	2	rim	7/28/2017	4.0	576	-1.923	0.006725	0.000022	0.05632	0.00019	0.704313	0.000070	0.01319	0.00080	0.704303	0.000081
SK08-150	3	rim	7/28/2017	4.0	580	-1.939	0.006721	0.000027	0.05629	0.00023	0.704405	0.000075	0.00807	0.00052	0.704399	0.000082
SK08-150	4	interstitial	7/28/2017	3.7	533	-1.918	0.006741	0.000027	0.05646	0.00022	0.704390	0.000082	0.00223	0.00002	0.704388	0.000084
SK08-150	5	core?	7/28/2017	3.6	520	-1.941	0.006719	0.000026	0.05627	0.00022	0.704375	0.000081	0.00233	0.00001	0.704373	0.000083
SK08-150	6	core?	7/28/2017	3.7	522	-1.943	0.006728	0.000027	0.05635	0.00022	0.704320	0.000072	0.00232	0.00002	0.704318	0.000074
SK08-150	7	core?	7/28/2017	4.3	612	-1.924	0.006728	0.000023	0.05635	0.00019	0.704507	0.000087	0.17700	0.00230	0.704368	0.000227
SK08-150	8	core?	7/28/2017	4.2	597	-1.925	0.006727	0.000021	0.05634	0.00018	0.704414	0.000067	0.00335	0.00010	0.704411	0.000070

SK08-150	9	core?	7/28/2017	3.9	546	-1.918	0.006709	0.000025	0.05619	0.00021	0.704408	0.000076	0.00261	0.00002	0.704406	0.000078
SK08-150	10	core	7/28/2017	4.0	560	-1.929	0.006717	0.000028	0.05625	0.00023	0.704421	0.000072	0.00240	0.00002	0.704419	0.000074
SK08-150	11	rim	7/28/2017	4.1	575	-1.923	0.006719	0.000027	0.05627	0.00022	0.704391	0.000074	0.00233	0.00004	0.704389	0.000076
SK08-150	12	core	7/28/2017	3.9	551	-1.924	0.006722	0.000024	0.05630	0.00020	0.704420	0.000086	0.00246	0.00002	0.704418	0.000088
SK08-150	13	core	7/28/2017	3.9	550	-1.916	0.006704	0.000027	0.05615	0.00023	0.704345	0.000073	0.00256	0.00002	0.704343	0.000075
SK08-150	14	rim	7/28/2017	3.9	550	-1.921	0.006737	0.000028	0.05642	0.00024	0.704441	0.000067	0.00261	0.00004	0.704439	0.000069
SK08-148	1	vesitiges in granophyre	7/28/2017	3.0	411	-1.953	0.006703	0.000041	0.05614	0.00034	0.704449	0.000088	0.15100	0.02200	0.704331	0.000223
SK08-148	2	vesitiges in granophyre	7/28/2017	6.2	857	-1.925	0.006731	0.000016	0.05637	0.00013	0.704353	0.000059	0.00392	0.00008	0.704350	0.000062
SK08-148	3	vesitiges in granophyre	7/28/2017	6.5	902	-1.926	0.006734	0.000013	0.05640	0.00011	0.704409	0.000049	0.00446	0.00009	0.704406	0.000053
SK08-148	4	vesitiges in granophyre	7/28/2017	2.6	356	-1.957	0.006705	0.000038	0.05616	0.00032	0.704415	0.000120	0.11480	0.00950	0.704325	0.000217
SK08-148	5	vesitiges in granophyre	7/28/2017	4.9	685	-1.943	0.006727	0.000018	0.05634	0.00015	0.704392	0.000069	0.01365	0.00005	0.704381	0.000080
SK08-148	6	vesitiges in granophyre	7/28/2017	2.9	405	-1.926	0.006698	0.000028	0.05610	0.00023	0.704385	0.000100	0.06060	0.00210	0.704338	0.000149
SK08-148	7	vesitiges in granophyre	7/28/2017	4.5	618	-1.935	0.006725	0.000021	0.05632	0.00017	0.704427	0.000062	0.02437	0.00033	0.704408	0.000081
SK08-148	8	vesitiges in granophyre	7/28/2017	4.9	677	-1.923	0.006734	0.000019	0.05640	0.00016	0.704329	0.000061	0.00710	0.00002	0.704323	0.000067
SK08-148	9	vesitiges in granophyre	7/28/2017	0.6	88	-1.903	0.006640	0.000160	0.05560	0.00130	0.705235	0.000410	2.77000	0.14000	0.703067	0.002688
SK08-103	1	rim	5/17/2017	3.0	450	-1.764	0.006699	0.000048	0.05611	0.00040	0.704332	0.000085	0.00498	0.00013	0.704328	0.000089
SK08-103	2	rim	5/17/2017	2.8	420	-1.791	0.006724	0.000060	0.05632	0.00050	0.704366	0.000090	0.00313	0.00003	0.704364	0.000092
SK08-103	3	rim	5/17/2017	3.1	458	-1.793	0.006717	0.000055	0.05626	0.00046	0.704423	0.000081	0.00573	0.00007	0.704419	0.000086
SK08-103	4	core	5/17/2017	3.1	458	-1.780	0.006714	0.000042	0.05623	0.00035	0.704346	0.000093	0.00261	0.00002	0.704344	0.000095
SK08-103	5	rim	5/17/2017	2.8	422	-1.774	0.006737	0.000054	0.05642	0.00046	0.704375	0.000110	0.01200	0.00006	0.704366	0.000119
SK08-103	6	rim	5/17/2017	3.0	451	-1.784	0.006730	0.000051	0.05636	0.00043	0.704423	0.000088	0.00292	0.00010	0.704421	0.000090
SK08-103	7	core	5/17/2017	3.6	528	-1.800	0.006736	0.000038	0.05642	0.00032	0.704339	0.000076	0.00248	0.00002	0.704337	0.000078
SK08-103	8	rim	5/17/2017	3.3	485	-1.797	0.006758	0.000041	0.05660	0.00034	0.704449	0.000087	0.00336	0.00002	0.704446	0.000090
SK08-103	9	rim	5/17/2017	3.1	461	-1.787	0.006739	0.000050	0.05644	0.00042	0.704406	0.000073	0.00584	0.00025	0.704401	0.000078
SK08-103	10	rim	5/17/2017	3.1	460	-1.782	0.006739	0.000061	0.05644	0.00051	0.704461	0.000081	0.00251	0.00002	0.704459	0.000083
SK08-103	1	interstitial	7/28/2017	4.3	612	-1.960	0.006727	0.000020	0.05634	0.00017	0.704425	0.000071	0.05280	0.00092	0.704384	0.000113
SK08-103	2	interstitial	7/28/2017	3.0	423	-1.963	0.006656	0.000033	0.05575	0.00028	0.704644	0.000095	0.06820	0.00260	0.704591	0.000150
SK08-103	3	core	7/28/2017	3.4	483	-1.953	0.006735	0.000034	0.05641	0.00029	0.704351	0.000091	0.00318	0.00003	0.704349	0.000094
SK08-103	4	interstitial	7/28/2017	4.0	567	-1.923	0.006736	0.000024	0.05642	0.00020	0.704367	0.000061	0.00292	0.00009	0.704365	0.000063
SK08-103	5	interstitial	7/28/2017	4.4	619	-1.941	0.006745	0.000022	0.05649	0.00019	0.704363	0.000070	0.00242	0.00002	0.704361	0.000072
SK08-103	6	interstitial	7/28/2017	4.4	630	-1.936	0.006750	0.000023	0.05653	0.00019	0.704464	0.000060	0.00842	0.00027	0.704457	0.000067
SK08-103	7	rim	7/28/2017	4.7	670	-1.970	0.006740	0.000021	0.05645	0.00018	0.704414	0.000059	0.00251	0.00008	0.704412	0.000061
SK08-103	8	core	7/28/2017	4.6	659	-1.960	0.006729	0.000017	0.05636	0.00015	0.704420	0.000062	0.00237	0.00013	0.704418	0.000064
SK08-103	9	core	7/28/2017	3.9	562	-1.976	0.006729	0.000024	0.05635	0.00020	0.704451	0.000070	0.00238	0.00003	0.704449	0.000072

SK08-103	10	core	7/28/2017	3.4	477	-1.989	0.006718	0.000033	0.05627	0.00028	0.704507	0.000070	0.07050	0.00740	0.704452	0.000131
SK08-103	11	rim	7/28/2017	3.3	474	-2.020	0.006717	0.000031	0.05626	0.00026	0.704357	0.000081	0.01394	0.00084	0.704346	0.000093
SK08-103	12	core	7/28/2017	3.1	446	-1.991	0.006717	0.000031	0.05626	0.00026	0.704422	0.000084	0.03850	0.00410	0.704392	0.000117

Vicinity of Sandwich Horizon

SK08-110	1	core	11/29/2017	12.6	748	-1.673	0.006742	0.000017	0.05646	0.00014	0.704375	0.000034	0.00502	0.00004	0.704371	0.000038
SK08-110	2	rim	11/29/2017	12.3	734	-1.670	0.006740	0.000017	0.05645	0.00014	0.704406	0.000038	0.00448	0.00002	0.704402	0.000042
SK08-110	3	core	11/29/2017	12.6	751	-1.672	0.006743	0.000017	0.05648	0.00014	0.704408	0.000032	0.00437	0.00001	0.704405	0.000035
SK08-110	4	core	11/29/2017	11.7	701	-1.680	0.006740	0.000019	0.05645	0.00016	0.704381	0.000035	0.00692	0.00011	0.704376	0.000041
SK08-110	5	rim	11/29/2017	10.7	642	-1.676	0.006743	0.000018	0.05647	0.00015	0.705206	0.000034	0.06930	0.00140	0.705152	0.000089
SK08-110	6	core	11/29/2017	9.4	563	-1.719	0.006739	0.000019	0.05644	0.00016	0.704448	0.000044	0.02264	0.00032	0.704430	0.000062
SK08-110	7	core	11/29/2017	12.1	727	-1.674	0.006748	0.000015	0.05652	0.00013	0.704385	0.000034	0.00487	0.00006	0.704381	0.000038
SK08-110	8	rim	11/29/2017	9.9	593	-1.719	0.006738	0.000018	0.05644	0.00015	0.704441	0.000041	0.00918	0.00003	0.704434	0.000048
SK08-110	9	core	11/29/2017	11.4	688	-1.674	0.006749	0.000018	0.05653	0.00015	0.704514	0.000038	0.00543	0.00004	0.704510	0.000042
SK08-110	10	rim?	11/29/2017	11.8	714	-1.668	0.006356	0.000054	0.05323	0.00045	0.704418	0.000040	0.01373	0.00067	0.704407	0.000051

SK11-58	1	core	5/18/2017	2.6	449	-1.866	0.006730	0.000060	0.05636	0.00050	0.704407	0.000093	0.02446	0.00079	0.704388	0.000113
SK11-58	2	core	5/18/2017	2.5	430	-1.881	0.006741	0.000062	0.05646	0.00052	0.704385	0.000110	0.01322	0.00082	0.704375	0.000121
SK11-58	3	?	5/18/2017	2.2	383	-1.883	0.006737	0.000075	0.05642	0.00063	0.704505	0.000130	0.09070	0.00150	0.704434	0.000202
SK11-58	4	core	5/18/2017	2.6	455	-1.859	0.006521	0.000076	0.05461	0.00064	0.704345	0.000110	0.02880	0.00190	0.704322	0.000134
SK11-58	5	?	5/18/2017	2.3	404	-1.869	0.006738	0.000057	0.05643	0.00048	0.704416	0.000091	0.01093	0.00067	0.704407	0.000100
SK11-58	6	?	5/18/2017	2.3	402	-1.873	0.006685	0.000051	0.05599	0.00043	0.704405	0.000130	0.01700	0.00190	0.704392	0.000145
SK11-58	7	core	5/18/2017	2.1	368	-1.837	0.006702	0.000067	0.05613	0.00056	0.704295	0.000130	0.00814	0.00005	0.704289	0.000136
SK11-58	8	core	5/18/2017	2.0	352	-1.858	0.006723	0.000053	0.05631	0.00044	0.704315	0.000130	0.00756	0.00016	0.704309	0.000136
SK11-58	9	?	5/18/2017	2.5	433	-1.879	0.006747	0.000056	0.05650	0.00047	0.704432	0.000094	0.01941	0.00097	0.704417	0.000110
SK11-58	10	?	5/18/2017	2.6	451	-1.879	0.006736	0.000054	0.05642	0.00045	0.704453	0.000099	0.02110	0.00160	0.704436	0.000117
SK11-58	11	core	5/18/2017	2.3	400	-1.878	0.006711	0.000070	0.05620	0.00059	0.704325	0.000100	0.00924	0.00011	0.704318	0.000107
SK11-58	12	core	5/18/2017	2.4	414	-1.871	0.006730	0.000055	0.05636	0.00046	0.704415	0.000100	0.00597	0.00009	0.704410	0.000105
SK11-58	1	?	7/28/2017	3.7	532	-1.954	0.006730	0.000023	0.05636	0.00019	0.704567	0.000076	0.09080	0.00730	0.704496	0.000153
SK11-58	2	?	7/28/2017	3.2	458	-1.957	0.006732	0.000028	0.05638	0.00024	0.704382	0.000080	0.02880	0.00220	0.704359	0.000104
SK11-58	3	?	7/28/2017	3.2	459	-1.958	0.006730	0.000026	0.05636	0.00022	0.704375	0.000093	0.01990	0.00110	0.704359	0.000109
SK11-58	4	?	7/28/2017	3.0	420	-1.968	0.006729	0.000034	0.05636	0.00028	0.704445	0.000094	0.01355	0.00044	0.704434	0.000105
SK11-58	5	?	7/28/2017	3.8	543	-1.961	0.006731	0.000027	0.05637	0.00023	0.704674	0.000086	0.18460	0.00310	0.704530	0.000233
SK11-58	6	core?	7/28/2017	3.4	490	-1.953	0.006750	0.000028	0.05653	0.00023	0.704462	0.000094	0.01098	0.00067	0.704453	0.000103
SK11-58	7	rim?	7/28/2017	3.5	496	-1.940	0.006733	0.000030	0.05639	0.00025	0.704359	0.000076	0.00741	0.00027	0.704353	0.000082

SK11-58	8	core	7/28/2017	3.5	502	-1.956	0.006726	0.000032	0.05633	0.00027	0.704456	0.000071	0.03430	0.00200	0.704429	0.000099
---------	---	------	-----------	-----	-----	--------	----------	----------	---------	---------	----------	----------	---------	---------	----------	----------

Layered Series

90-22-31.1	1	core	3/3/2017	4.0	405	-1.632	0.006749	0.000024	0.05652	0.00020	0.704381	0.000066	0.00266	0.00002	0.704379	0.000068
90-22-31.1	2	rim	3/3/2017	4.4	439	-1.633	0.006748	0.000017	0.05652	0.00014	0.704428	0.000072	0.00521	0.00024	0.704424	0.000076
90-22-31.1	3	core	3/3/2017	4.3	431	-1.633	0.006732	0.000023	0.05638	0.00020	0.704328	0.000081	0.00452	0.00039	0.704324	0.000085
90-22-31.1	4	rim	3/3/2017	3.8	390	-1.629	0.006731	0.000027	0.05637	0.00022	0.704364	0.000077	0.00373	0.00004	0.704361	0.000080
90-22-31.1	5	rim	3/3/2017	3.9	399	-1.633	0.006738	0.000027	0.05643	0.00023	0.704392	0.000074	0.00448	0.00022	0.704388	0.000078
90-22-31.1	6	core	3/3/2017	3.9	399	-1.640	0.006730	0.000023	0.05636	0.00020	0.704352	0.000072	0.00391	0.00007	0.704349	0.000075
90-22-31.1	7	core?	3/3/2017	4.2	425	-1.625	0.006745	0.000021	0.05649	0.00017	0.704406	0.000070	0.00299	0.00005	0.704404	0.000072
90-22-31.1	8	core	3/3/2017	3.8	390	-1.639	0.006673	0.000025	0.05589	0.00021	0.704463	0.000065	0.01170	0.00230	0.704454	0.000076
90-22-31.1	9	rim	3/3/2017	3.8	393	-1.619	0.006743	0.000024	0.05647	0.00020	0.704395	0.000068	0.00694	0.00036	0.704390	0.000074
90-22-31.1	10	inclusion	3/3/2017	4.4	455	-1.647	0.006733	0.000022	0.05639	0.00018	0.704364	0.000076	0.00631	0.00022	0.704359	0.000081
90-22-31.1	11	core	3/3/2017	4.0	417	-1.638	0.006723	0.000025	0.05631	0.00021	0.704363	0.000073	0.00637	0.00014	0.704358	0.000078
90-22-31.1	12	core?	3/3/2017	4.1	424	-1.626	0.006727	0.000024	0.05634	0.00020	0.704355	0.000066	0.00298	0.00011	0.704353	0.000068
90-22-87.7	1	rim	3/3/2017	4.2	447	-1.623	0.006725	0.000024	0.05632	0.00020	0.704359	0.000076	0.00688	0.00059	0.704354	0.000082
90-22-87.7	2	core	3/3/2017	4.0	423	-1.617	0.006744	0.000025	0.05648	0.00021	0.704382	0.000076	0.00320	0.00002	0.704379	0.000079
90-22-87.7	3	rim	3/3/2017	4.0	420	-1.622	0.006747	0.000020	0.05651	0.00017	0.704425	0.000083	0.00635	0.00032	0.704420	0.000088
90-22-87.7	4	core	3/3/2017	4.0	421	-1.625	0.006734	0.000022	0.05640	0.00018	0.704448	0.000064	0.00288	0.00002	0.704446	0.000066
90-22-87.7	5	inclusion	3/3/2017	4.0	425	-1.615	0.006731	0.000027	0.05638	0.00022	0.704371	0.000073	0.00382	0.00007	0.704368	0.000076
90-22-87.7	6	core	3/3/2017	4.1	428	-1.617	0.006738	0.000021	0.05644	0.00017	0.704398	0.000072	0.00334	0.00002	0.704395	0.000075
90-22-87.7	7	rim	3/3/2017	3.9	413	-1.625	0.006745	0.000026	0.05649	0.00021	0.704374	0.000085	0.00681	0.00015	0.704369	0.000090
90-22-87.7	8	core	3/3/2017	3.9	414	-1.621	0.006725	0.000027	0.05633	0.00023	0.704431	0.000075	0.00515	0.00019	0.704427	0.000079
90-22-87.7	9	core	3/3/2017	4.1	428	-1.617	0.006738	0.000022	0.05643	0.00019	0.704431	0.000072	0.00280	0.00004	0.704429	0.000074
90-22-87.7	10	inclusion	3/3/2017	4.1	436	-1.621	0.006745	0.000021	0.05649	0.00017	0.704436	0.000076	0.00536	0.00006	0.704432	0.000080
90-22-87.7	11	inclusion	3/3/2017	4.0	423	-1.618	0.006738	0.000023	0.05643	0.00019	0.704345	0.000065	0.00369	0.00014	0.704342	0.000068
90-22-87.7	12	inclusion	3/3/2017	4.0	420	-1.625	0.006739	0.000022	0.05644	0.00019	0.704372	0.000073	0.01390	0.00120	0.704361	0.000085
90-22-384.0	1	core	3/3/2017	3.2	336	-1.631	0.006716	0.000028	0.05625	0.00023	0.704368	0.000093	0.00582	0.00003	0.704363	0.000098
90-22-384.0	2	inclusion	3/3/2017	3.2	334	-1.632	0.006741	0.000027	0.05646	0.00023	0.704443	0.000081	0.00874	0.00004	0.704436	0.000088
90-22-384.0	3	rim	3/3/2017	3.2	336	-1.631	0.006734	0.000029	0.05640	0.00024	0.704385	0.000100	0.00632	0.00018	0.704380	0.000105
90-22-384.0	4	core	3/3/2017	3.1	330	-1.634	0.006723	0.000033	0.05631	0.00028	0.704380	0.000096	0.00395	0.00002	0.704377	0.000099
90-22-384.0	5	rim	3/3/2017	3.1	329	-1.628	0.006738	0.000030	0.05643	0.00025	0.704299	0.000080	0.00967	0.00004	0.704291	0.000088
90-22-384.0	6	inclusion	3/3/2017	3.3	350	-1.629	0.006732	0.000027	0.05639	0.00023	0.704405	0.000083	0.02360	0.00008	0.704387	0.000102

90-22-384.0	7	inclusion	3/3/2017	3.2	336	-1.633	0.006752	0.000024	0.05655	0.00020	0.704344	0.000081	0.03415	0.00014	0.704317	0.000108
90-22-384.0	8	inclusion	3/3/2017	3.2	337	-1.635	0.006749	0.000028	0.05652	0.00023	0.704407	0.000081	0.01799	0.00006	0.704393	0.000095
90-22-384.0	9	rim	3/3/2017	3.1	332	-1.631	0.006742	0.000030	0.05647	0.00025	0.704340	0.000077	0.00611	0.00003	0.704335	0.000082
90-22-384.0	10	core	3/3/2017	3.1	326	-1.634	0.006747	0.000030	0.05651	0.00025	0.704359	0.000093	0.01705	0.00006	0.704346	0.000106
90-22-481.8	1	rim	3/3/2017	3.2	343	-1.629	0.006711	0.000031	0.05621	0.00026	0.704366	0.000084	0.00381	0.00004	0.704363	0.000087
90-22-481.8	2	core	3/3/2017	3.3	347	-1.626	0.006729	0.000024	0.05636	0.00020	0.704347	0.000088	0.00376	0.00008	0.704344	0.000091
90-22-481.8	3	core	3/3/2017	3.2	344	-1.630	0.006740	0.000028	0.05645	0.00023	0.704375	0.000100	0.00357	0.00006	0.704372	0.000103
90-22-481.8	4	core	3/3/2017	3.3	354	-1.632	0.006730	0.000027	0.05637	0.00023	0.704515	0.000085	0.00605	0.00004	0.704510	0.000090
90-22-481.8	5	rim	3/3/2017	3.3	353	-1.630	0.006749	0.000030	0.05652	0.00025	0.704417	0.000073	0.00599	0.00006	0.704412	0.000078
90-22-481.8	6	core	3/3/2017	3.3	350	-1.623	0.006729	0.000027	0.05635	0.00023	0.704368	0.000079	0.00716	0.00092	0.704362	0.000085
90-22-481.8	7	rim	3/3/2017	3.4	357	-1.622	0.006708	0.000029	0.05618	0.00024	0.704416	0.000087	0.01740	0.00180	0.704402	0.000102
90-22-481.8	8	core	3/3/2017	3.3	350	-1.626	0.006736	0.000031	0.05642	0.00026	0.704406	0.000088	0.00630	0.00004	0.704401	0.000093
90-22-481.8	9	inclusion	3/3/2017	3.4	359	-1.633	0.006727	0.000033	0.05634	0.00027	0.704370	0.000086	0.00560	0.00014	0.704366	0.000090
90-22-481.8	10	rim	3/3/2017	3.2	342	-1.636	0.006727	0.000029	0.05634	0.00024	0.704389	0.000094	0.00464	0.00004	0.704385	0.000098
90-22-481.8	11	rim	3/3/2017	3.3	350	-1.632	0.006730	0.000030	0.05636	0.00026	0.704418	0.000082	0.00703	0.00007	0.704412	0.000088
90-22-481.8	12	core	3/3/2017	3.3	348	-1.626	0.006720	0.000029	0.05628	0.00024	0.704434	0.000056	0.00446	0.00005	0.704431	0.000060
90-22-648.4	1	core	11/29/2017	5.9	350	-1.631	0.006765	0.000035	0.05666	0.00029	0.704227	0.000056	0.01245	0.00011	0.704217	0.000066
90-22-648.4	2	core	11/29/2017	5.9	349	-1.633	0.006764	0.000032	0.05665	0.00027	0.704312	0.000057	0.00977	0.00007	0.704304	0.000065
90-22-648.4	3	rim	11/29/2017	6.1	360	-1.630	0.006757	0.000041	0.05659	0.00034	0.704372	0.000056	0.01182	0.00016	0.704363	0.000065
90-22-648.4	4	rim	11/29/2017	6.0	356	-1.630	0.006760	0.000038	0.05662	0.00032	0.704313	0.000056	0.00651	0.00017	0.704308	0.000061
90-22-648.4	5	core	11/29/2017	6.2	367	-1.625	0.006767	0.000035	0.05667	0.00029	0.704269	0.000057	0.01960	0.00100	0.704254	0.000073
90-22-648.4	6	core	11/29/2017	6.2	368	-1.626	0.006775	0.000037	0.05674	0.00031	0.704291	0.000050	0.02080	0.00110	0.704275	0.000067
90-22-648.4	7	rim	11/29/2017	6.2	365	-1.629	0.006757	0.000041	0.05659	0.00035	0.704396	0.000053	0.00904	0.00014	0.704389	0.000060
90-22-648.4	8	rim	11/29/2017	6.5	381	-1.626	0.006773	0.000035	0.05672	0.00029	0.704342	0.000056	0.00787	0.00011	0.704336	0.000062
90-22-648.4	9	rim	11/29/2017	6.2	364	-1.625	0.006765	0.000035	0.05666	0.00029	0.704420	0.000065	0.01665	0.00065	0.704407	0.000079
90-22-648.4	10	core	11/29/2017	6.2	363	-1.628	0.006749	0.000035	0.05652	0.00029	0.704333	0.000052	0.01510	0.00009	0.704321	0.000064
90-22-648.4	11	core	11/29/2017	6.0	349	-1.630	0.006763	0.000038	0.05664	0.00032	0.704316	0.000066	0.01094	0.00058	0.704307	0.000075
90-22-648.4	12	core	11/29/2017	6.2	365	-1.625	0.006764	0.000040	0.05665	0.00034	0.704368	0.000055	0.00729	0.00005	0.704362	0.000061
90-22-648.4	13	core	11/29/2017	6.2	362	-1.630	0.006765	0.000033	0.05666	0.00028	0.704372	0.000061	0.01419	0.00010	0.704361	0.000072
90-22-648.4	14	rim	11/29/2017	6.3	366	-1.628	0.006775	0.000036	0.05674	0.00030	0.704361	0.000053	0.01098	0.00011	0.704352	0.000062
90-22-893.6	1	core	3/2/2017	3.8	329	-1.674	0.006732	0.000025	0.05639	0.00021	0.704324	0.000074	0.00558	0.00007	0.704320	0.000078
90-22-893.6	2	core	3/2/2017	3.9	331	-1.675	0.006738	0.000029	0.05643	0.00024	0.704364	0.000075	0.00402	0.00006	0.704361	0.000078
90-22-893.6	3	rim	3/2/2017	3.8	327	-1.674	0.006749	0.000027	0.05652	0.00023	0.704349	0.000075	0.00770	0.00004	0.704343	0.000081

90-22-893.6	4	core	3/2/2017	3.7	320	-1.675	0.006742	0.000027	0.05646	0.00023	0.704306	0.000077	0.00795	0.00005	0.704300	0.000083
90-22-893.6	5	rim	3/2/2017	3.8	327	-1.673	0.006725	0.000026	0.05633	0.00022	0.704392	0.000092	0.00394	0.00003	0.704389	0.000095
90-22-893.6	6	core	3/2/2017	3.8	322	-1.685	0.006748	0.000023	0.05651	0.00019	0.704325	0.000076	0.00707	0.00005	0.704319	0.000082
90-22-893.6	7	rim	3/2/2017	3.7	318	-1.681	0.006732	0.000025	0.05638	0.00021	0.704303	0.000082	0.00756	0.00047	0.704297	0.000088
90-22-893.6	8	core	3/2/2017	3.7	314	-1.682	0.006733	0.000028	0.05639	0.00023	0.704418	0.000087	0.01393	0.00082	0.704407	0.000099
90-22-893.6	9	core	3/2/2017	3.8	323	-1.681	0.006738	0.000033	0.05643	0.00028	0.704360	0.000089	0.00904	0.00012	0.704353	0.000096
90-22-893.6	10	inclusion	3/2/2017	3.7	318	-1.675	0.006750	0.000025	0.05653	0.00021	0.704354	0.000076	0.01099	0.00003	0.704345	0.000085
458256	1	rim	3/2/2017	3.8	325	-1.670	0.006726	0.000026	0.05633	0.00022	0.704435	0.000078	0.01127	0.00046	0.704426	0.000087
458256	2	interstitial	3/2/2017	3.8	329	-1.668	0.006690	0.000025	0.05603	0.00021	0.704574	0.000086	0.13350	0.00880	0.704470	0.000197
458256	3	rim	3/2/2017	3.7	322	-1.668	0.006735	0.000028	0.05641	0.00024	0.704338	0.000081	0.00711	0.00028	0.704332	0.000087
458256	4	core	3/2/2017	3.7	319	-1.670	0.006736	0.000025	0.05641	0.00021	0.704346	0.000076	0.01107	0.00007	0.704337	0.000085
458256	5	rim	3/2/2017	3.7	322	-1.667	0.006736	0.000027	0.05641	0.00023	0.704375	0.000080	0.00883	0.00012	0.704368	0.000087
458256	6	core	3/2/2017	3.8	328	-1.671	0.006737	0.000023	0.05642	0.00019	0.704402	0.000074	0.00988	0.00010	0.704394	0.000082
458256	7	rim	3/2/2017	3.7	316	-1.677	0.006767	0.000024	0.05667	0.00020	0.704509	0.000079	0.00547	0.00005	0.704505	0.000083
458256	8	core	3/2/2017	3.7	315	-1.676	0.006743	0.000023	0.05648	0.00019	0.704342	0.000075	0.00564	0.00014	0.704338	0.000080
458256	9	core	3/2/2017	3.7	316	-1.676	0.006744	0.000029	0.05648	0.00025	0.704521	0.000077	0.00720	0.00013	0.704515	0.000083
458256	10	core	3/2/2017	3.9	333	-1.672	0.006731	0.000027	0.05637	0.00023	0.704386	0.000068	0.00794	0.00015	0.704380	0.000074
458257	1	core	3/2/2017	3.7	319	-1.671	0.006771	0.000027	0.05671	0.00023	0.704438	0.000085	0.00810	0.00026	0.704432	0.000092
458257	2	interstitial	3/2/2017	3.8	333	-1.680	0.006743	0.000025	0.05647	0.00021	0.704393	0.000079	0.00561	0.00027	0.704389	0.000084
458257	3	inclusion	3/2/2017	3.8	331	-1.676	0.006749	0.000023	0.05652	0.00019	0.704366	0.000070	0.00627	0.00007	0.704361	0.000075
458257	4	inclusion	3/2/2017	3.8	325	-1.677	0.006726	0.000025	0.05633	0.00021	0.704422	0.000071	0.01078	0.00009	0.704414	0.000080
458257	5	core	3/2/2017	3.7	324	-1.675	0.006743	0.000026	0.05647	0.00022	0.704464	0.000073	0.00707	0.00011	0.704458	0.000079
458257	6	interstitial	3/2/2017	3.8	326	-1.675	0.006732	0.000029	0.05638	0.00024	0.704326	0.000067	0.00926	0.00010	0.704319	0.000074
458257	7	rim	3/2/2017	3.6	314	-1.674	0.006772	0.000024	0.05672	0.00020	0.704361	0.000071	0.00512	0.00026	0.704357	0.000075
458257	8	core	3/2/2017	3.7	319	-1.673	0.006747	0.000026	0.05651	0.00022	0.704356	0.000091	0.00310	0.00010	0.704354	0.000094
458257	9	core	3/2/2017	3.7	316	-1.675	0.006730	0.000029	0.05637	0.00024	0.704344	0.000078	0.00554	0.00010	0.704340	0.000082
458257	10	core	3/2/2017	3.7	321	-1.674	0.006732	0.000027	0.05638	0.00023	0.704352	0.000080	0.00519	0.00030	0.704348	0.000084
458286	1	core	11/29/2017	4.9	302	-1.676	0.006757	0.000042	0.05659	0.00035	0.704427	0.000058	0.01199	0.00011	0.704418	0.000067
458286	2	core	11/29/2017	5.0	312	-1.675	0.006745	0.000036	0.05649	0.00030	0.704307	0.000070	0.01268	0.00009	0.704297	0.000080
458286	3	rim	11/29/2017	4.8	299	-1.677	0.006743	0.000051	0.05647	0.00042	0.704383	0.000058	0.00888	0.00007	0.704376	0.000065
458286	4	core	11/29/2017	4.5	280	-1.669	0.006295	0.000060	0.05272	0.00050	0.704430	0.000070	0.00916	0.00024	0.704423	0.000077
458286	5	rim	11/29/2017	4.9	304	-1.683	0.006734	0.000046	0.05640	0.00039	0.704443	0.000057	0.00717	0.00007	0.704437	0.000063
458286	6	core	11/29/2017	4.9	306	-1.680	0.006752	0.000039	0.05655	0.00033	0.704359	0.000074	0.00704	0.00010	0.704353	0.000080

458286	7	rim	11/29/2017	4.9	309	-1.678	0.006756	0.000039	0.05658	0.00033	0.704400	0.000062	0.00720	0.00006	0.704394	0.000068
458286	8	rim	11/29/2017	4.9	306	-1.681	0.006749	0.000040	0.05653	0.00033	0.704348	0.000065	0.00711	0.00008	0.704342	0.000071
458286	9	inclusion	11/29/2017	4.8	301	-1.679	0.006757	0.000037	0.05659	0.00031	0.704406	0.000066	0.00931	0.00007	0.704399	0.000073
458286	10	inclusion	11/29/2017	4.9	309	-1.678	0.006741	0.000037	0.05645	0.00031	0.704338	0.000068	0.00767	0.00005	0.704332	0.000074
458286	11	inclusion	11/29/2017	4.8	298	-1.678	0.006749	0.000045	0.05653	0.00037	0.704379	0.000071	0.00790	0.00006	0.704373	0.000077
458286	12	core	11/29/2017	5.1	319	-1.678	0.006752	0.000037	0.05655	0.00031	0.704676	0.000054	0.01346	0.00013	0.704665	0.000065
458277	1	rim	3/2/2017	3.6	289	-1.653	0.006729	0.000024	0.05636	0.00020	0.704357	0.000067	0.00916	0.00010	0.704350	0.000074
458277	2	rim	3/2/2017	3.8	303	-1.656	0.006740	0.000028	0.05645	0.00023	0.704366	0.000086	0.00947	0.00006	0.704359	0.000093
458277	3	core	3/2/2017	3.7	298	-1.656	0.006758	0.000027	0.05660	0.00023	0.704319	0.000066	0.01073	0.00029	0.704311	0.000075
458277	4	rim	3/2/2017	3.7	301	-1.651	0.006755	0.000029	0.05657	0.00024	0.704386	0.000070	0.00737	0.00005	0.704380	0.000076
458277	5	core	3/2/2017	3.6	288	-1.653	0.006753	0.000026	0.05656	0.00022	0.704364	0.000084	0.00830	0.00008	0.704358	0.000091
458277	6	cire	3/2/2017	3.6	288	-1.653	0.006683	0.000034	0.05597	0.00028	0.704375	0.000094	0.02969	0.00021	0.704352	0.000117
458277	7	rim	3/2/2017	3.9	314	-1.656	0.006749	0.000024	0.05652	0.00020	0.704357	0.000075	0.00609	0.00006	0.704352	0.000080
458277	8	rim	3/2/2017	4.1	330	-1.654	0.006746	0.000023	0.05650	0.00019	0.704400	0.000068	0.00492	0.00009	0.704396	0.000072
458277	9	?	3/2/2017	0.2	17	-1.567	N.D.	0.000530	N.D.	0.00440	0.707395	0.001100	0.01190	0.00100	0.707386	0.001110
458277	10	rim	3/2/2017	3.6	287	-1.651	0.006733	0.000030	0.05639	0.00025	0.704331	0.000088	0.00884	0.00008	0.704324	0.000095
458277	11	rim	3/2/2017	3.6	288	-1.660	0.006741	0.000028	0.05646	0.00024	0.704425	0.000077	0.00995	0.00008	0.704417	0.000085
458277	12	core	3/2/2017	3.5	284	-1.658	0.006744	0.000028	0.05648	0.00023	0.704401	0.000082	0.00783	0.00015	0.704395	0.000088
458277	13	core	3/2/2017	3.6	290	-1.653	0.006754	0.000028	0.05656	0.00023	0.704377	0.000072	0.00706	0.00009	0.704371	0.000078
458277	14	rim	3/2/2017	3.7	294	-1.657	0.006731	0.000026	0.05638	0.00022	0.704398	0.000080	0.01041	0.00055	0.704390	0.000089
458203	1	rim	11/29/2017	4.7	298	-1.678	0.006733	0.000043	0.05639	0.00036	0.704286	0.000060	0.00709	0.00005	0.704280	0.000066
458203	2	core	11/29/2017	4.6	297	-1.679	0.006734	0.000041	0.05640	0.00035	0.704232	0.000074	0.00662	0.00008	0.704227	0.000079
458203	3	rim	11/29/2017	4.9	311	-1.681	0.006744	0.000042	0.05648	0.00036	0.704281	0.000060	0.00710	0.00004	0.704275	0.000066
458203	4	core	11/29/2017	4.6	295	-1.680	0.006740	0.000045	0.05645	0.00037	0.704288	0.000062	0.00940	0.00005	0.704281	0.000069
458203	5	rim	11/29/2017	4.7	298	-1.678	0.006766	0.000054	0.05667	0.00045	0.704362	0.000070	0.00994	0.00006	0.704354	0.000078
458203	6	core	11/29/2017	4.7	301	-1.682	0.006745	0.000043	0.05649	0.00036	0.704279	0.000077	0.00979	0.00005	0.704271	0.000085
458203	7	core	11/29/2017	4.6	295	-1.686	0.006749	0.000039	0.05653	0.00032	0.704375	0.000069	0.00989	0.00006	0.704367	0.000077
458203	8	core	11/29/2017	4.8	308	-1.687	0.006740	0.000046	0.05645	0.00038	0.704304	0.000069	0.00843	0.00004	0.704297	0.000076
458203	9	rim	11/29/2017	4.7	302	-1.683	0.006745	0.000047	0.05649	0.00039	0.704311	0.000062	0.00974	0.00007	0.704303	0.000070
458203	10	rim	11/29/2017	4.7	306	-1.685	0.006764	0.000042	0.05665	0.00035	0.704311	0.000065	0.01191	0.00007	0.704302	0.000074
458203	11	core	11/29/2017	4.7	305	-1.685	0.006757	0.000046	0.05659	0.00039	0.704356	0.000061	0.01002	0.00006	0.704348	0.000069
458203	12	core	11/29/2017	4.6	296	-1.679	0.006780	0.000050	0.05678	0.00042	0.704232	0.000070	0.00575	0.00003	0.704227	0.000075
458231	1	core	3/2/2017	3.6	295	-1.651	0.006730	0.000027	0.05637	0.00023	0.704312	0.000072	0.00548	0.00005	0.704308	0.000076

458231	2	rim	3/2/2017	3.7	301	-1.652	0.006758	0.000030	0.05660	0.00025	0.704303	0.000078	0.00770	0.00005	0.704297	0.000084
458231	3	rim	3/2/2017	3.7	303	-1.652	0.006730	0.000025	0.05636	0.00021	0.704300	0.000083	0.00549	0.00007	0.704296	0.000087
458231	4	core	3/2/2017	3.7	302	-1.653	0.006733	0.000024	0.05639	0.00020	0.704318	0.000083	0.00740	0.00088	0.704312	0.000089
458231	5	core	3/2/2017	3.7	300	-1.652	0.006733	0.000026	0.05639	0.00022	0.704322	0.000080	0.00478	0.00003	0.704318	0.000084
458231	6	rim	3/2/2017	3.8	306	-1.657	0.006752	0.000027	0.05655	0.00022	0.704360	0.000071	0.00676	0.00003	0.704355	0.000076
458231	7	core	3/2/2017	3.7	301	-1.653	0.006746	0.000024	0.05650	0.00020	0.704326	0.000085	0.00532	0.00003	0.704322	0.000089
458231	8	core	3/2/2017	3.8	310	-1.655	0.006740	0.000027	0.05645	0.00023	0.704317	0.000074	0.00511	0.00003	0.704313	0.000078
458231	9	rim	3/2/2017	3.9	312	-1.649	0.006738	0.000027	0.05643	0.00022	0.704301	0.000074	0.00890	0.00005	0.704294	0.000081
458231	10	rim	3/2/2017	3.8	303	-1.656	0.006737	0.000027	0.05642	0.00022	0.704379	0.000082	0.00643	0.00003	0.704374	0.000087
458231	11	interstitial	3/2/2017	3.7	298	-1.650	0.006748	0.000026	0.05651	0.00022	0.704315	0.000100	0.00814	0.00003	0.704309	0.000106
458231	12	interstitial	3/2/2017	3.8	303	-1.651	0.006744	0.000027	0.05648	0.00022	0.704331	0.000073	0.00542	0.00008	0.704327	0.000077
458220	1	core	3/2/2017	3.1	267	-1.676	0.006724	0.000029	0.05632	0.00024	0.704219	0.000092	0.02406	0.00059	0.704200	0.000111
458220	2	rim	3/2/2017	3.4	288	-1.678	0.006734	0.000031	0.05640	0.00026	0.704246	0.000074	0.00925	0.00016	0.704239	0.000081
458220	3	rim	3/2/2017	3.3	279	-1.678	0.006720	0.000031	0.05628	0.00026	0.704301	0.000078	0.01008	0.00016	0.704293	0.000086
458220	4	core	3/2/2017	3.2	271	-1.676	0.006724	0.000032	0.05631	0.00027	0.704294	0.000090	0.00640	0.00100	0.704289	0.000096
458220	5	core	3/2/2017	3.2	268	-1.672	0.006722	0.000027	0.05630	0.00023	0.704268	0.000079	0.00337	0.00005	0.704265	0.000082
458220	6	rim	3/2/2017	3.3	277	-1.673	0.006704	0.000027	0.05615	0.00023	0.704319	0.000083	0.00861	0.00013	0.704312	0.000090
458220	7	core	3/2/2017	3.2	274	-1.678	0.006739	0.000031	0.05644	0.00026	0.704264	0.000084	0.00500	0.00010	0.704260	0.000088
458220	8	rim	3/2/2017	3.4	284	-1.678	0.006738	0.000032	0.05643	0.00027	0.704241	0.000079	0.00739	0.00032	0.704235	0.000085
458220	9	core	3/2/2017	3.2	269	-1.677	0.006741	0.000032	0.05646	0.00027	0.704236	0.000083	0.00451	0.00004	0.704232	0.000087
458220	10	rim	3/2/2017	3.2	268	-1.678	0.006761	0.000036	0.05663	0.00030	0.704256	0.000089	0.00547	0.00002	0.704252	0.000093
458218	1	core	11/29/2017	4.6	273	-1.662	0.006723	0.000048	0.05631	0.00040	0.704215	0.000073	0.00582	0.00004	0.704210	0.000078
458218	2	core	11/29/2017	4.5	272	-1.668	0.006741	0.000049	0.05646	0.00041	0.704244	0.000071	0.00572	0.00006	0.704240	0.000076
458218	3	rim	11/29/2017	4.7	283	-1.669	0.006720	0.000038	0.05628	0.00031	0.704251	0.000064	0.00905	0.00015	0.704244	0.000071
458218	4	rim	11/29/2017	5.0	301	-1.670	0.006740	0.000039	0.05645	0.00033	0.704262	0.000065	0.00685	0.00005	0.704257	0.000070
458218	5	core	11/29/2017	4.6	277	-1.666	0.006749	0.000042	0.05652	0.00035	0.704203	0.000062	0.00711	0.00009	0.704197	0.000068
458218	6	core	11/29/2017	4.8	286	-1.667	0.006743	0.000044	0.05648	0.00037	0.704169	0.000056	0.00858	0.00007	0.704162	0.000063
458218	7	rim	11/29/2017	4.9	294	-1.667	0.006737	0.000037	0.05642	0.00031	0.704216	0.000071	0.01260	0.00004	0.704206	0.000081
458218	8	rim	11/29/2017	4.6	279	-1.668	0.006665	0.000054	0.05582	0.00046	0.704288	0.000077	0.02550	0.00560	0.704268	0.000101
458218	9	core	11/29/2017	4.9	293	-1.671	0.006758	0.000040	0.05660	0.00033	0.704208	0.000059	0.00723	0.00008	0.704202	0.000065
458218	10	rim	11/29/2017	4.9	296	-1.673	0.006733	0.000042	0.05639	0.00035	0.704252	0.000066	0.01104	0.00012	0.704243	0.000075
458218	11	core?	11/29/2017	5.0	305	-1.672	0.006725	0.000037	0.05632	0.00031	0.704211	0.000059	0.00946	0.00030	0.704204	0.000067
458218	12	rim	11/29/2017	5.0	305	-1.670	0.006735	0.000046	0.05641	0.00038	0.704204	0.000061	0.00563	0.00002	0.704200	0.000065
458218	13	core	11/29/2017	4.5	272	-1.665	0.006719	0.000056	0.05627	0.00047	0.704199	0.000068	0.00451	0.00008	0.704195	0.000072

458218	14	core	11/29/2017	4.7	283	-1.662	0.006749	0.000050	0.05653	0.00042	0.704141	0.000071	0.00733	0.00009	0.704135	0.000077
458218	15	rim	11/29/2017	4.6	278	-1.667	0.006743	0.000040	0.05648	0.00033	0.704214	0.000072	0.01048	0.00007	0.704206	0.000080
458218	16	rim	11/29/2017	4.5	276	-1.665	0.006718	0.000051	0.05626	0.00042	0.704191	0.000060	0.00399	0.00006	0.704188	0.000063
458214	1	rim	11/29/2017	5.2	296	-1.623	0.006728	0.000038	0.05635	0.00032	0.704071	0.000067	0.00550	0.00004	0.704067	0.000071
458214	2	rim	11/29/2017	5.5	312	-1.629	0.006748	0.000039	0.05652	0.00033	0.704176	0.000057	0.00552	0.00002	0.704172	0.000061
458214	3	core	11/29/2017	4.9	278	-1.627	0.006737	0.000049	0.05643	0.00041	0.704214	0.000070	0.00775	0.00079	0.704208	0.000077
458214	4	core	11/29/2017	5.3	300	-1.623	0.006749	0.000040	0.05652	0.00033	0.704175	0.000062	0.00716	0.00012	0.704169	0.000068
458214	5	core	11/29/2017	5.0	282	-1.620	0.006766	0.000047	0.05666	0.00039	0.704149	0.000065	0.00552	0.00004	0.704145	0.000069
458214	6	rim?	11/29/2017	5.2	292	-1.623	0.006743	0.000039	0.05648	0.00033	0.704183	0.000059	0.00588	0.00009	0.704178	0.000064
458214	7	rim	11/29/2017	5.1	290	-1.626	0.006410	0.000087	0.05369	0.00073	0.704268	0.000060	0.00675	0.00015	0.704263	0.000065
458214	8	rim	11/29/2017	5.5	310	-1.633	0.006740	0.000035	0.05645	0.00029	0.704221	0.000061	0.00911	0.00040	0.704214	0.000068
458214	9	rim	11/29/2017	5.1	287	-1.620	0.006740	0.000040	0.05645	0.00033	0.704137	0.000061	0.00442	0.00003	0.704134	0.000064
458214	10	core	11/29/2017	5.2	290	-1.624	0.006762	0.000048	0.05663	0.00040	0.704205	0.000068	0.00485	0.00002	0.704201	0.000072
458214	11	core	11/29/2017	5.2	294	-1.622	0.006754	0.000043	0.05657	0.00036	0.704141	0.000061	0.00429	0.00002	0.704138	0.000064
458214	12	rim	11/29/2017	5.1	283	-1.629	0.006718	0.000045	0.05626	0.00038	0.704202	0.000070	0.00436	0.00030	0.704199	0.000074
458214	13	rim	11/29/2017	5.6	311	-1.628	0.006726	0.000048	0.05633	0.00040	0.704165	0.000068	0.00701	0.00002	0.704160	0.000074
458214	14	core	11/29/2017	5.3	298	-1.621	0.006741	0.000040	0.05645	0.00033	0.704186	0.000065	0.00418	0.00002	0.704183	0.000068
458214	15	rim	11/29/2017	5.4	303	-1.629	0.006756	0.000046	0.05658	0.00038	0.704150	0.000063	0.00169	0.00002	0.704149	0.000064
458214	16	interstitial	11/29/2017	5.2	288	-1.628	0.006741	0.000039	0.05645	0.00032	0.704214	0.000058	0.01063	0.00032	0.704206	0.000067
458213	1	core	3/2/2017	3.0	254	-1.676	0.006739	0.000034	0.05644	0.00028	0.704175	0.000100	0.00533	0.00011	0.704171	0.000104
458213	2	core	3/2/2017	3.2	274	-1.674	0.006732	0.000031	0.05638	0.00026	0.704120	0.000084	0.00784	0.00004	0.704114	0.000090
458213	3	rim	3/2/2017	3.0	254	-1.676	0.006731	0.000036	0.05637	0.00030	0.704026	0.000084	0.00314	0.00003	0.704024	0.000086
458213	4	core?	3/2/2017	3.1	262	-1.677	0.006737	0.000034	0.05643	0.00028	0.704169	0.000088	0.00568	0.00035	0.704165	0.000093
458213	5	rim	3/2/2017	3.1	265	-1.680	0.006725	0.000032	0.05632	0.00027	0.704141	0.000090	0.00359	0.00002	0.704138	0.000093
458213	6	core	3/2/2017	3.1	264	-1.672	0.006727	0.000032	0.05634	0.00026	0.704115	0.000100	0.00429	0.00006	0.704112	0.000103
458213	7	rim	3/2/2017	3.2	273	-1.676	0.006717	0.000028	0.05626	0.00024	0.704079	0.000075	0.00325	0.00009	0.704076	0.000078
458213	8	inclusion	3/2/2017	3.0	251	-1.683	0.006714	0.000034	0.05623	0.00028	0.704085	0.000084	0.00289	0.00009	0.704083	0.000086
458213	9	inclusion	3/2/2017	3.1	262	-1.679	0.006728	0.000031	0.05635	0.00026	0.704137	0.000092	0.00215	0.00003	0.704135	0.000094
458213	10	inclusion	3/2/2017	3.1	257	-1.680	0.006727	0.000033	0.05634	0.00028	0.704090	0.000087	0.00109	0.00003	0.704089	0.000088
458213	1	core	7/28/2017	1.8	265	-1.963	0.006733	0.000061	0.05639	0.00051	0.704035	0.000140	0.00286	0.00007	0.704033	0.000142
458213	2	core	7/28/2017	2.0	288	-1.957	0.006754	0.000046	0.05657	0.00038	0.704285	0.000110	0.00545	0.00009	0.704281	0.000114
458213	3	core	7/28/2017	2.0	289	-1.945	0.006712	0.000039	0.05621	0.00033	0.704175	0.000140	0.00366	0.00004	0.704172	0.000143
458213	4	rim	7/28/2017	2.1	305	-1.946	0.006716	0.000037	0.05625	0.00031	0.704105	0.000110	0.00900	0.00110	0.704098	0.000118
458213	5	rim	7/28/2017	2.1	307	-1.947	0.006724	0.000039	0.05632	0.00033	0.704195	0.000140	0.00541	0.00021	0.704191	0.000144

458213	6	rim	7/28/2017	2.1	310	-1.951	0.006737	0.000040	0.05643	0.00034	0.704145	0.000100	0.00753	0.00046	0.704139	0.000106
458213	7	rim	7/28/2017	2.1	304	-1.942	0.006716	0.000044	0.05625	0.00037	0.704245	0.000110	0.00416	0.00012	0.704242	0.000113
458213	8	rim	7/28/2017	2.0	294	-1.945	0.006730	0.000043	0.05636	0.00036	0.704075	0.000120	0.00404	0.00010	0.704072	0.000123
458213	9	core	7/28/2017	1.9	270	-1.940	0.006733	0.000040	0.05639	0.00033	0.704095	0.000140	0.00764	0.00096	0.704089	0.000147
458213	10	core	7/28/2017	1.9	279	-1.932	0.006700	0.000039	0.05612	0.00033	0.703995	0.000120	0.00464	0.00026	0.703991	0.000124
458213	11	core	7/28/2017	2.0	292	-1.931	0.006759	0.000051	0.05661	0.00043	0.704136	0.000099	0.00432	0.00014	0.704133	0.000102
458213	12	rim	7/28/2017	2.0	292	-1.940	0.006711	0.000053	0.05621	0.00045	0.704075	0.000120	0.00401	0.00017	0.704072	0.000123
458213	13	rim	7/28/2017	2.1	301	-1.943	0.006712	0.000040	0.05622	0.00034	0.704005	0.000120	0.00523	0.00004	0.704001	0.000124
458213	14	rim	7/28/2017	2.0	289	-1.940	0.006706	0.000048	0.05616	0.00040	0.704015	0.000140	0.34000	0.11000	0.703749	0.000492
458211	1	rim	3/2/2017	3.4	274	-1.655	0.006716	0.000028	0.05625	0.00024	0.704172	0.000083	0.00402	0.00022	0.704169	0.000086
458211	2	core	3/2/2017	3.4	278	-1.657	0.006702	0.000027	0.05613	0.00023	0.704128	0.000077	0.00541	0.00040	0.704124	0.000082
458211	3	core	3/2/2017	3.4	277	-1.662	0.006722	0.000028	0.05630	0.00023	0.704130	0.000075	0.00207	0.00007	0.704128	0.000077
458211	4	rim	3/2/2017	3.4	274	-1.653	0.006740	0.000031	0.05645	0.00026	0.704133	0.000079	0.02060	0.00280	0.704117	0.000097
458211	5	rim	3/2/2017	3.5	285	-1.653	0.006732	0.000026	0.05638	0.00022	0.704296	0.000078	0.00314	0.00002	0.704294	0.000080
458211	6	core	3/2/2017	3.3	268	-1.645	0.006724	0.000032	0.05632	0.00027	0.704093	0.000077	0.00455	0.00031	0.704089	0.000081
458211	7	core(?)	3/2/2017	3.3	266	-1.648	0.006734	0.000033	0.05640	0.00027	0.704213	0.000078	0.00339	0.00004	0.704210	0.000081
458211	8	rim	3/2/2017	3.4	276	-1.650	0.006757	0.000029	0.05659	0.00025	0.704169	0.000090	0.00204	0.00002	0.704167	0.000092
458211	9	core	3/2/2017	3.3	269	-1.642	0.006726	0.000029	0.05633	0.00024	0.704191	0.000078	0.00387	0.00013	0.704188	0.000081
458211	10	core	3/2/2017	3.4	273	-1.646	0.006735	0.000033	0.05640	0.00027	0.704185	0.000080	0.00442	0.00003	0.704182	0.000083
458211	11	rim	3/2/2017	3.4	278	-1.649	0.006730	0.000031	0.05636	0.00026	0.704181	0.000083	0.00366	0.00002	0.704178	0.000086
458211	12	inclusion	3/2/2017	3.6	295	-1.651	0.006745	0.000028	0.05649	0.00024	0.704204	0.000081	0.00261	0.00002	0.704202	0.000083
458211	13	inclusion	3/2/2017	3.2	263	-1.647	0.006744	0.000023	0.05648	0.00019	0.704130	0.000075	0.00497	0.00037	0.704126	0.000079
458211	14	inclusion	3/2/2017	3.3	264	-1.655	0.006729	0.000028	0.05636	0.00023	0.704206	0.000088	0.00134	0.00002	0.704205	0.000089
458211	1	core	7/28/2017	2.0	282	-1.965	0.006722	0.000044	0.05630	0.00037	0.704215	0.000140	0.01056	0.00048	0.704207	0.000149
458211	2	core	7/28/2017	2.0	292	-1.965	0.006729	0.000048	0.05636	0.00040	0.704265	0.000110	0.00177	0.00025	0.704264	0.000112
458211	3	core	7/28/2017	2.2	308	-1.958	0.006713	0.000045	0.05623	0.00037	0.704235	0.000120	0.00844	0.00050	0.704228	0.000127
458211	4	rim	7/28/2017	2.2	317	-1.958	0.006723	0.000032	0.05631	0.00027	0.704215	0.000110	0.01100	0.00130	0.704206	0.000120
458211	5	rim	7/28/2017	2.0	293	-1.953	0.006713	0.000047	0.05623	0.00039	0.704245	0.000120	0.00344	0.00038	0.704242	0.000123
458211	6	rim	7/28/2017	2.1	308	-1.955	0.006738	0.000040	0.05643	0.00033	0.704255	0.000120	0.00198	0.00004	0.704253	0.000122
458211	7	core	7/28/2017	1.9	275	-1.982	0.006730	0.000045	0.05636	0.00037	0.704205	0.000120	0.00339	0.00020	0.704202	0.000123
458211	8	core	7/28/2017	2.0	289	-1.978	0.006717	0.000043	0.05626	0.00036	0.704305	0.000130	0.01060	0.00120	0.704297	0.000139
458211	9	core	7/28/2017	2.1	300	-1.962	0.006725	0.000050	0.05632	0.00042	0.704095	0.000130	0.01180	0.00120	0.704086	0.000140
458211	10	rim	7/28/2017	2.0	294	-1.973	0.006743	0.000050	0.05647	0.00041	0.704275	0.000130	0.00830	0.00035	0.704269	0.000137
458211	11	rim	7/28/2017	2.1	302	-1.971	0.006727	0.000037	0.05634	0.00031	0.704235	0.000120	0.00395	0.00008	0.704232	0.000123
458211	12	rim	7/28/2017	2.1	309	-1.966	0.006728	0.000046	0.05635	0.00038	0.704285	0.000120	0.00339	0.00012	0.704282	0.000123

458211	13	core	7/28/2017	2.2	323	-1.967	0.006725	0.000039	0.05632	0.00033	0.704256	0.000099	0.01690	0.00120	0.704243	0.000113
458211	14	core	7/28/2017	2.2	317	-1.966	0.006703	0.000045	0.05614	0.00038	0.704187	0.000096	0.00471	0.00024	0.704183	0.000100
458211	15	rim	7/28/2017	2.4	344	-1.973	0.006729	0.000031	0.05636	0.00026	0.704305	0.000100	0.00674	0.00007	0.704300	0.000105
458211	16	rim	7/28/2017	2.4	339	-1.972	0.006726	0.000041	0.05633	0.00035	0.704225	0.000110	0.01162	0.00088	0.704216	0.000120

Secondary Standard

T21	N.A.	N.A.	5/17/2017	6.3	976	-1.814	0.006724	0.000029	0.05632	0.00025	0.704630	0.000050	0.00484	0.00002	N.A.	N.A.
T21	N.A.	N.A.	11/29/2017	15.3	912	-1.633	0.006747	0.000015	0.05651	0.00012	0.704642	0.000030	0.00615	0.00002	N.A.	N.A.
T21	N.A.	N.A.	7/28/2017	7.2	1045	-1.953	0.006736	0.000013	0.05641	0.00011	0.704656	0.000044	0.00748	0.00006	N.A.	N.A.
T21	N.A.	N.A.	7/28/2017	7.1	1027	-1.883	0.006742	0.000012	0.05646	0.00010	0.704660	0.000046	0.00787	0.00004	N.A.	N.A.
T21	N.A.	N.A.	7/28/2017	7.3	1042	-1.931	0.006732	0.000009	0.05638	0.00007	0.704661	0.000050	0.00808	0.00004	N.A.	N.A.
T21	N.A.	N.A.	5/17/2017	6.2	915	-1.814	0.006743	0.000028	0.05647	0.00023	0.704662	0.000054	0.00500	0.00002	N.A.	N.A.
T21	N.A.	N.A.	7/28/2017	7.5	1064	-1.928	0.006736	0.000015	0.05641	0.00013	0.704665	0.000050	0.00861	0.00007	N.A.	N.A.
T21	N.A.	N.A.	5/18/2017	5.8	990	-1.855	0.006731	0.000030	0.05637	0.00025	0.704667	0.000055	0.00524	0.00002	N.A.	N.A.
T21	N.A.	N.A.	11/29/2017	16.9	984	-1.659	0.006738	0.000012	0.05643	0.00010	0.704667	0.000030	0.00600	0.00001	N.A.	N.A.
T21	N.A.	N.A.	7/28/2017	7.2	1035	-1.837	0.006737	0.000013	0.05642	0.00011	0.704667	0.000043	0.00746	0.00002	N.A.	N.A.
T21	N.A.	N.A.	7/28/2017	7.5	1032	-1.862	0.006744	0.000011	0.05648	0.00010	0.704669	0.000052	0.00729	0.00009	N.A.	N.A.
T21	N.A.	N.A.	5/18/2017	6.1	974	-1.827	0.006739	0.000026	0.05644	0.00022	0.704670	0.000058	0.00488	0.00002	N.A.	N.A.
T21	N.A.	N.A.	3/2/2017	11.8	989	-1.686	0.006745	0.000008	0.05649	0.00007	0.704673	0.000039	0.00497	0.00002	N.A.	N.A.
T21	N.A.	N.A.	3/2/2017	12.7	1041	-1.661	0.006731	0.000008	0.05637	0.00007	0.704674	0.000033	0.00538	0.00002	N.A.	N.A.
T21	N.A.	N.A.	7/28/2017	7.4	1042	-1.897	0.006727	0.000012	0.05634	0.00010	0.704675	0.000048	0.00620	0.00002	N.A.	N.A.
T21	N.A.	N.A.	11/29/2017	15.5	962	-1.685	0.006738	0.000016	0.05644	0.00013	0.704676	0.000033	0.00656	0.00001	N.A.	N.A.
T21	N.A.	N.A.	7/28/2017	7.3	997	-1.864	0.006736	0.000014	0.05642	0.00012	0.704677	0.000045	0.00682	0.00001	N.A.	N.A.
T21	N.A.	N.A.	3/3/2017	10.4	1034	-1.636	0.006741	0.000008	0.05646	0.00006	0.704679	0.000039	0.00493	0.00001	N.A.	N.A.
T21	N.A.	N.A.	11/29/2017	15.4	980	-1.685	0.006739	0.000012	0.05644	0.00010	0.704685	0.000032	0.00628	0.00001	N.A.	N.A.
T21	N.A.	N.A.	7/28/2017	7.4	1038	-1.835	0.006736	0.000016	0.05642	0.00014	0.704686	0.000052	0.00645	0.00005	N.A.	N.A.
T21	N.A.	N.A.	7/28/2017	7.4	1009	-1.933	0.006737	0.000012	0.05643	0.00010	0.704688	0.000045	0.00652	0.00005	N.A.	N.A.
T21	N.A.	N.A.	5/18/2017	5.7	958	-1.832	0.006737	0.000026	0.05643	0.00022	0.704690	0.000068	0.00522	0.00004	N.A.	N.A.
T21	N.A.	N.A.	11/29/2017	16.6	961	-1.632	0.006748	0.000014	0.05652	0.00012	0.704690	0.000027	0.00572	0.00001	N.A.	N.A.
T21	N.A.	N.A.	11/29/2017	16.1	976	-1.680	0.006741	0.000008	0.05646	0.00007	0.704690	0.000032	0.00598	0.00001	N.A.	N.A.
T21	N.A.	N.A.	11/29/2017	17.2	963	-1.652	0.006741	0.000014	0.05645	0.00012	0.704691	0.000029	0.00633	0.00001	N.A.	N.A.
T21	N.A.	N.A.	5/17/2017	6.6	977	-1.809	0.006731	0.000024	0.05637	0.00020	0.704693	0.000050	0.00507	0.00002	N.A.	N.A.
T21	N.A.	N.A.	5/18/2017	5.9	1003	-1.852	0.006738	0.000021	0.05643	0.00017	0.704693	0.000056	0.00483	0.00002	N.A.	N.A.
T21	N.A.	N.A.	3/3/2017	15.7	N.D.	-1.735	0.006737	0.000005	N.D.	N.D.	0.704699	0.000032	0.00631	0.00004	N.A.	N.A.
T21	N.A.	N.A.	3/3/2017	9.3	974	-1.624	0.006735	0.000009	0.05641	0.00008	0.704699	0.000041	0.00498	0.00001	N.A.	N.A.

T21	N.A.	N.A.	7/28/2017	7.5	1081	-1.945	0.006732	0.000013	0.05638	0.00011	0.704699	0.000050	0.00499	0.00002	N.A.	N.A.
T21	N.A.	N.A.	5/18/2017	5.6	986	-1.866	0.006734	0.000023	0.05640	0.00020	0.704699	0.000062	0.00531	0.00002	N.A.	N.A.
T21	N.A.	N.A.	11/29/2017	16.4	921	-1.643	0.006738	0.000014	0.05643	0.00012	0.704701	0.000029	0.00668	0.00001	N.A.	N.A.
T21	N.A.	N.A.	3/3/2017	14.9	N.D.	-1.698	0.006735	0.000007	N.D.	N.D.	0.704702	0.000035	0.00597	0.00001	N.A.	N.A.
T21	N.A.	N.A.	11/29/2017	15.8	961	-1.676	0.006744	0.000017	0.05648	0.00014	0.704706	0.000031	0.00687	0.00001	N.A.	N.A.
T21	N.A.	N.A.	11/29/2017	17.7	1001	-1.638	0.006741	0.000010	0.05646	0.00008	0.704707	0.000033	0.00523	0.00001	N.A.	N.A.
T21	N.A.	N.A.	3/2/2017	11.7	1017	-1.670	0.006739	0.000009	0.05644	0.00008	0.704708	0.000037	0.00526	0.00001	N.A.	N.A.
T21	N.A.	N.A.	11/29/2017	15.6	929	-1.675	0.006741	0.000013	0.05646	0.00011	0.704710	0.000030	0.00719	0.00001	N.A.	N.A.
T21	N.A.	N.A.	11/29/2017	14.8	960	-1.694	0.006745	0.000018	0.05649	0.00015	0.704711	0.000028	0.00601	0.00002	N.A.	N.A.
T21	N.A.	N.A.	11/29/2017	17.6	990	-1.641	0.006739	0.000015	0.05644	0.00013	0.704716	0.000027	0.00561	0.00001	N.A.	N.A.
T21	N.A.	N.A.	3/2/2017	12.5	998	-1.663	0.006740	0.000009	0.05645	0.00008	0.704718	0.000038	0.00577	0.00002	N.A.	N.A.
T21	N.A.	N.A.	5/18/2017	6.2	1022	-1.837	0.006742	0.000023	0.05646	0.00019	0.704720	0.000058	0.00475	0.00002	N.A.	N.A.
T21	N.A.	N.A.	11/29/2017	17.7	983	-1.643	0.006738	0.000011	0.05643	0.00009	0.704724	0.000032	0.00545	0.00001	N.A.	N.A.
T21	N.A.	N.A.	5/17/2017	6.3	929	-1.808	0.006728	0.000018	0.05635	0.00015	0.704727	0.000056	0.00513	0.00002	N.A.	N.A.
T21	N.A.	N.A.	11/29/2017	17.2	982	-1.654	0.006736	0.000011	0.05642	0.00009	0.704730	0.000029	0.00575	0.00001	N.A.	N.A.
T21	N.A.	N.A.	7/28/2017	7.0	1066	-1.996	0.006724	0.000015	0.05631	0.00013	0.704748	0.000047	0.00580	0.00003	N.A.	N.A.
T21	N.A.	N.A.	7/28/2017	7.3	1041	-1.950	0.006731	0.000012	0.05637	0.00010	0.704793	0.000048	0.00702	0.00002	N.A.	N.A.

Primary Standard

AMNH-107160	N.A.	N.A.	3/2/2017	8.8	724	-1.659	0.006735	0.000013	0.05641	0.00011	0.704391	0.000051	0.00104	0.00001	N.A.	N.A.
AMNH-107160	N.A.	N.A.	3/2/2017	7.7	670	-1.665	0.006737	0.000012	0.05642	0.00010	0.704376	0.000046	0.00107	0.00001	N.A.	N.A.
AMNH-107160	N.A.	N.A.	3/2/2017	9.1	744	-1.661	0.006737	0.000012	0.05643	0.00010	0.704361	0.000037	0.00102	0.00001	N.A.	N.A.
AMNH-107160	N.A.	N.A.	3/2/2017	7.5	649	-1.666	0.006742	0.000014	0.05647	0.00011	0.704371	0.000047	0.00107	0.00001	N.A.	N.A.
AMNH-107160	N.A.	N.A.	3/2/2017	7.9	641	-1.654	0.006736	0.000011	0.05641	0.00009	0.704377	0.000045	0.00106	0.00001	N.A.	N.A.
AMNH-107160	N.A.	N.A.	3/2/2017	7.6	656	-1.667	0.006740	0.000013	0.05645	0.00011	0.704357	0.000045	0.00106	0.00001	N.A.	N.A.
AMNH-107160	N.A.	N.A.	3/2/2017	7.1	580	-1.653	0.006734	0.000014	0.05640	0.00011	0.704361	0.000055	0.00109	0.00001	N.A.	N.A.
AMNH-107160	N.A.	N.A.	3/2/2017	7.5	646	-1.667	0.006739	0.000012	0.05644	0.00010	0.704378	0.000047	0.00107	0.00001	N.A.	N.A.
AMNH-107160	N.A.	N.A.	3/2/2017	7.6	615	-1.655	0.006732	0.000013	0.05639	0.00011	0.704378	0.000051	0.00104	0.00001	N.A.	N.A.
AMNH-107160	N.A.	N.A.	3/2/2017	7.7	660	-1.672	0.006737	0.000012	0.05643	0.00010	0.704372	0.000047	0.00104	0.00001	N.A.	N.A.
AMNH-107160	N.A.	N.A.	3/2/2017	7.5	605	-1.649	0.006743	0.000014	0.05647	0.00011	0.704360	0.000043	0.00107	0.00001	N.A.	N.A.
AMNH-107160	N.A.	N.A.	3/2/2017	7.6	647	-1.677	0.006737	0.000011	0.05643	0.00009	0.704382	0.000040	0.00103	0.00001	N.A.	N.A.
AMNH-107160	N.A.	N.A.	3/2/2017	7.6	613	-1.651	0.006731	0.000012	0.05638	0.00010	0.704362	0.000049	0.00106	0.00001	N.A.	N.A.
AMNH-107160	N.A.	N.A.	3/2/2017	7.8	660	-1.681	0.006748	0.000012	0.05652	0.00010	0.704352	0.000046	0.00100	0.00001	N.A.	N.A.
AMNH-107160	N.A.	N.A.	3/2/2017	7.8	623	-1.652	0.006734	0.000012	0.05640	0.00010	0.704386	0.000051	0.00104	0.00001	N.A.	N.A.
AMNH-107160	N.A.	N.A.	3/2/2017	7.8	657	-1.685	0.006750	0.000012	0.05653	0.00010	0.704378	0.000049	0.00099	0.00001	N.A.	N.A.

AMNH-107160	N.A.	N.A.	3/2/2017	7.8	621	-1.654	0.006735	0.000014	0.05640	0.00012	0.704373	0.000048	0.00105	0.00001	N.A.	N.A.
AMNH-107160	N.A.	N.A.	3/3/2017	6.4	637	-1.627	0.006736	0.000013	0.05641	0.00011	0.704364	0.000050	0.00102	0.00001	N.A.	N.A.
AMNH-107160	N.A.	N.A.	3/3/2017	9.6	N.D.	-1.734	0.006737	0.000009	N.D.	N.D.	0.704375	0.000040	0.00134	0.00001	N.A.	N.A.
AMNH-107160	N.A.	N.A.	3/3/2017	6.2	642	-1.623	0.006726	0.000014	0.05634	0.00012	0.704366	0.000051	0.00100	0.00001	N.A.	N.A.
AMNH-107160	N.A.	N.A.	3/3/2017	9.3	N.D.	-1.715	0.006746	0.000011	N.D.	N.D.	0.704373	0.000039	0.00127	0.00001	N.A.	N.A.
AMNH-107160	N.A.	N.A.	3/3/2017	6.1	645	-1.627	0.006728	0.000015	0.05635	0.00012	0.704388	0.000056	0.00102	0.00001	N.A.	N.A.
AMNH-107160	N.A.	N.A.	3/3/2017	9.2	N.D.	-1.697	0.006746	0.000011	N.D.	N.D.	0.704349	0.000044	0.00130	0.00001	N.A.	N.A.
AMNH-107160	N.A.	N.A.	3/3/2017	6.2	663	-1.623	0.006738	0.000015	0.05644	0.00012	0.704371	0.000058	0.00110	0.00002	N.A.	N.A.
AMNH-107160	N.A.	N.A.	3/3/2017	9.0	N.D.	-1.699	0.006736	0.000009	N.D.	N.D.	0.704381	0.000037	0.00127	0.00001	N.A.	N.A.
AMNH-107160	N.A.	N.A.	3/3/2017	6.0	634	-1.621	0.006735	0.000014	0.05641	0.00012	0.704396	0.000055	0.00104	0.00001	N.A.	N.A.
AMNH-107160	N.A.	N.A.	3/3/2017	5.8	612	-1.617	0.006742	0.000014	0.05646	0.00012	0.704343	0.000051	0.00104	0.00001	N.A.	N.A.
AMNH-107160	N.A.	N.A.	3/3/2017	5.6	593	-1.624	0.006740	0.000015	0.05645	0.00012	0.704376	0.000051	0.00110	0.00003	N.A.	N.A.
AMNH-107160	N.A.	N.A.	5/17/2017	4.5	664	-1.802	0.006728	0.000032	0.05635	0.00026	0.704375	0.000067	0.00107	0.00001	N.A.	N.A.
AMNH-107160	N.A.	N.A.	5/17/2017	4.4	678	-1.813	0.006720	0.000039	0.05629	0.00033	0.704361	0.000076	0.00106	0.00001	N.A.	N.A.
AMNH-107160	N.A.	N.A.	5/17/2017	4.0	587	-1.797	0.006735	0.000031	0.05641	0.00026	0.704354	0.000074	0.00107	0.00001	N.A.	N.A.
AMNH-107160	N.A.	N.A.	5/17/2017	3.9	621	-1.811	0.006721	0.000030	0.05629	0.00025	0.704417	0.000078	0.00108	0.00001	N.A.	N.A.
AMNH-107160	N.A.	N.A.	5/17/2017	3.9	577	-1.798	0.006727	0.000037	0.05634	0.00031	0.704389	0.000076	0.00104	0.00001	N.A.	N.A.
AMNH-107160	N.A.	N.A.	5/17/2017	4.1	608	-1.801	0.006722	0.000033	0.05630	0.00027	0.704367	0.000078	0.00108	0.00002	N.A.	N.A.
AMNH-107160	N.A.	N.A.	5/17/2017	4.3	634	-1.812	0.006715	0.000031	0.05624	0.00026	0.704370	0.000059	0.00108	0.00001	N.A.	N.A.
AMNH-107160	N.A.	N.A.	5/18/2017	4.3	716	-1.824	0.006731	0.000032	0.05638	0.00027	0.704356	0.000078	0.00107	0.00002	N.A.	N.A.
AMNH-107160	N.A.	N.A.	5/18/2017	4.2	709	-1.843	0.006723	0.000037	0.05631	0.00031	0.704380	0.000074	0.00110	0.00002	N.A.	N.A.
AMNH-107160	N.A.	N.A.	5/18/2017	4.0	631	-1.817	0.006738	0.000045	0.05643	0.00038	0.704369	0.000075	0.00105	0.00001	N.A.	N.A.
AMNH-107160	N.A.	N.A.	5/18/2017	4.2	713	-1.852	0.006736	0.000039	0.05642	0.00033	0.704415	0.000078	0.00110	0.00001	N.A.	N.A.
AMNH-107160	N.A.	N.A.	5/18/2017	3.8	608	-1.824	0.006736	0.000038	0.05642	0.00032	0.704304	0.000087	0.00103	0.00002	N.A.	N.A.
AMNH-107160	N.A.	N.A.	5/18/2017	3.9	676	-1.860	0.006759	0.000036	0.05661	0.00031	0.704322	0.000074	0.00112	0.00001	N.A.	N.A.
AMNH-107160	N.A.	N.A.	5/18/2017	3.7	600	-1.827	0.006722	0.000031	0.05630	0.00026	0.704432	0.000083	0.00104	0.00001	N.A.	N.A.
AMNH-107160	N.A.	N.A.	5/18/2017	4.2	739	-1.864	0.006738	0.000032	0.05643	0.00026	0.704382	0.000067	0.00105	0.00001	N.A.	N.A.
AMNH-107160	N.A.	N.A.	5/18/2017	4.0	664	-1.834	0.006719	0.000030	0.05627	0.00025	0.704314	0.000067	0.00106	0.00001	N.A.	N.A.
AMNH-107160	N.A.	N.A.	5/18/2017	4.0	682	-1.842	0.006715	0.000038	0.05624	0.00031	0.704383	0.000071	0.00106	0.00002	N.A.	N.A.
AMNH-107160	N.A.	N.A.	5/18/2017	3.9	669	-1.856	0.006714	0.000043	0.05623	0.00036	0.704399	0.000077	0.00105	0.00002	N.A.	N.A.
AMNH-107160	N.A.	N.A.	7/28/2017	5.1	775	-1.983	0.006723	0.000016	0.05631	0.00013	0.704376	0.000051	0.00110	0.00004	N.A.	N.A.
AMNH-107160	N.A.	N.A.	7/28/2017	5.4	755	-1.898	0.006727	0.000019	0.05634	0.00016	0.704376	0.000061	0.00109	0.00002	N.A.	N.A.
AMNH-107160	N.A.	N.A.	7/28/2017	5.2	711	-1.863	0.006729	0.000021	0.05635	0.00017	0.704371	0.000053	0.00107	0.00001	N.A.	N.A.
AMNH-107160	N.A.	N.A.	7/28/2017	5.4	762	-1.930	0.006733	0.000018	0.05639	0.00015	0.704369	0.000070	0.00104	0.00003	N.A.	N.A.
AMNH-107160	N.A.	N.A.	7/28/2017	4.5	668	-1.967	0.006726	0.000020	0.05633	0.00017	0.704328	0.000066	0.00106	0.00003	N.A.	N.A.
AMNH-107160	N.A.	N.A.	7/28/2017	4.9	676	-1.886	0.006735	0.000020	0.05641	0.00017	0.704346	0.000054	0.00108	0.00002	N.A.	N.A.

AMNH-107160	N.A.	N.A.	7/28/2017	5.3	742	-1.836	0.006736	0.000020	0.05642	0.00017	0.704371	0.000054	0.00101	0.00001	N.A.	N.A.
AMNH-107160	N.A.	N.A.	7/28/2017	5.1	721	-1.946	0.006722	0.000019	0.05630	0.00016	0.704372	0.000057	0.00101	0.00001	N.A.	N.A.
AMNH-107160	N.A.	N.A.	7/28/2017	5.3	765	-1.938	0.006727	0.000019	0.05634	0.00016	0.704402	0.000068	0.00102	0.00002	N.A.	N.A.
AMNH-107160	N.A.	N.A.	7/28/2017	5.1	704	-1.859	0.006740	0.000016	0.05645	0.00013	0.704392	0.000049	0.00107	0.00002	N.A.	N.A.
AMNH-107160	N.A.	N.A.	7/28/2017	5.0	725	-1.842	0.006736	0.000017	0.05642	0.00014	0.704371	0.000064	0.00108	0.00002	N.A.	N.A.
AMNH-107160	N.A.	N.A.	7/28/2017	5.4	770	-1.933	0.006721	0.000016	0.05629	0.00013	0.704374	0.000064	0.00100	0.00001	N.A.	N.A.
AMNH-107160	N.A.	N.A.	7/28/2017	5.0	701	-1.928	0.006729	0.000018	0.05636	0.00015	0.704394	0.000063	0.00105	0.00002	N.A.	N.A.
AMNH-107160	N.A.	N.A.	7/28/2017	4.9	684	-1.878	0.006734	0.000021	0.05640	0.00018	0.704382	0.000059	0.00104	0.00002	N.A.	N.A.
AMNH-107160	N.A.	N.A.	7/28/2017	4.9	706	-1.948	0.006737	0.000024	0.05643	0.00020	0.704376	0.000061	0.00102	0.00001	N.A.	N.A.
AMNH-107160	N.A.	N.A.	7/28/2017	5.3	718	-1.930	0.006732	0.000017	0.05639	0.00014	0.704359	0.000051	0.00110	0.00002	N.A.	N.A.
AMNH-107160	N.A.	N.A.	7/28/2017	5.6	810	-1.868	0.006727	0.000017	0.05634	0.00014	0.704357	0.000056	0.00120	0.00004	N.A.	N.A.
AMNH-107160	N.A.	N.A.	7/28/2017	5.2	749	-1.947	0.006727	0.000016	0.05634	0.00013	0.704354	0.000068	0.00104	0.00002	N.A.	N.A.
AMNH-107160	N.A.	N.A.	7/28/2017	4.9	701	-1.946	0.006752	0.000020	0.05655	0.00017	0.704375	0.000049	0.00102	0.00001	N.A.	N.A.
AMNH-107160	N.A.	N.A.	7/28/2017	5.0	722	-1.958	0.006741	0.000021	0.05646	0.00017	0.704371	0.000051	0.00100	0.00001	N.A.	N.A.
AMNH-107160	N.A.	N.A.	11/29/2017	11.8	704	-1.626	0.006768	0.000019	0.05668	0.00016	0.704333	0.000033	0.00105	0.00001	N.A.	N.A.
AMNH-107160	N.A.	N.A.	11/29/2017	12.1	683	-1.633	0.006752	0.000019	0.05655	0.00016	0.704392	0.000042	0.00106	0.00001	N.A.	N.A.
AMNH-107160	N.A.	N.A.	11/29/2017	12.2	693	-1.647	0.006744	0.000024	0.05649	0.00020	0.704369	0.000034	0.00105	0.00001	N.A.	N.A.
AMNH-107160	N.A.	N.A.	11/29/2017	11.5	686	-1.669	0.006745	0.000021	0.05649	0.00018	0.704394	0.000033	0.00103	0.00001	N.A.	N.A.
AMNH-107160	N.A.	N.A.	11/29/2017	14.0	835	-1.634	0.006719	0.000063	0.05627	0.00052	0.704661	0.000072	0.00599	0.00002	N.A.	N.A.
AMNH-107160	N.A.	N.A.	11/29/2017	12.0	675	-1.629	0.006742	0.000021	0.05647	0.00018	0.704358	0.000036	0.00105	0.00001	N.A.	N.A.
AMNH-107160	N.A.	N.A.	11/29/2017	11.5	670	-1.651	0.006757	0.000019	0.05659	0.00016	0.704373	0.000035	0.00104	0.00001	N.A.	N.A.
AMNH-107160	N.A.	N.A.	11/29/2017	11.3	680	-1.665	0.006755	0.000020	0.05657	0.00017	0.704359	0.000035	0.00105	0.00001	N.A.	N.A.
AMNH-107160	N.A.	N.A.	11/29/2017	12.0	705	-1.621	0.006765	0.000021	0.05666	0.00018	0.704374	0.000040	0.00104	0.00001	N.A.	N.A.
AMNH-107160	N.A.	N.A.	11/29/2017	12.0	675	-1.633	0.006751	0.000018	0.05654	0.00015	0.704357	0.000036	0.00104	0.00001	N.A.	N.A.
AMNH-107160	N.A.	N.A.	11/29/2017	11.3	671	-1.656	0.006752	0.000020	0.05655	0.00017	0.704374	0.000034	0.00105	0.00001	N.A.	N.A.
AMNH-107160	N.A.	N.A.	11/29/2017	11.4	696	-1.667	0.006747	0.000021	0.05651	0.00017	0.704369	0.000033	0.00103	0.00001	N.A.	N.A.
AMNH-107160	N.A.	N.A.	11/29/2017	11.9	693	-1.622	0.006756	0.000018	0.05658	0.00015	0.704338	0.000038	0.00103	0.00001	N.A.	N.A.
AMNH-107160	N.A.	N.A.	11/29/2017	11.7	658	-1.639	0.006749	0.000022	0.05653	0.00018	0.704391	0.000035	0.00105	0.00000	N.A.	N.A.
AMNH-107160	N.A.	N.A.	11/29/2017	11.3	680	-1.667	0.006752	0.000018	0.05655	0.00015	0.704360	0.000040	0.00106	0.00000	N.A.	N.A.
AMNH-107160	N.A.	N.A.	11/29/2017	11.0	675	-1.670	0.006751	0.000020	0.05654	0.00017	0.704366	0.000040	0.00105	0.00001	N.A.	N.A.
AMNH-107160	N.A.	N.A.	11/29/2017	11.9	682	-1.625	0.006745	0.000016	0.05649	0.00013	0.704369	0.000036	0.00106	0.00001	N.A.	N.A.
AMNH-107160	N.A.	N.A.	11/29/2017	11.6	651	-1.641	0.006745	0.000017	0.05649	0.00014	0.704337	0.000037	0.00106	0.00001	N.A.	N.A.
AMNH-107160	N.A.	N.A.	11/29/2017	11.6	707	-1.671	0.006757	0.000023	0.05659	0.00019	0.704376	0.000037	0.00102	0.00000	N.A.	N.A.
AMNH-107160	N.A.	N.A.	11/29/2017	10.6	661	-1.671	0.006738	0.000017	0.05644	0.00014	0.704326	0.000041	0.00107	0.00001	N.A.	N.A.
AMNH-107160	N.A.	N.A.	11/29/2017	12.0	680	-1.622	0.006746	0.000016	0.05650	0.00014	0.704341	0.000037	0.00106	0.00001	N.A.	N.A.
AMNH-107160	N.A.	N.A.	11/29/2017	12.6	704	-1.648	0.006745	0.000017	0.05649	0.00014	0.704391	0.000034	0.00103	0.00001	N.A.	N.A.

AMNH-107160	N.A.	N.A.	11/29/2017	10.6	666	-1.678	0.006744	0.000016	0.05649	0.00014	0.704391	0.000036	0.00106	0.00000	N.A.	N.A.
AMNH-107160	N.A.	N.A.	11/29/2017	12.1	681	-1.626	0.006748	0.000019	0.05651	0.00016	0.704374	0.000035	0.00105	0.00001	N.A.	N.A.
AMNH-107160	N.A.	N.A.	11/29/2017	11.0	697	-1.678	0.006751	0.000017	0.05654	0.00015	0.704378	0.000038	0.00104	0.00001	N.A.	N.A.
AMNH-107160	N.A.	N.A.	11/29/2017	12.0	666	-1.631	0.006755	0.000022	0.05657	0.00019	0.704393	0.000034	0.00106	0.00001	N.A.	N.A.
AMNH-107160	N.A.	N.A.	11/29/2017	10.6	681	-1.679	0.006749	0.000021	0.05653	0.00018	0.704343	0.000038	0.00105	0.00001	N.A.	N.A.
AMNH-107160	N.A.	N.A.	11/29/2017	10.1	659	-1.681	0.006752	0.000024	0.05655	0.00020	0.704407	0.000042	0.00108	0.00001	N.A.	N.A.

* The textural positions of the analyses are indicated when they could be confidently classified based on micr-XRF maps. Question marks indicate cases where positions could not be confidently classified.

† Sr concentrations are estimated by comparing the ⁸⁸Sr signal to BCR-2G, with a known Sr concentration. They are considered to be semi-quantitative in absence of a matrix-matched Sr concentration standard.

§ Bold italic lines are analyses that were excluded from the weighted mean of a sample.

TABLE DR3. SAMPLE LOCATIONS

Sample	Zone	Profile	Stratigraphic height (m)	latitude (°N)	longitude (°W)
<u>Upper Border Series</u>					
SK08-113	LZa'	Hammerpas	3135	68.148500	31.594230
SK08-189	LZa'	Skaergaardsbugt	3134	68.129222	31.706500
SK08-70	LZa'	Sydtoppen	3128	68.144998	31.646326
SK08-114	LZa'	Hammerpas	3108	68.148635	31.594938
SK08-115	LZa'	Hammerpas	3104	68.148745	31.595666
SK08-65	LZa'	Sydtoppen	3104	68.144694	31.644417
SK08-116	LZa'	Hammerpas	3054	68.148861	31.596528
SK08-117	LZa'	Hammerpas	3017	68.148944	31.597056
SK08-118	LZa'	Hammerpas	2984	68.149250	31.597750
SK08-1	LZb'	Brødretoppen	2922	68.151600	31.635600
SK08-125	LZb'	Hammerpas	2841	68.150472	31.602500
SK08-14	LZb'	Brødretoppen	2803	68.151826	31.642118
SK08-13	LZb'	Brødretoppen	2803	68.151826	31.642118
SK08-199	LZb'	Kilen	2793	68.155111	31.595083
SK08-129	LZc'	Hammerpas	2706	68.151917	31.607028
SK08-137	MZ'	Hammerpas	2613	68.153639	31.619750
SK08-138	MZ'	Hammerpas	2613	68.153633	31.619757
SK08-140	UZa'	Hammerpas	2535	68.154944	31.621278
SK08-156	UZb'	Kilen	2460	68.156833	31.599113
SK08-150	UZb'/UZc'	Kilen	2334	68.160803	31.596438
SK08-148	UZb'/UZc'	Kilen	2290	68.161050	31.597097
SK08-103	UZc'	Kilen	2273	68.161194	31.597161
<u>Sandwich Horizon</u>					
SK08-110	SH	Kilen	2177	68.161916	31.597598
SK11-58	SH	N.D.	2177	68.166521	31.655410
<u>Layered Series</u>					

90-22-31.1	UZc	LS Reference Profile	2061	68.159762	31.673027
90-22-87.7	UZb	LS Reference Profile	2004	68.159762	31.673027
90-22-384.0	UZb	LS Reference Profile	1708	68.159762	31.673027
90-22-481.8	UZa	LS Reference Profile	1610	68.159762	31.673027
90-22-648.4	UZa	LS Reference Profile	1443	68.159762	31.673027
90-22-893.6	UZa	LS Reference Profile	1198	68.159762	31.673027
458256	MZ	LS Reference Profile	1003	68.185983	31.681083
458257	MZ	LS Reference Profile	1003	68.185983	31.681083
458286	LZc	LS Reference Profile	847	68.188783	31.714283
458277	LZb	LS Reference Profile	703	68.191150	31.715483
458203	LZb	LS Reference Profile	558	68.211183	31.686650
458231	LZb	LS Reference Profile	367	68.211083	31.694100
458220	LZa	LS Reference Profile	173	68.210600	31.710000
458218	LZa	LS Reference Profile	159	68.210700	31.713433
458214	LZa	LS Reference Profile	107	68.210900	31.720217
458213	LZa	LS Reference Profile	84	68.210883	31.722050
458211	LZa	LS Reference Profile	7	68.211300	31.725367
